Title

CHEMICAL TRANSPORT REACTION ANALYSIS FOR CRYSTAL GROWTH OF BINARY AND TERNARY CHALCOGENIDES

Author

Agnihotri, Rajani Bhushan.

Publication Date

1972-12-01

LBL-1404

CHEMICAL TRANSPORT REACTION ANALYSIS FOR CRYSTAL GROWTH OF BINARY AND TERNARY CHALCOGENIDES

Rajani Bhushan Agnihotri

(M. S. Thesis)

December 1972

Prepared for the U. S. Atomic Energy Commission under Contract W-7405-ENG-48

LBL-1404

DISCLAIMER

CHEMICAL TRANSPORT REACTION ANALYSIS FOR CRYSTAL GROWTH OF BINARY AND TERNARY CHALCOGENIDES

Contents

ABSTRACT v

I. GENERAL INTRODUCTION 1

Tables 7

Bibliography 11

Figure Captions 14

Figures 15

II. CHEMICAL TRANSPORT IN A CLOSED SYSTEM

A. Introduction 17

B. Chemical Transport of Group II-VI Compounds with Halogens as Transport Agents 27

1. Diffusion Controlled Transport 27

2. Results and Discussion 32

C. Chemical Transport AB_2X_4 Compounds with Halogens as Transport Agents 36

1. Diffusion Controlled Transport 40

2. Results and Discussion 43

Tables 44

Bibliography 58

Figure Captions 60

Figures 61

III. MAGNETIC SUSCEPTIBILITY

A. Magnetic Behavior of 2-3 Spinels 73

B. Experimental Setup for Measuring Magnetic Susceptibility 78

III.B. continued

1. The Faraday Method 79

2. Coil Design 80

3. Coil Construction 80

4. Experimental Observations 81

5. Conclusions 82

Bibliography 83

Figure Captions 84

Figures 85

APPENDICES

Appendix 1A: Mathematical Modelling of the Transport of II-VI Compounds 90

Appendix 1B: Mathematical Modelling of the Transport of AB_2X_4 Compounds 101

Appendix 2: Thermodynamic Calculations 111

Appendix 3: Determination of Gas-Phase Diffusivity . . 121

Appendix 4: Computer Program 124

ACKNOWLEDGEMENTS 132

CHEMICAL TRANSPORT REACTION ANALYSIS FOR CRYSTAL GROWTH OF BINARY AND TERNARY CHALCOGENIDES

Rajani Bhushan Agnihotri

Inorganic Materials Research Division, Lawrence Berkeley Laboratory and Department of Chemical Engineering; University of California Berkeley, California

ABSTRACT

The chemical transport crystal growth of binary and ternary chalcogenides in a closed container using halogens as transport agents is analyzed for diffusion controlled kinetics in terms of thermodynamics of gas solid equilibria, temperature conditions and initial transport agent concentration.

The Stefan-Maxwell transport equations for multi-component gaseous diffusion are integrated and related to phase equilibria to predict the growth rates of CdS, ZnS and MnS using I_2 as a transport agent under varying transport conditions. Concentration profiles for the gaseous species are also predicted as a function of position along the transport path. The chemical transport of ternary chalcogenides (AB_2X_4) is analyzed similarly. The importance of magnetic susceptibility for characterization of the compound is shown. A magnetic coil system developed to produce a linear field gradient for measuring magnetic susceptibility by the Faraday method is described.

I. GENERAL INTRODUCTION

Chalcogen compounds have attracted much interest because of their variety of magnetic electrical and optical properties. Many chalcogenides are industrially important as photoconductors, magnetic semiconductors and chemical catalysts. Binary chalcogenides such as CdS and ZnS are well-known for their electro-optical properties. CdS[1] is also used in electromechanical transducers and ultrasonic amplifiers. Generally, the chalcogenides of zinc and cadmium are utilised chiefly as luminescent and photoconducting materials.[2] They are also semiconductors. Single crystals of tin and lead sulfide, selenide and tellurides have attracted interest in the semiconducting properties of these compounds arising from their use as infrared photodetectors.[2] Many semiconductors of the II-VI compounds family can be made p- or n-type by a simple change in stoichiometry.

Ternary chalcogenide spinels, AB_2X_4 (X=S, Se, Te) exhibit unusual magnetic and electrical properties. These compounds are in the same family as ferrites which are used in microwave devices, memory devices in computers, magnetic heads in tape recorders and other device applications. The exchange interactions in ferrites (which are oxyspinels) are always negative so that these substances are ferri- or antiferromagnetic. In chalcogenide spinels, however, positive exchange interactions are possible giving rise to ferri-, ferro-, antiferromagnetism, a helical spin configuration and so on. Spinels of the type (A = Fe^{2+}, Mn^{2+}, Co^{2+}) are ferrimagnetic semiconductors, $ZnCr_2X_4$ (X=S, Se) spinels are antiferromagnetic and semiconducting,

A Cr_2X_4 ($A=Cd^{2+}$, Hg^{2+}, X=S, Se) are ferromagnetic insulators excepting $HgCr_2S_4$ which is a metamagnetic insulator.[3] On the other hand compounds of the type $CuCr_2X_4$ (X=S, Se, Te) are ferromagentic and exhibit metallic conduction.[4] Finally, three compounds CuV_2S_4, $CuRh_2S_4$ and $CuRh_2Se_4$ have been found to be superconductors.[5,6]

The series of ternary chalcogenides M Cr_2X_4 (M = Pb, Sr, Ba, Eu and X = S, Se) are known to crystallize in a hexagonal structure. These compounds are found to be ferrimagnetic semiconductors except for $PbCr_2Se_4$ which has a metallic type of conductivity dependance on temperature. Because of their structure these compounds are expected to exhibit highly amiotropic physical properties in contrast to the cubic spinels.[7]

Rare earth chalcogenides such as EuX (X=O, S, Se, Te) are magnetic semiconductors.[8] Ternary chalcogenides of the form $EuLn_2X_4$ (Ln = Lanthanides, X = S, Se) also have magnetic ordering.[9]

We can see that for an understanding of the physics and chemistry of these materials, crystals are a prerequisite. One can use a polycrystalline sample for many studies but for a study of structure and transport properties as well as industrial applications, a reasonably large single crystal is needed. Grain boundaries in polycrystals give rise to impurity segregation and particle scattering and thus single crystals are also required for optical studies as well as for a determination of any transport properties. Single crystals are also required for studies on magnetic anisotropy and electromagnetic coupling.

Currently there are various methods by which it is known single crystals of chalcogen compounds can be prepared. These are

i) closed tube vapor transport

ii) Open tube vapor transport (epitaxial process)

iii) Growth from solution

iv) Solid state reactions

v) Hydrothermal crystal growth

vi) Liquid transport. (Growth from liquid phase by a chemical reaction)

One form of vapor transport is the simple sublimation-condensation process. This can be done for compounds that have high volatility. CdS and ZnS are best grown by this technique.[10,11] However, dissociation of the compound in the vapor phase is considerable so that a more realistic reaction for the "sublimation" process is

$$CdS_{(s)} \rightleftharpoons Cd_{(g)} + S_{(g)} \quad .$$

The Piper-Polich method[12] of moving the vapor zone separating the source material and the single crystal product through a temperature gradient has become the method of choice, since the thermal gradient stabilizes single crystal growth.

Crystal growth from the melt becomes difficult for materials having high melting points or which show appreciable dissociation at the melting point. To obtain single crystals of such materials vapor phase growth methods are used.

To minimize contamination from containers, and to improve growth rates, it is preferrable to carry out methods for growing crystals at temperatures well below the melting point of the material involved.

This can be achieved through chemical transport reactions, a term introduced by Schafer.[13] Instead of directly vaporizing a solid at high temperatures, the solid could be reacted at a lower temperature to form volatile chemical intermediates. These intermediates can be reacted back to the solid at a different temperature utilizing the temperature dependance of the chemical equilibrium involved.

In this work, we will focus our attention on the closed tube chemical transport method for preparing single crystals of binary and ternary chalcogenides.

In this technique, a silica (quartz) ampoule is evacuated, partly filled with the source material and a volatile transport agent and placed in a controlled two-zone furnace. (Fig. 1). Since halides are generally more volatile than other metallic salts, the transport agent is often a halogen or a halogen-containing compound. The reaction follows the general reaction equilibrium,

$$A_{(s)} + B_{(g)} \rightleftharpoons C_{(g)} + D_{(g)}$$

where A is the solid to be transported, B is the transport agent and C and D the volatile intermediates. The different II-VI chalcogenides that have been grown by this method are given in Table I.
A very good case for the use of a transport agent in growth experiments, even when the compounds have high vapor pressure, is when an alloy crystal product is desired to be formed from compounds having different vapor pressures at the same temperature. Cherin et al[33] found that because CdS had a much higher vapor pressure than ZnS at a given temperature,

it is impossible to grow "mixed" (alloy) crystals of $Cd_xZn_{1-x}S$ by sublimation.[34] However, with I_2 as a transport agent, the equilibrium constants in the reactions of CdS and ZnS are close enough for co-transport to be possible. Several other studies have been made of this reaction.[35-38]

Chemical vapor transport is the principle technique available to synthesize many ternary chalcogenide spinels, even in the polycrystalline form. It is useful particularly for those ternary and quarternary compounds that melt incongruently or that have high equilibrium dissociation pressures at their melting points due to one or more volatile components. These difficulties are frequently encountered in chalcogenide spinels. A list of ternary chalcogenides that have been prepared by the closed tube chemical transport process is given in Table II.

Gibart et al[39] obtained an improvement in the size of the single crystals by pulling the ampoule slowly through the temperature gradient. One could explain this result as follows: As the first single crystals are formed, they extend spatially, causing the next crystal zone of deposition to be at a slightly different temperature for a fixed profile. Hence if the ampoule is displaced continuously with respect to the fixed thermal profile, the deposition will take place at a more constant temperature. It is obvious that the pulling rate must be closely related to the crystal deposition rate. Gibart et al.[39] increased the size of $FeCr_2S_4$ crystals from 2-4 mm to 15 × 6 × 0.6 mm by pulling.

Another improvement on the ordinary closed tube method is the ampoule designed by Widmer.[40] This double-wall (Fig. 2) permits the outer evacuated jacket to reduce the radial temperature gradient in the ampoule and also to protect the growth region from convective heat currents in the furnace tube. $CdCr_2S_4$ crystals were improved in size from 0.2 to 0.6 mm to 4 × 6 × 3 mm by this method.

In this work, attention has been centered on crystal growth by the chemical transport method. We apply thermodynamic and diffusivity data and assume certain chemical equilibria for the equations of motion of the gaseous chemical intermediates that are formed by the reaction of the transport agent and the solids to be transported. A model based on the Stefan-Maxwell equations is proposed and solved to obtain rates of product formation as a function of imput variables to the system e.g. temperature conditions, transport agent and transport agent feed. We can also predict the pressure in the ampoule and the concentrations of the various species as a function of position in the ampoule.

Also since the magnetic properties of the ternary chalcogenide spinels are so varied, we have included a section which outlines simply the magnetic behavior of these compounds. Since magnetic susceptibility is an important tool in characterizistic of their structure, a set of magnetic deflection coils that produce a linear magnetic field gradient was designed for use in the Faraday method.

Table I. Chemical transport of II-VI compounds in a closed tube.

Compound	Agent	Temp. Profile (°C)	Transport Agent (mg/cc)	Linear Growth Rate (cm/sec)	Ref.
CdS	I_2	$\bar{T}$=830, ΔT=15	4.0	1.0×10^{-6}	14
	I_2	850→650	5.0		15,16
CdSe	I_2	1000→500	5.0		15,16
	I_2				17
CdTe	I_2				18,19
ZnS	I_2	1050→750			15,16
	I_2	1050→770	5.0		20
	I_2	1050→900			21
	Cl_2	1200→1060			22
	I_2				23
	I_2				24
	I_2				25
ZnS(cubic)	I_2				26
ZnSe	I_2	1050-800	4.0	1.0×10^{-6}	15,16
	I_2	785-780			27
	I_2	$\bar{T}$=850,ΔT=5	5.0	2.0×10^{-6}	28
	I_2				29

Table I. continued

Compound	Agent	Temp. Profile (°C)	Transport Agent (mg/cc)	Linear Growth Rate (cm/sec)	Ref.
ZnSe(cubic)	HCl, Br_2 I_2				28
ZnTe	I_2				23
ZnAs	I_2				23
MnS	I_2	1000-550			15,16
HgS	Cl_2				30
FeS, CoS, NiS	Cl_2				31
EuTe	I_2	$\bar{T}$=1680, ΔT=95	1.35	2.0×10^{-7}	32
EuSe	I_2	$\bar{T}$=1650, ΔT=68	1.0	4.0×10^{-8}	32
FeS	I_2	900-700			13
CrTe	I_2	1025-850			13

Table II. Chemical transport of ternary chalcogenides (AB_2X_4)

Substance	Transport Agent	Temp. Profile (°C)	Rate	Ref.
$CdCr_2S_4$	Cl_2	825-775		41,42
	$CrCl_3$			43
$CdCr_2Se_4$	$CdCl_2$-Se-$CdCr_2Se_4$	800-700		44
$HgCr_2S_4$	Cl_2	900-780		45
$HgCr_2Se_4$	$CrCl_3$	700-670/10 cm		46
ACr_2S_4 (A=Cd,Zn,Mn)	$AlCl_3$	1000-800		47
ACr_2Se_4 (A=Cd,Zn,Hg Cu)	$AlCl_3$	900-600		47
$CuCr_2Se_4$	I_2	1150-1100		4
$CoCr_2S_4$	I_2	1150-1000		48
	$CrBr_3$			39
$FeCr_2S_4$	Cl_2	1100-1000		39
$ZnGa_2S_4$	I_2	1100-1000		16
$CdGa_2S_4$	I_2	650-600		16
$HgGa_2S_4$	I_2	1100-1000		16
$ZnGa_2Se_4$	I_2	1100-1000		16
$CdGa_2Se_4$	I_2	950-750		16
$HgGa_2Se_4$	I_2	760-700		16
$ZnIn_2S_4$	I_2	750-700		15,16
	I_2	750-700		49

Table II continued

Substance	Transport Agent	Temp. Profile (°C)	Rate	Ref.
$CdIn_2S_4$	I_2	850÷750		15,16
	I_2	850-750		49
$HgIn_2S_4$	I_2	950-650		15,16
$ZnIn_2Se_4$	I_2	700-650		15,16
$CdIn_2Se_4$	I_2	650-600		15,16
$HgIn_2Se_4$	I_2	750-700	Fast (51)	50
$MnIn_2S_4$	I_2	1100-1000	Low (51)	50
$CoIn_2S_4$	I_2	850-800	Very low (51)	50
$CoCr_2S_4$	NH_4Cl	1150-1000	Very low (51)	50
Cr_2S_3	Br_2		Medium	51
$GeFe_2S_4$	I_2		Medium	51
$GeMn_2S_4$	I_2		Low	51
$SiMn_2S_4$	I_2		Low	51

BIBLIOGRAPHY

1. R. Laudise, The Growth of Single Crystals (Prentice-Hall, Inc., New Jersey, 1970) p. 34.

2. N. B. Hannay, Semiconductors (Reinhold Pub. Corp., N. Y., 1959).

3. V. J. Folen and G. H. Stauss, Landolt-Bornstein, Gr. III, Vol. 4, Pt.b,p.619.

4. F. K. Lotgering, Proceedings of International Conference on Magnetism, Nottingham, England, 1964 (Inst. Phys. and Physical Society, London, 1965) p. 533.

5. N. H. Van Maaren, G. M. Schaeffer and F. K. Lotgering, Phys. Letters 25A, 238 (1967).

6. M. Robbins, R. H. Willens and R. C. Miller, Solid State Comm. 5, 933 (1967).

7. F. Okamoto, et al., Proc. Intl. Conf. on Ferrites, Kyoto 1970. (University of Tokyo Press, 1971).

8. S. Methfessel and D. C. Mattis, Handbuch der Physik 18, (Springer-Verlag, Berlin, 1968) p. 389.

9. F. Hulliger and O. Vogt, Phys. Letters 21 (2), 138-9 (1966).

10. S. J. Czyzak, D. C. Reynolds, et al., J. Appl. Phys. 23, 932 (1952).

11. D. C. Reynolds, The Art and Science of Growing Crystals, edited by J. J. Gilman (Wiley, New York, 1963) p. 62.

12. W. W. Piper and S. J. Polich, J. Appl. Phys. 32, 1278 (1961).

13. H. Schafer, Chemical Transport Reactions (Academic Press, N. Y. & London 1964).

14. E. Kaldis, J. Cryst. Growth 5, 376-90 (1969).

15. R. Nitsche, J. Phys. Chem. Solids 17, 163 (1960).

16. R. Nitsche, et al., J. Phys. Chem. Solids 21, 199 (1961).

17. W. Kleber, I. Mietz and U. Elasser, Krist. Tech. 2 (3), 327-38 (1967).

18. C. Piaget, Rev. Phys. Appl. 1 (3), 201-3 (1966).

19. W. Akutagawa and K. Zanio, J. Cryst. Growth 11, 191-6 (1971).

20. Rumyantsev, et al., Soviet Physics Crystallography 10, 212 (1965).

21. F. Jona and G. Mandel, J. Phys. Chem. Solids 25, 187 (1964).

22. K. Patek, et al., Czech J. Phys. B 12, 313 (1962).

23. H. Hartmann, Growth of Crystals 7, 220-3 (1969).

24. A. J. Horodecki, A. Kawski and J. Czajko, Bull. Acad. Pol. Sci. Ser. Sci. Math. Astron. Phys. 16 (10), 831-3 (1968).

25. K. Recker and R. Schoepe, J. Cryst. Growth 9, 189-92 (1971).

26. S. Ujiie and Y. Kotera, J. Cryst. Growth 10, 320-2 (1971).

27. E. Kaldis, J. Phys. Chem. Solids 26, 1701 (1965).

28. S. G. Parker and J. E. Pinnell, Trans. Met. Soc. AIME, 245 (3), 451-5 (1969).

29. A. A. Simanovskii, Growth of Crystals 7, 224-32 (1969).

30. E. H. Carlson, J. Cryst. Growth 1 (5), 271-7 (1967).

31. R. J. Bouchard, J. Cryst. Growth 2 (1), 40-4 (1968).

32. E. Kaldis, J. Cryst. Growth 3-4, 146-9 (1968).

33. P. Cherin, E. L. Lind and E. M. Davis, J. Electrochem. Soc. 117, 233 (1970).

34. F. L. Chan, Advances in X-Ray Analysis, Vol. 5, edited by W. M. Mueller (Plenum Press, N. Y. 1961) p. 142.

35. E. A. Davis and E. L. Lind, J. Phys. Chem. Solids 29, 79 (1968).

36. E. A. Davis, R. E. Drews and E. L. Lind, Solid State Commun. 5, 573 (1967).

37. R. E. Drews, E. A. Davis and A. G. Leiger, Phys. Rev. Letters 18, 1194 (1967).

38. E. A. Lind, E. A. Davis and G. Luzowsky, II-VI Compound Semiconductors, edited by P. J. Thomas (Benjamin, Inc. 1967).

39. P. Gibart, et al., Conf. on Crystal Growth and Epitaxy from the Vapor Phase, Zurich, 1970.

40. R. Widmer, J. Cryst. Growth 8, 216-8 (1971).

41. G. Harbeke and H. Pinch, Phys. Rev. Letters 17, 1090 (1966).

42. S. B. Berger and H. Pinch, J. Appl. Phys. 38, 949 (1967).

43. F. Okamoto and T. Oka, presented at meeting of the Japanese Physical Society, 1970.

44. F. H. Wehmeier, J. Cryst. Growth 5, 26 (1969).

45. G. Harbeke, S. B. Berger and F. P. Emmenegger, Solid State Comm. 6, 553 (1968).

46. T. Takahashi, J. Cryst. Growth 6, 319 (1970).

47. H. D. Lutz, et al., Monatsh. Chemie 101, 519 (1970).

48. R. Nitsche, in Crystal Growth, edited by H. S. Peiser (Pergamon, Oxford, 1967) p. 215.

49. Shionoya and Tamoto, J. Phys. Soc. Japan 19, 1142 (1964).

50. R. Nitsche, Fortschr. Miner 44 (2), 231-87 (1967).

51. R. Nitsche, private communication with Professor L. F. Donaghey.

Figure Captions

Fig. 1. Schematic diagram of the assembly for chemical transport reactions in a closed ampoule.

Fig. 2. Double-walled ampoule by Widmer.[40]

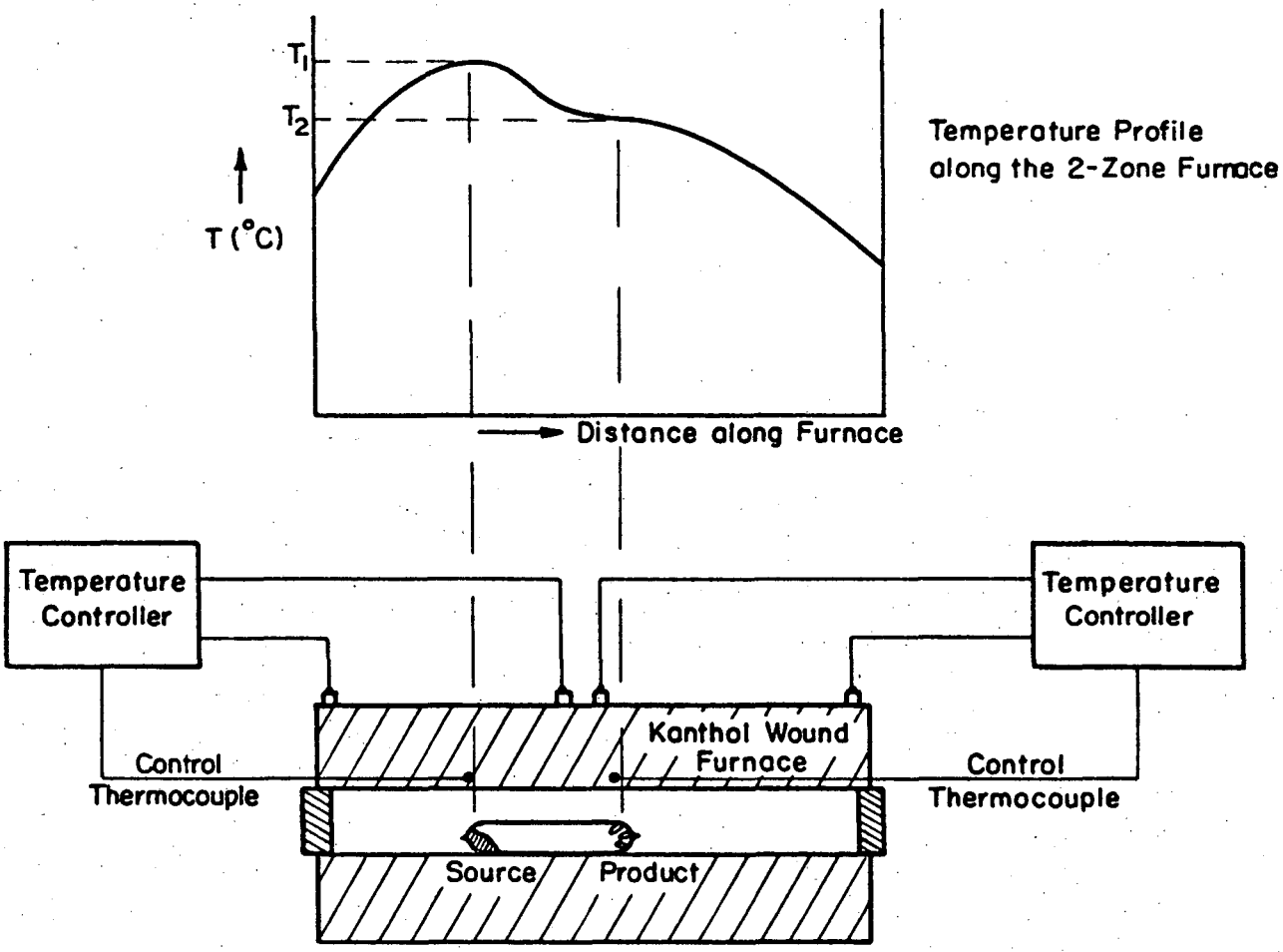
T1
T2
T (°C)
Temperature Profile
along the 2-Zone Furnace
Distance along Furnace
Temperature
Controller
Temperature
Controller
Kanthol Wound
Furnace
Control
Thermocouple
Control
Thermocouple
Source
Product
XBL7212-7339

Fig. 1

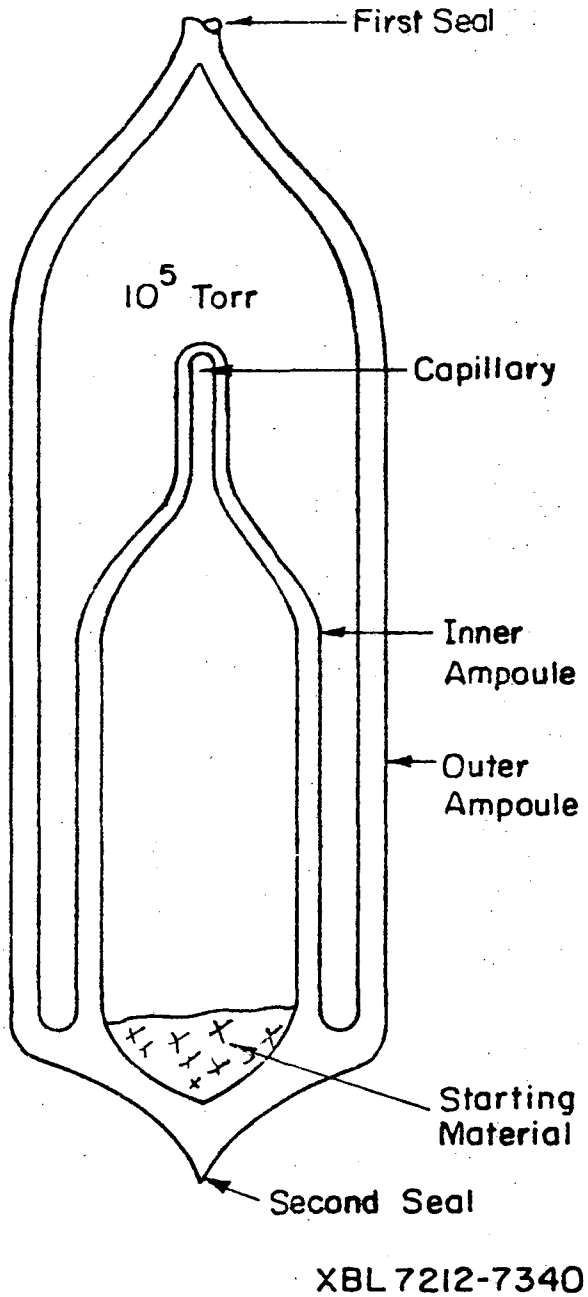
First Seal
10^5 Torr
Capillary
Inner Ampoule
Outer Ampoule
Starting Material
Second Seal
XBL 7212-7340

Fig. 2

II. CHEMICAL TRANSPORT IN A CLOSED SYSTEM

A. Introduction

The term chemical transport was put forward by Schafer et al.[1] to describe the fact that a chemical compound can be converted to a more volatile chemical intermediate at one temperature and then can be reobtained at a different temperature where the equilibrium favors the formation of the original compound. Thus for a reaction of the type

$$A_{(s)} + B_{(g)} \rightleftharpoons C_{(g)} + D_{(g)}$$

the ΔG_{rxn} would change with temperature according to

$$\frac{\partial}{\partial T} (\Delta G/T) = -\frac{\Delta H}{T^2}$$

where ΔH is the heat of reaction. Hence the different equilibrium constants at different temperatures will cause a concentration gradient to exist in the reaction vessel, in our case a closed, evacuated ampoule.

The chemical transport process can be divided into three parts:

i) Heterogeneous equilibrium at the source end, at a temperature, T_1.

ii) Transport of the gaseous species formed in i) to the other end of the ampoule at a temperature T_2.

iii) Heterogeneous equilibrium at this product end at T_2.

Schafer[1] outlines the various mechanisms by which transport can occur.

i) Molecular flow: This mechanism dominates at extremely low pressure, $P < 10^{-3}$ atm.

ii) Diffusion: This is the controlling transport process in the ranges of temperature and pressure used generally for chemical transport (e.g., $10^{-3} < P < 3$ atm, and for 400 to 1100°C.). When this process is generally the rate determining step, then reaction equilibrium is established between the solid substances and the transport species.

iii) Thermal convection: At pressures of $P > 3$ atm thermal convection has an important contribution to the chemical transport.

We will concentrate more on the diffusion process. If the reactions are carried out at the medium temperature range, diffusion is the slowest step only for the higher total pressures. As the pressure is lowered, diffusive transport increases until it ceases to be the slowest step. Then the calculated transport rate assuming diffusion to be rate controlling will be smaller than the actual rate at low pressures. One can in general, expect that the diffusion range will extend to lower pressures with increasing temperatures. It is also possible to expand the diffusion range by the choice of tube dimensions, especially by choosing a narrow diffusion path.[1]

The mass flux in a situation where there exist both concentration and thermal gradients is excellently treated by Bird, Stewart and Lightfoot.[2] The mass flux, j_i is

$$j_i = j_i^{(x)} + j_i^{(p)} + j_i^{(g)} + j_i^{(T)}$$

where

$j_i^{(x)}$ is the concentration or ordinary diffusion flux,

$j_i^{(p)}$ the pressure diffusion flux,

and

$j_i^{(g)}$, the forced diffusion, flux

$j_i^{(T)}$, the thermal diffusion flux.

For a closed system, $j_i^{(p)} = 0$ because of equal pressure throughout the ampoule. Also $j_i^{(g)} = 0$ because the only external force is gravity and that has an equal effect on all regions if the ampoule is horizontal or nearly so. Thus

$$j_i \cong j_k^{(x)} + j_i^{(T)}$$

where

$$j_i^{(T)} = - D_i^T \nabla \ell n T \quad .$$

The thermal diffusion coefficient D_1^T is known to be negligible compared to that for molecular diffusion. In our range of pressure, $10^{-3} < P < 3$ atm we are neglecting any thermal contribution to mass transport. Consequently the mass flux is simply,

$$j_i \cong j_k^{(x)}$$

where for multicomponent diffusion

$$j_i^{(x)} = \frac{c^2}{\rho RT} \sum_{j=1}^{n} M_i M_j D_{ij} \left[x_j \sum_{\substack{k=1 \\ k\neq j}}^{n} \left(\frac{\partial \bar{G}_j}{\partial x_k} \right)_{\substack{T,p,x_s \\ s\neq j,k}} \nabla x \right]$$

where c is the total molar concentration, ρ the gas density,

M is the Molecular weight

$\bar{G}_j$, the partial molal free enthalpy, and

D_{ij}, the multicomponent diffusion coefficient.

For $n > 2$, it can be shown that generally $D_{ij} \neq D_{ji}$.

For a high temperature and a low pressure system, we assume the vapor species to behave roughly like an ideal gas. Then the mass flux is simply

$$j_i = \frac{c^2}{\rho} \sum_{j=1}^{n} M_i M_j D_{ij} \nabla x_j . \qquad i=1, 2, \ldots n$$

For an n-component ideal-gas mixture there is a relation between D_{ij} (the diffusivity of the pair i-j in a multicomponent mixture) and $\hat{D}_{ij}$ (the diffusivity of the pair i-j in a binary mixture).[3] The D_{ij}'s are not convenient to use because they are concentration dependent. Besides $\hat{D}_{ij}$ has the added advantage that $\hat{D}_{ij} = \hat{D}_{ji}$ and is independent of the composition.

Curtis and Hirschfelder[3] converted the above equation to the form

$$\nabla x_i = \sum_{j=1}^{n} \frac{1}{c\hat{D}_{ij}} (x_i N_j - x_i N_i) ,$$

N_i = Molar flux of component i with respect to fixed coordinates.

The set of such equations is called the Stefan-Maxwell equations. They constitute the starting point of many multicomponent diffusion problems.

Although many researchers have applied the chemical transport process in a closed tube few have analyzed the diffusion process involved.

Schafer and his co-workers[4,5] developed an approximate theory relating the rate of transport to various macroscopic parameters: e.g. the relative amount of vapor solvent, temperature etc. In the reaction

$$iA_{(s,\ell)} + kB_{(g)} = jC_{(g)}$$

the solid substance A is transported from the region at temperature T_2 to where the temperature is T_1. If the number of moles of solid substance A is known, then the number of moles of solid substance A that has been transported can be obtained from the stoichiometry of the reaction:

$$n_A = \frac{i}{k} n_B = \frac{i}{j} n_C$$

If the reaction proceeds with a change in the number of moles ($k \neq j$), the requirement of an equal total pressure in the tube will give rise to a flow of the entire mass, along with the diffusion process. Then the number of moles of transported gas is

$$n_B = Dqt \frac{dc_B}{ds} \frac{k(C_B+C_C)}{j\ C_B+k\ C_C}$$

where C_i = concentration of species i; s = length of ampoule; q = cross section of the diffusion path; t = time. The third factor due to the flow is equal to 1 for k=j. Without an appreciable error this factor is set = 1. Converting concentrations to partial pressures, $P_{C(2)}-P_{C(1)} = \Delta P_C$, Schafer obtained

$$n_C = \frac{Dqt}{SRt} \Delta P_C \text{ (moles)}$$

and

$$n_A = \frac{i}{j} \cdot \frac{Dqt}{sRT} \cdot \Delta P_c \quad \text{(moles)} . \tag{1}$$

The diffusion coefficient D is expressed as a function of temperature with D_o measured at $\Sigma P_o = 1$ atm and $T_o = 273°K$:

$$D = D_o \frac{\Sigma P_o}{\Sigma P} \left(\frac{T}{T_o}\right)^{1.8} . \tag{2}$$

On combining Eqs. (1) and (2) we obtain the number of moles of A transported,

$$n_A = \frac{i}{j} \cdot \frac{\Delta P_c}{\Sigma P} \cdot \frac{D_o \Sigma P_o T^{0.8} qt}{T_o^{1.8} sR} .$$

For more than two gaseous components e.g.

$$iA_{(s)} + kB_{(g)} = jC_{(g)} + \ell D_{(g)} \tag{3}$$

we will have

$$P_C : P_D = j : \ell$$

and a stationery state of mass transport in the tube will require

$$D_B \cdot \frac{1}{k} \cdot \Delta P_B = D_C \cdot \frac{1}{j} \cdot \Delta P_c = D_D \cdot \frac{1}{\ell} \cdot \Delta P_D$$

where D_B, D_C and D_D are the diffusion coefficients for the gases B, C and D in the gas mixture. This consideration only holds for the condition that the reaction of Eq. 3 involves no change in the number of moles, i.e. $k = j + \ell$. When the transport reaction produces a change in the number

of moles, the flow of the mass in its entirety must be taken into account. Schafer acknowledges this but does not offer a solution to this problem. Schafer simplifies his estimate of the transport rate further by using approximate diffusion coefficients.[6]

Mandel and Lever in a series of papers treat the theoretical case with greater detail. Mandel[7] used the simple diffusion expression,

$$(\text{Flux})_i = (\text{Diffusivity})_i(\text{Area})(\text{Concentration Gradient})_i$$

This approximation, however, does not take into account the flow term caused by a difference between the moles generated and initial number of moles. Mandel's later paper[8], an apologia, seeks to justify the above approximation rather than to obtain the exact solution to the Stefan-Maxwell equations. Furthermore, the diffusion coefficients of the individual gaseous compounds are assumed to be those of a mixture rather than binary diffusion coefficients. The partial pressures of the different species in the tube are given by further approximations.

In Part (3) of his initial paper,[7] Mandel treats the effect of surface reaction rates on the product formation rate.

Subsequently, Lever[9] treats the problem of multiple reaction equilibria for vapor transport. Here, thermal diffusion is neglected and the flow is expressed very simply in terms of the diffusion coefficient and a simple parameter describing the overall gas composition, without reference to individual molecular species. Mandel[11] extends this to transport of several solids by using coupling parameters that can be determined from a (N-1) dimensional equation set where N is the

number of equilibria. In a later work Lever[10] also treats the problem of a single heterogeneous equilibrium and the transport of a solid therefrom.

Our approach to the problem of chemical transport differs from those above in that we take the Stefan-Maxwell equations as our basis, and do not approximate these or the actual concentrations of gaseous along the transport path. Using the stoichiometry of the reactions involved, the Stefan-Maxwell equations are solved assuming gas-solid reactions at ends of the transport path. We use binary diffusion coefficients because of the advantages outlined earlier, but assume the diffusivities are constant and have values corresponding to the mean temperature along the transport path.

Since we are interested in a rigorous statement and solution of the chemical transport process, we cannot approximate the diffusion equations as done by Schafer[1] and Mandel[7]. However, we do have to make the following assumptions.

1. The transport process occurs at steady state,
2. The total pressure in the tube is constant and independent of position. This constraint means that the total molar concentration is constant throughout the tube.
3. We neglect the change in partial molal volume of the gaseous species due to temperature changes.
4. Since the pressure is low (10^{-2} - 3 atm) and the temperatures are high (~700°-1000°C) the ideal gas assumption for the gaseous species is valid as an equation of state.

5. The chemical transport agent (in this case a halogen) introduced in the tube is of known quantity and is in the gaseous state at the temperatures in question.

The problem of simulating the transport conditions operating under diffusional control then reduces to the solving of the Stefan-Maxwell equations of motion of the gaseous species subject to the boundary conditions of the problem. These are

i) The heterogeneous equilibria at the two ends:

$$iA_{(s)} + kB_{(g)} \rightleftharpoons jC_{(g)} + \ell D_{(g)} \quad ,$$

where the equilibrium constants $K = P_C^j \, P_D^\ell \, P_B^{-k}$ are deduced from a free energy calculation (See App. 2).

ii) The conservation of the transport agent introduced into the closed tube.

The unknowns for a system of N gaseous species are the concentrations of (N-1) species and the mass flux of one species. From stoichiometry this flux is related to the flux of all other gaseous species. Hence we have N unknowns. The number of equations needed, N, in general consist of the transport agent conservation and the heterogeneous equilibria at the ends of the tube. For a simple transport problem involving binary chalcogenides, we have a 3 dimensional problem (ie. N=3), while for a ternary chalcogenide or spinel, N=4. Various degrees of refinement in the model are required by an increase in N to 5 or 6.

In the problem, the binary diffusivities of the various gaseous species are obtained as outlined in App. 3.

For a solution of the problem, we require to find i) the concentration of the various species as a function of position along the tube, and ii) the mass fluxes and hence the product rate of formation of the solid phase.

B. Chemical Transport of Group II-VI Compounds with Halogens Transport Agents

Single crystals of the divalent chalcogenides can be grown in the vapor phase by sublimation or by chemical transport with various transport agents, e.g. NH_4Cl, H_2, halogens etc. On sublimation of the compound, the gaseous species are the elements themselves while with H_2, the metal and the corresponding hydrogen chalcogenide gas are formed, e.g.

$$MX + H_2 \rightleftharpoons M(g) + H_2X \qquad (A)$$

where X is S, Se or Te and M is a divalent cation.

With free halogens as transport agents, the temperatures of transport are considerably reduced below those required for sublimation. If I_2 is added, the gaseous metal is bound in the iodide form, and the equilibrium is consequently shifted in favor of the gaseous participant in the reaction. The general reaction can be represented by

$$MX_{(s)} + I_{2(g)} \rightleftharpoons MI_{2(g)} + 0.5\ X_{2(g)} \qquad (B)$$

1. Diffusion Controlled Transport

The one-dimensional transport process is shown in Fig. 1. The directions of diffusion of the various gaseous species are also shown in the figure. We designate the gas phase species I_2, MI_2 and X_2 by the subscripts 1, 2 and 3 respectively.

The multicomponent (Stefan-Maxwell) diffusion equations are

$$\nabla x_i = \sum_{j=1}^{3} \frac{1}{c\hat{D}_{ij}} (x_i N_j - x_j N_i) \qquad i = 1, 2, 3. \tag{1}$$

Also, in the gas phase, for all z

$$\sum_{i-1}^{3} x_i(z) = 1 \tag{1a}$$

where

x_i is the mole fraction of the species i

N_i is the molar flux of the species i with respect to fixed coordinates,

c is the total molar concentration,

$\hat{D}_{ij}$ is the binary diffusion coefficient for the species pair i,j

and z is the distance along the ampoule

Because of the above constraint, only two of the set of equations (1) for the species MI_2, S_2 and I_2 are independent. These reduce to the form (see Appendix 1A) in terms of the product flux J

$$\nabla x_1 = a_1 x_1 + b_1 x_2 + d_1 \tag{1b}$$

$$\nabla x_2 = a_2 x_1 + b_2 x_2 + d_2 \tag{1c}$$

where

$$a_1 = \frac{J}{c}\left(\frac{1}{\hat{D}_{12}} - \frac{1}{2\hat{D}_{13}}\right) \qquad a_2 = \frac{J}{c}\left(\frac{1}{\hat{D}_{23}} - \frac{1}{\hat{D}_{21}}\right)$$

$$b_1 = \frac{J}{c}\left(\frac{1}{\hat{D}_{12}} - \frac{1}{\hat{D}_{13}}\right) \qquad b_2 = \frac{J}{c}\left(\frac{3}{2\hat{D}_{23}} - \frac{1}{\hat{D}_{21}}\right)$$

$$d_1 = \frac{J}{c\hat{D}_{13}} \qquad d_2 = -\frac{J}{c\hat{D}_{23}}$$

The integrated solutions for these equations are

$$x_1 = \frac{b_2d_1-b_1d_2}{a_2b_1-a_1b_2} + \lambda_1 e^{m_1 z} + \lambda_2 e^{m_2 z}$$

$$x_2 = \frac{a_1d_2-a_2d_1}{a_2b_1-a_1b_2} + \frac{a_2\lambda_1}{m_1-b_2} e^{m_1 z} + \frac{a_2\lambda_2}{m_2-b_2} e^{m_2 z} \quad \text{, and } x_3 = 1-x_1-x_2$$

where

$$m_1, m_2 = \frac{(a_1+b_2)}{2} \pm \frac{1}{2}\sqrt{(a_1+b_2)^2-4(a_1b_2-a_2b_1)}.$$

Generally, it has been found that the discriminent is negative and so we have imaginary roots. Then we can represent the solutions as

$$x_1 = \alpha_1 + e^{sz}(c_1 \cos rz + c_2 \sin rz)$$

and

$$x_2 = \alpha_2 + e^{sz}(c_3 \cos rz + c_4 \sin rz)$$

$$x_3 = 1 - x_1 - x_2$$

where r and s are given by

$$r = (m_1-m_2)/2i, \qquad s = (m_1+m_2)/2$$

$$c_1 = \lambda_1 + \lambda_2 \qquad c_2 = (\lambda_1 - \lambda_2)$$

$$c_3 = a_2\left[\frac{\lambda_1}{m_1-b_2} + \frac{\lambda_2}{m_2-b_2}\right] \qquad c_4 = ia_2\left[\frac{\lambda_1}{m_1-b_2} - \frac{\lambda_2}{m_2-b_2}\right]$$

$$\alpha_1 = \frac{b_2d_1-b_1d_2}{a_2b_1-a_1b_2} \quad \text{and} \quad \alpha_2 = \frac{a_1d_2-a_2d_1}{a_2b_1-a_1b_2}$$

To obtain a particular solution to the above general solutions for x_1, x_2 and x_3 we must know the values of the quantities λ_1, λ_2 and J (which is implicit in the constants a_1, b_1 $\cdots$ etc.). These three unknowns require three equations. These equations are

i) the heterogeneous equilibrium at the source end,

$$K_1 = K_{z=0} = \left.\frac{x_2 x_3^{1/2}}{x_1}\right|_{z=0} (cRT_1)^{1/2} \tag{2}$$

ii) the heterogeneous equilibrium at the product end

$$K_2 = K_{z=L} = \left.\frac{x_2 x_3^{1/2}}{x_1}\right|_{z=L} (cRT_2)^{1/2} \tag{3}$$

iii) and the overall iodine balance in the closed tube.

If ϵ is the concentration of I_2 initially fed to the system (moles/cm^3) and if A is the uniform cross section area of the tube, then

$$A\epsilon L = A_c \int_0^L (x_1+x_2)\,dz \tag{4}$$

This leads to the relation developed in App. 1A, Sec. II.

We also need to know the total concentration of all gaseous species in the tube, $\bar{c}$. This is obtained from the relation (see App. 1, Sec. II).

$$K_1 = \frac{\left(\frac{\bar{c}}{\epsilon} - 1\right)^{3/2}}{3 - \frac{2\bar{c}}{\epsilon}} \quad (4RT_1\epsilon)^{1/2} \tag{5}$$

Once $\bar{c}$ is calculated from Eq. 5, the system of three non-linear algebraic simultaneous equations, Eqs. 2, 3 and 4 can be solved for the unknowns λ_1, λ_2 and J.

These equations were solved on the CDC 6600 at the Lawrence Berkeley Laboratory, and on the CDC 6400 at the University of California Computer Center, Berkeley, California. Details of the computational method and the program are given in Appendix 4.

2. Results and Discussion

The computed results of the simulated transport problem are given in Tables (1-6). Using these we have plotted the product flux as a function of the iodine feed and the temperature gradient across the ampoule. It has been found in general that

i) For a given temperature gradient at the temperature in question, 1100°K, the product formation rate increases with the amount of iodine initially fed to the system. (Fig. 2, 4, 6)

ii) The product rate, for the same iodine feed, increases with the temperature gradient. (Figs. 3, 5, 7)

Results obtained for CdS, MnS and ZnS transport by I_2 bear out the above except for MnS where the product rate undergoes a weak maximum as a function of the iodine feed. This result could be connected to the fact that only in MnS were K_1 and K_2 less than unity. With increasing ΔT, this maximum shifts to the right (Fig. 4) corresponding to increased concentrations of the transport agent.

The concentrations of the various gaseous species as a function of position along the ampoule involve exponential and trigonometric function dependence.

$$x(I_2) = -2 + (c_1 \cos rz + c_2 \sin rz) \exp(sz)$$

$$x(MI_2) = 2 + (c_3 \cos rz + c_4 \sin rz) \exp(sz)$$

$$x(S_2) = 1 - x(I_2) - x(MI_2)$$

where x is concentration, z is distance along the ampoule and r, s, c_1, c_2, c_3 and c_4 are parameters found for a particular transport condition. The nonlinearity of the concentration profiles is indicated by r and

s. These quantities are, however, so minor as to effectually give a linear concentration gradient. As a general rule, the nonlinearity increases with both iodine feed and temperature gradient (Tables 2, 4, 6) except for a weak maximum observed for MnS (Table 4).

Better product formation rates were obtained for cases where K_1 and K_2 (the equilibrium constants at either end of the tube) were closer to unity. Thus, product rates were lower for CdS than for ZnS or MnS. One important factor in choosing the temperatures in the tube is that they have to be higher than the boiling points of the intermediate halides. If not, the solid or liquid halide formed would envelope the depositing chalcogenide and the reaction would stop. Therefore, for CdS, the temperatures were such that $K_{1,2}$ were very high and consequently the yield was low.

Kaldis[12] carried out the chemical transport of CdS with I_2. His experimental results are shown in Fig. 12. The comparison of product rates with a change in ΔT is interesting. The curve for CdS is linear for $\Delta T \geqslant 55°C$ and below this, there is a hump near the origin. Kaldis suggests that the heterogeneous rate reaction could be the rate determining step in this region. Above $\Delta T = 55°C$, the linear variation is similar to the curve we have obtained (Fig. 3) except that our curve is more nonlinear. Though we have not calculated the transport rate for ZnSe, the linear variation for this compound is similar to the variation for ZnS (Fig. 7).

In another experiment, he found that the chemical transport rate at $T = 1130°C$ decreases when the iodine is added to the ampoule concentration. Since the sublimation of CdS occurs rapidly at this temperature, the

transport process is actually a combination of sublimation and chemical transport by the halide. The experimental transport rates are approximately a factor of ten higher than those predicted by the above theory. The effect of thermal convection and sublimation transport or incorrect thermodynamic data could be the source of the difference.

The limitations on the accuracy of our results stem principally from errors in the thermodynamic data, and from errors in estimating diffusivity. Both of these are inevitable because of the exploratory applications to which chemical transport is applied. Data for many compounds in which we are interested has not yet been measured. In addition, some error accompanies the assumptions made:

1) In actuality, there is a great probability of multiple reaction equilibria but the reasonable assumption is that one gas-solid reaction predominates.

2) Sulfur is assumed present only in the form of S_2. This is true to a large extent because at high temperatures the polymers S_4, S_6, S_8 break down into S_2 and the equilibrium heavily favors S_2.

3) The dissociation of iodine, $I_2 \rightleftharpoons 2I$, was neglected. The species I would involve another diffusing species and also another term in the reaction equilibria. We have lumped the monatomic iodine with the diatomic molecule. Generally the concentration of I does not exceed a few % of I at typical transport temperatures.

4) The results which we have obtained do not take into account the sublimation reaction, which is assumed much slower than the chemical transport reaction considered.

The simulation of chemical transport of Group II-VI compounds has several incentives. In addition to comparing the suitability of different halogens and other compounds as transport agents, the solution method proposed allows a prediction of the product compound formation rate for diffusion controlled transport under different conditions of temperature, initial transport agent concentration and choice of transport agent. The method allows a prediction of the concentration profiles for various species along the transport path, can provide the total pressure in the transport tube, and can provide data for predicting the optimum conditions for crystal growth.

The actual production of crystals by chemical transport correlated with the predictions of this study are not considered here. Rather, it is assumed that i) a single transport reaction equilibrium applies and ii) diffusion is the rate determining step. If the actual experimental results are close to the ones we have predicted, it will tend to support these starting premises.

C. Chemical Transport of AB_2X_4 Compounds with Halogens as Transport Agents

By an analysis of the chemical transport process we hope to predict the yield of ternary chalcogenide crystals transported in a closed tube. Since diffusion in the gas phase rather than the gas-solid reactions is assumed to be rate controlling, no conclusion can be made on crystal size but rather the mass rate is calculated.

In order to set up transport equations we need to know first the chemical reactions involved in such a transport process. Here the actual transport reactions become important as are the gas phase species.

Wehmeier[13] proposed the following reactions for the transport of AB_2X_4 compounds with halogens.

$$AB_2X_{4(s)} + 4\ Y_{2(y)} \rightleftharpoons AY_{2(g)} + 2BY_{3(g)} + 2X_{2(g)} \quad (1)$$

$$AX_{(s)} + Y_{2(g)} \rightleftharpoons AY_{2(g)} + 0.5X_{2(g)} \quad (2)$$

$$B_2X_{3(s)} + 3Y_{2(g)} \rightleftharpoons 2BY_{3(g)} + 1.5X_{2(g)} \quad (3)$$

where X and Y are the chalcogen and transport agent respectively. Thus, if the separated binary chalcogenides are introduced as source compounds, the binary halides are formed at the source end. These then form the solid ternary at the product end.

Lutz et al.[14] when referring to the transport of Cr_2S_3 with I_2, postulate the formation of CrI_2. This additional gas phase species is important, considering the fact that many AB_2X_4 compounds contain chromium. On the other hand, Nitsche et al.[15] propose the following reactions.

When the starting material is a mixture of powdered AS and B_2S_3, and I_2 as the transport agent , then the transport reactions are

$$AS_{(s)} + I_{2(g)} = AI_{2(g)} + \frac{1}{2} S_{2(g)} \quad (4)$$

$$B_2S_{3(s)} + 3I_{2(g)} \rightarrow 2BI_{3(g)} + \frac{3}{2} S_2 \quad (5)$$

$$B_2S_{3(s)} + BI_{3(g)} = 3BI_{(g)} + \frac{3}{2} S_{2(g)} \quad (6)$$

The further postulation is that when the binary sulfides are reformed in the cooler zone of the ampoule by displacement of the equilibriums of Reactions (4) and (6) to the left they react to form the ternary compound.

Thus far, we have the formation of the mono-, bi- and trihalides in the gas phase. Nelson and Sharpe[16] have probed the stabilities and interrelation of the different halides for the first transition series. But, in the absence of conclusive tests, we are not sure of the species present in the vapor phase. Pinch and Ekstrom[17] divided chromium compounds into two groups. The first group contained spinels with high-vapor-pressure metals (e.g. Zn, Cd, Hg) as divalent cations. For this group, divalent cations would be transported as monatomic vapor,

$$ACr_2X_{4(s)} \rightleftharpoons A_{(g)} + \frac{1}{2} X_{2(g)} + Cr_2X_{3(s)}. \quad (7)$$

The Cr ions would be transported as a tri-halide,

$$3Cl_{2(g)} + Cr_2X_{3(s)} \rightleftharpoons 2CrCl_{3(g)} + \frac{3}{2}X_{2(g)} \quad (8)$$

$$Cr_2X_{3(s)} + mX_{2(g)} \rightleftharpoons CrX_{n(g)} \quad (9)$$

The reaction of Eq. (7) is the decomposition reaction for the spinel. However, if additional elemental metal were suppled in the starting material, it would be transported also in elemental form. The above authors also put forward the formation of ACl_2 in the vapor phase,

$$ACr_2X_{4(s)} + 4\ Cl_{2(g)} \rightleftharpoons ACl_{2(g)} + 2CrCl_{3(g)} + 2X_{2(g)}. \qquad (10)$$

The second group of spinels proposed by Pinch and Ekstrom contains divalent transition metal ions (Mn, Fe, Co) or a mixture of mono- and trivalent ions ($Cu_{1/2}Ga_{1/2}$, $Ag_{1/2}In_{1/2}$, or $Cu_{1/2}Fe_{1/2}$).

Probable reactions are then

$$M^{2+}Cr_2S_{4(s)} + 4Cl_{2(g)} \rightleftharpoons M^{2+}Cl_{2(g)} + 2CrCl_{3(g)} + 2S_{2(g)} \qquad (11)$$

$$M^{1+}_{1/2}\ M^{3+}_{1/2}\ Cr_2X_{4(s)} + 4Cl_{2(g)} \rightleftharpoons \tfrac{1}{2}M^{1+}Cl_{(g)} + \tfrac{1}{2}M^{3+}Cl_{3(g)} + 2CrCl_{3(g)} + 2S_{2(g)}. \qquad (12)$$

As seen from Table II in Part I for growth of spinels, iodine is a favored transport agent. This is because generally the iodine reaction has the lowest ΔG_{rxn} value and thus the most favored equilibrium position required for transport. However, if I_2 is used above 600 °C, some dissociation into elemental iodine will occur. This dissociation will give rise to another gas species in the tube.

Therefore, without further information on definite chemical species participating in the ternary transport reactions we assumed the following simplest reactions in order to simulate the conditions in the ampoule. We set up transport equations which would predict the mole fractions of gas species in the ampoule and thus predict the rate of product formation in the ampoule,

$$AX_{(s)} + I_{2(g)} \rightleftharpoons AI_{2(g)} + \frac{1}{2} X_{2(g)} \quad (13)$$

$$B_2X_{3(s)} + 3I_{2(g)} \rightleftharpoons 2BI_3 + \frac{3}{2} X_{2(g)} \quad (14)$$

$$AI_{2(g)} + 2BI_{3(g)} + 2X_{2(g)} \rightleftharpoons AB_2X_{4(s)} + 4I_{2(g)} \quad (15)$$

Here I_2 can represent any halogen while AB_2X_4 is the general form of a ternary compound.

The closed vessel geometry and direction of diffusing species are shown schematically in Fig. 11. At one end of the closed vessel, Reaction Eqs. (13) and (14) apply to stoichiometric mixtures of binary chalcogenides AX and B_2X_3 held at a temperature T_1. The halides that are formed after reaction with the halogen diffuse to the other end of the ampoule where Reaction Eq. (15) applies at temperature T_2. At this end, the gaseous species react to form the solid spinel. The free energy conditions should be such that the binary chalcogenides are not formed again at the product end. To ensure this Wehmeier [13] has proposed the following ΔG functions

$$\Delta G_{(13)} = \Delta G^{o}_{(13)} + 0.3\ \Delta G^{o}_{(15)} + RT \ln \frac{p^{0.2}_{(15)}\ (I_2)}{2^{0.7}}$$

and

$$\Delta G_{(14)} = \Delta G^{o}_{(14)} + 0.7\ \Delta G^{o}_{(15)} + RT \ln \frac{2^{0.7}}{p^{0.2}_{(15)}\ (I_2)}$$

For a successful reaction, the free energy of the binary transport reactions (13) and (14) postulated above are negative. If either binary reaction has a positive value of ΔG, decomposition of the ternary phase will occur. The quantities needed in the above equations are the partial pressure of the transport agent $p_{(15)}(I_2)$ and the standard free energies

for Eqs.(15), (14) and (13). One stumbling block here is the difficulty in estimating the free energy of formation of the ternary compounds. Even the estimation from their partition functions is difficult because of a dearth of spectroscopic data. Hence we have to approximate the chemical equilibrium at the product end.

The three different processes occurring in the ampoule are then a) formation of AI_2, BI_3, etc. at T_1, b) diffusion of these species to the product zone and c) formation of solid AB_2X_4 at T_2. Of these three steps, we assume that the rate limiting is b) i.e., the diffusion process. Steps a) and c) are at equilibrium.

1. Diffusion Controlled Transport

The multicomponent diffusion equations in the gas phase are[2]

$$\nabla x_i = \sum_{j=1}^{n} \frac{1}{c\hat{D}_{ij}} (x_i N_j - x_j N_i).$$

In our case i = 4.

Let us represent the different substances I_2, AI_2, BI_3 and X_2 by the subscripts 1, 2, 3 and 4 respectively.

The diffusion equations obtained are then

$$\nabla x_1 = \frac{1}{c}\left[\frac{1}{\hat{D}_{12}} (x_1N_2-x_2N_1) + \frac{1}{\hat{D}_{13}} (x_1N_3-x_3N_1) + \frac{1}{\hat{D}_{14}} (x_1N_4-x_4N_1)\right]$$

$$\nabla x_2 = \frac{1}{c}\left[\frac{1}{\hat{D}_{21}} (x_2N_1-x_1N_2) + \frac{1}{\hat{D}_{23}} (x_2N_3-x_3N_2) + \frac{1}{\hat{D}_{24}} (x_2N_4-x_4N_2)\right]$$

$$\nabla x_3 = \frac{1}{c}\left[\frac{1}{\hat{D}_{31}} (x_3N_1-x_1N_3) + \frac{1}{\hat{D}_{32}} (x_3N_2-x_2N_3) + \frac{1}{\hat{D}_{34}} (x_3N_4-x_4N_3)\right]$$

where $x_4 = 1-x_1-x_2-x_3$

c, the total concentration, is obtained by using conversion criteria at the source end (see App. 1B, Sec. II).

Solving these equations (see App. 1B, Sec. I) we obtain

$$x_1 = \lambda_1 + z(a_1\lambda_1 + b_2\lambda_2 + c_1\lambda_3) + \frac{z^2}{2}(a_1'\lambda_1 + b_1'\lambda_2 + c_1'\lambda_3) - (\mathring{a}_1 d_1 + \mathring{b}_1 d_2 + \mathring{c}_1 d_3)$$

$$x_2 = \lambda_2 + z(a_2\lambda_1 + b_2\lambda_2 + c_2\lambda_3) + \frac{z^2}{2}(a_2'\lambda_1 + b_2'\lambda_2 + c_2'\lambda_3) - (\mathring{a}_2 d_1 + \mathring{b}_2 d_2 + \mathring{c}_2 d_3)$$

$$x_3 = \lambda_3 + z(a_3\lambda_1 + b_3\lambda_2 + c_3\lambda_3) + \frac{z^2}{2}(a_3'\lambda_1 + b_3'\lambda_2 + c_3'\lambda_3) - (\mathring{a}_3 d_1 + \mathring{b}_3 d_2 + \mathring{c}_3 d_3)$$

$$x_4 = 1 - \sum_{i=1}^{3} x_i \ .$$

Here a, b, c etc. are as defined in Appendix 1B, while λ_1, λ_2 and λ_3 are constants. These three constants (λ_1, λ_2 and λ_3) together with J, the product flux, constitute the four unknown quantities. We need four boundary or initial conditions to solve for these unknowns. The four boundary conditions are then

1) The equilibrium constant K_{1A} for Eq. (13) at the source end at T_1,

$$K_{1A} = \frac{(P_{AI_2})(P_{x_2}^{1/2})}{(P_{I_2})} = \left.\frac{x_2 x_4^{1/2}}{x_1}\right|_{z=0} (cRT_1)^{1/2}$$

ii) The equilibrium constant K_{1B} for Eq. (14) at the source end at T_1,

$$K_{1B} = \frac{(P_{BI_3})^2 (P_{x_2})^{3/2}}{(P_{I_2})^3} = \left.\frac{x_3^2 x_4^{3/2}}{x_1^3}\right|_{z=0} (cRT_1)^{1/2}$$

iii) The equilibrium constant K_2 for Eq. (15) at the product end at T_2,

$$K_2 = \frac{4(P_{I_2})^4}{(P_{AI_2})(P_{BI_3})^2 (P_{S_2})^2} = \left.\frac{4x_1^4}{x_2 x_3^2 x_2^2}\right|_{z=L} (cRT_2)^{-1}$$

iv) Iodine fed in the system is equal to the iodine present in different compounds containing iodine I_2, AI_2, BI_3. If I_o is the initial iodine concentration (moles/cm^3)

$$I_o = A\int_0^L c(x_1 + x_2 + \tfrac{3}{2}x_3)\,dz.$$

This relation is evaluated in App. 1B, Sec. II

v) Conversion equilibria at the source end. This is given in App. 1B, Sec. II.

2. Results and Discussions

The transport problem for the AB_2X_4 compounds was reduced to a four dimensional set of nonlinear algebraic equations in four real variables. We know that the mole fraction of any species has to lie between 0 and 1. This constraint, when applied at $z = 0$, led to the placing of limits on the value of three of our variables. These were $4 \leq \lambda_1 \leq 5$, $-1 \leq \lambda_2 \leq 0$ and $-2 \leq \lambda_3 \leq -1$. In addition we must have $J \geq 0$ since the product flux is always positive. Because the equation set was nonlinear, however, only an approximate solution could be found for any given set of conditions since convergence was slow and not always towards a solution within bounds. In general, we could not obtain a satisfactory solution to this problem.

After the initial variable values were set within their respective ranges, the method of computation was the unconstrained minimization technique using the Newton Raphson method with internally approximated gradients. This method was generally unsuccessful. Davidon's method of variable metric miminization also failed to produce a convergence within the required ranges. One reason for the failure to converge to a solution could be the lack of accurate data. Thermodynamic data on Eq. 15 was scarce and for the severe limiting ranges that we imposed on our variables, any inaccuracy could be significant. In general the available methods work best when the variable magnitudes are comparable. In our problem, however, the product flux J differed from the mole fractions x_i by many orders of magnitude.

Table 1. Cadmium sulfide transport by iodine. Product rates of formation for various transport condition.

Serial No.	Source Temp, T_1 (°K)	Product Temp, T_2 (°K)	Iodine Feed (moles/cc)$\times 10^6$	Pressure in ampoule (atm.)	Conversion in reaction at source	Total concn. in ampoule (moles/cc)$\times 10^6$	Product Rate (Gm/sq.cm/hr)$\times 10^3$
I (1)	1125	1100	.100	.0137	.9933	.1497	.04263
2			.200	.0273	.9906	.2991	.05985
3	$K_{1125} = 10.04$	$K_{1100} = 8.92$	.500	.0681	.9852	.7463	.09330
4			1.000	.1360	.9793	1.490	.1299
5			2.000	.2712	.9710	2.971	.1797
6			5.000	.6744	.9553	7.388	.2722
7			10.000	1.341	.9385	14.69	.3675
8			20.000	2.662	.9161	29.16	.4879
II (1)	1150	1100	.100	.0138	.9939	.1497	.0792
2	$K_{1150} = 11.21$	$K_{1100} = 8.92$	.200	.0276	.9914	.2991	.1113
3			.500	.0689	.9866	.7466	.1736
4			1.000	.1376	.9812	1.491	.2418
5			2.000	.2744	.9737	2.974	.3349
6			5.000	.6827	.9593	7.398	.5084
7			10.000	1.358	.9438	14.72	.6877
8			20.000	2.698	.9232	29.23	.9157

Table 1. (Continued)

Serial No.	Source Temp, T_1 (°K)	Product Temp, T_2 (°K)	Iodine Feed (moles/cc)×10^6	Pressure in ampoule (atm.)	Conversion in reaction at source	Total concn. in ampoule (moles/cc)×10^6	Product Rate (Gm/sq.cm/hr)×10^3
III (1)	1200	1100	.100	.0141	.9949	.1497	.1385
2	$K_{1200} = 13.70$	$K_{1100} = 8.92$	.200	.0282	.9928	.2993	.1946
3			.500	.0704	.9887	.7472	.3040
4			1.000	.1407	.9842	1.492	.4240
5			2.000	.2807	.9779	2.978	.5881
6			5.000	.6989	.9656	7.414	.8957
7			10.000	1.392	.9524	14.76	1.216
8			20.000	2.766	.9346	29.35	1.626

Table 2. CdS transport by Iodine. Parameters for concentration profiles along the closed ampoule.

Serial No.	Source Temp, T_1 (°K)	Product Temp, T_2 (°K)	Iodine Feed (moles/cc)×10^6	R	S	C_1	C_2	C_3	C_4
I (1)	1125	1100	.100	.00001	.00003	2.00448	-.8302	-1.3364	-.1697
2	$K_{1125} = 10.04$	$K_{1100} = 8.92$	.200	.00002	.00004	2.0063	-.8310	-1.3376	-.1699
3			.500	.00003	.00007	2.0099	-.8326	-1.3400	-.1701
4			1.000	.00004	.00009	2.0139	-.8344	-1.3427	-.1704
5			2.000	.00005	.00013	2.0195	-.8368	-1.3465	-.1708
6			5.000	.00008	.00019	2.0302	-.8415	-1.3437	-.1716
7			10.000	.00011	.00026	2.0419	-.8466	-1.3616	-.1724
8			20.000	.00015	.00035	2.0576	-.8535	-1.3721	-.1735
II (1)	1150	1100	.100	.00002	.00006	2.0041	-.8301	-1.3361	-.1696
2	$K_{1150} = 11.21$	$K_{1100} = 8.92$	.200	.00003	.00008	2.0057	-.8309	-1.3372	-.1697
3			.500	.00005	.00012	2.0090	-.8324	-1.3395	-.1699
4			1.000	.00007	.00017	2.0126	-.8341	-1.3420	-.1701
5			2.000	.00010	.00024	2.0177	-.8365	-1.3454	-.1704
6			5.000	.00015	.00036	2.0275	-.8411	-1.3521	-.1710
7			10.000	.00020	.00048	2.0382	-.8460	-1.3594	-.1716
8			20.000	.00027	.00064	2.0526	-.8526	-1.3692	-.1725

Table 2. (Continued)

Serial No.	Source Temp, T_1 (°K)	Product Temp, T_2 (°K)	Iodine Feed (moles/cc)$\times 10^6$	R	S	C_1	C_2	C_3	C_4
III (1)	1200	1100	.100	.00004	.00010	2.0034	-.8300	-1.3357	-.1695
2			.200	.00006	.00013	2.0048	-.8308	-1.3367	-.1695
3	$K_{1200} = 13.70$	$K_{1100} = 8.92$	.500	.00009	.00021	2.0075	-.8322	-1.3386	-.1696
4			1.000	.00012	.00029	2.0106	-.8338	-1.3408	-.1697
5			2.000	.00017	.00041	2.0149	-.8360	-1.3438	-.1698
6			5.000	.00026	.00062	2.0232	-.8403	-1.3496	-.1700
7			10.000	.00035	.00084	2.0322	-.8450	-1.3559	-.1703
8			20.000	.00047	.00112	2.0446	-.8512	-1.3645	-.1707

Table 3. MnS transport by Iodine. Product rates of formation for various transport conditions.

Serial No.	Source Temp, T_1 (°K)	Product Temp, T_2 (°K)	Iodine Feed (moles/cc)$\times 10^6$	Pressure in ampoule (atm.)	Conversion in reaction at source	Total concn. in ampoule (moles/cc)$\times 10^6$	Product Rate (Gm/sq.cm/hr)$\times 10^3$
I (1)	1125	1100	.100	.0128	.8009	.1400	1.620
2			.200	.0251	.7466	.2747	1.893
3	$K_{1125} = .2445$	$K_{1100} = .1851$	.500	.0608	.6639	.6660	2.182
4			1.000	.1185	.5959	1.298	2.313
5			2.000	.2306	.5260	2.526	2.353
6			5.000	.5557	.4355	6.089	2.269
7			10.000	1.082	.3713	11.86	2.123
8			20.000	2.111	.3128	23.13	1.929
II (1)	1150	1100	.100	.0131	.8358	.1418	92.99*
2			.200	.0257	.7876	.2788	3.564
3	$K_{1150} = .3197$	$K_{1100} = .1851$	.500	.0626	.7116	.6779	4.184
4			1.000	.1221	.6467	1.323	4.496
5			2.000	.2379	.5779	2.578	4.633
6			5.000	.5735	.4857	6.214	4.537
7			10.000	1.116	.4185	12.09	4.286
8			20.000	2.174	.3556	23.56	3.928

Table 3. (Continued)

Serial No.	Source Temp, T_1 (°K)	Product Temp, T_2 (°K)	Iodine Feed (moles/cc)×10^6	Pressure in ampoule (atm.)	Conversion in reaction at source	Total concn. in ampoule (moles/cc)×10^6	Product Rate (Gm/sq.cm/hr)×10^3
III (1)	1200	1100	.100	.0136	.8893	.1445	—*
2			.200	.0269	.8530	.2853	—*
3	$K_{1200} = .5317$	$K_{1100} = .1851$	.500	.0658	.7920	.6980	7.592
4			1.000	.1290	.7363	1.368	8.361
5			2.000	.2520	.6737	2.674	8.826
6			5.000	.6089	.5838	6.459	8.909
7			10.000	1.185	.5139	12.57	8.592
8			20.000	2.305	.4453	24.45	8.019

* = bad convergence.

Table 4. MnS transport by Iodine. Parameters for concentration profiles along the closed ampoule.

Serial No.	Source Temp, T_1 (°K)	Product Temp, T_2 (°K)	Iodine Feed (moles/cc)×10^6	R	S	C_1	C_2	C_3	C_4
I. (1)	1125	1100	.100	.00074	.00188	2.1422	-1.0193	-1.4306	-.1113
2	K_{1125} = .2445	K_{1100} = .1851	.200	.00087	.00220	2.1846	-1.0408	-1.4593	-.1127
3			.500	.00100	.00253	2.2523	-1.0746	-1.5050	-.1155
4			1.000	.00106	.00268	2.3113	-1.1034	-1.5447	-.1181
5			2.000	.00108	.00273	2.3753	-1.1341	-1.5875	-.1213
6			5.00	.00104	.002632	2.4636	-1.1758	-1.6463	-.1260
7			10.000	.00097	.00246	2.5302	-1.2068	-1.6906	-.1299
8			20.000	.00089	.00224	2.5943	-1.2362	-1.7330	-.1338
II (1)	1150	1100	.100	-	-	-	-	-	-*
2			.200	.00162	.00410	2.1524	-1.0334	-1.4402	-.1069
3	K_{1150} = .3197	K_{1100} = .1851	.500	.00190	.00481	2.2127	-1.0653	-1.4814	-.1084
4			1.000	.00204	.00517	2.2669	-1.0929	-1.5182	-.1103
5			2.000	.00211	.00533	2.3274	-1.1227	-1.5589	-.1129
6			5.000	.00206	.00522	2.4137	-1.1637	-1.6165	-.1173
7			10.000	.00195	.00493	2.4808	-1.1948	-1.6611	-.1213
8			20.000	.00179	.00452	2.5470	-1.2247	-1.7048	-.1256

Table 4. (Continued)

Serial No.	Source Temp, T_1 (°K)	Product Temp, T_2 (°K)	Iodine Feed (moles/cc)×10^6	R	S	C_1	C_2	C_3	C_4
III (1)	1200	1100	.100	-	-	-	-	-	-*
2			.200	-	-	-	-	-	-*
3	$K_{1200} = 0.5317$	$K_{1100} = 0.1851$	.500	.00339	.00858	2.1489	-1.0488	-1.4430	-.0978
4			1.000	.00373	.00945	2.1926	-1.0733	-1.4733	-.0981
5			2.000	.00394	.00998	2.2440	-1.1003	-1.5084	-.0995
6			5.000	.00398	.01007	2.3220	-1.1388	-1.5609	-.1028
7			10.000	.00384	.00971	2.3865	-1.1690	-1.6038	-.1064
8			20.000	.00358	.00906	2.4533	-1.1991	-1.6479	-.1108

* = bad convergence.

Table 5. ZnS transport by Iodine. Product rates of fromation for various transport conditions.

Serial No.	Source Temp, T_1 (°K)	Product Temp, T_2 (°K)	Iodine Feed (moles/cc)$\times 10^6$	Pressure in ampoule (atm.)	Conversion in reaction at source	Total concn. in ampoule (moles/cc)$\times 10^6$	Product Rate (Gm/sq.cm/hr)$\times 10^3$
I. (1)	1125	1100	.100	.0135	.9676	.1484	.2384
2			.200	.0270	.9550	.2955	.3255
3	$K_{1125} = 1.994$	$K_{1100} = 1.662$	.500	.0669	.9315	.7329	.4813
4			1.000	.1327	.9070	1.453	.6337
5			2.000	.2624	.8753	2.875	.8150
6			5.000	.6437	.8209	7.052	1.087
7			10.000	1.264	.7699	13.85	1.297
8			20.000	2.475	.7111	27.11	1.488
II (1)	1150	1100	.100	.0137	.9722	.1486	.4351
2			.200	.0273	.9613	.2961	.5956
3	$K_{1150} = 2.369$	$K_{1100} = 1.662$	.500	.0679	.9408	.7352	.8848
4			1.000	.1347	.9192	1.460	1.170
5			2.000	.2668	.8909	2.891	1.514
6			5.000	.6556	.8417	7.104	2.037
7			10.000	1.289	.7946	13.97	2.452
8			20.000	2.528	.7393	27.39	2.838

Table 5. (Continued)

Serial No.	Source Temp, T_1 (°K)	Product Temp, T_2 (°K)	Iodine Feed (moles/cc)×10^6	Pressure in ampoule (atm.)	Conversion in reaction at source	Total concn. in ampoule (moles/cc)×10^6	Product Rate (Gm/sq.cm/hr)×10^3
III (1)	1200	1100	.100	.0140	.9791	.1490	.7367
2			.200	.0280	.9708	.2971	1.012
3			.500	.0696	.9549	.7387	1.514
4	$K_{1200} = 3.248$	$K_{1100} = 1.662$	1.000	.1385	.9379	1.469	2.017
5			2.000	.2748	.9154	2.915	2.633
6			5.000	.6775	.8750	7.187	3.597
7			10.000	1.336	.8351	14.18	4.387
8			20.000	2.627	.7868	27.87	5.155

Table 6. ZnS transport by Iodine. Parameters for concentration profiles along the closed ampoule.

Serial No.	Source Temp, T_1 (°K)	Product Temp, T_2 (°K)	Iodine Feed (moles/cc)$\times 10^6$	R	S	C_1	C_2	C_3	C_4
I (1)	1125	1100	.100	.00009	.00023	2.0219	-.8651	-1.3482	-.1563
2	$K_{1125} = 1.994$	$K_{1100} = 1.662$	.200	.00013	.00032	2.0304	-.8692	-1.3541	-.1568
3			.500	.00019	.00047	2.0467	-.8768	-1.3651	-.1577
4			1.000	.00025	.00062	2.0640	-.8849	-1.3769	-.1587
5			2.000	.00032	.00080	2.0868	-.8954	-1.3923	-.1600
6			5.000	.00042	.00106	2.1270	-.9139	-1.4195	-.1624
7			10.000	.00050	.00127	2.1662	-.9316	-1.4459	-.1649
8			20.000	.00058	.00146	2.2131	-.9527	-1.4775	-.1680
II (1)	1150	1100	.100	.00017	.00042	2.0187	-.8646	-1.3464	-.1556
2	$K_{1150} = 2.369$	$K_{1100} = 1.662$	.200	.00023	.00058	2.0261	-.8684	-1.3515	-.1558
3			.500	.00034	.00086	2.0402	-.8757	-1.3613	-.1563
4			1.000	.00045	.00114	2.0554	-.8834	-1.3718	-.1568
5			2.000	.00058	.00147	2.0755	-.8935	-1.3856	-.1575
6			5.000	.00079	.00198	2.1114	-.9112	-1.4103	-.1591
7			10.000	.00095	.00238	2.1470	-.9283	-1.4346	-.1608
8			20.000	.00109	.00276	2.1903	-.9488	-1.4641	-.1632

Table 6. (Continued)

Serial No.	Source Temp, T_1 (°K)	Product Temp, T_2 (°K)	Iodine Feed (moles/cc)×10^6	R	S	C_1	C_2	C_3	C_4
III (1)	1200	1100	.100	.00028	.00070	2.0141	-.8638	-1.3436	-.1546
2			.200	.00038	.00097	2.0197	-.8673	-1.3477	-.1545
3	$K_{1200} = 3.248$	$K_{1100} = 1.662$	.500	.00057	.00144	2.0305	-.8740	-1.3556	-.1542
4			1.000	.00076	.00192	2.0422	-.8811	-1.3641	-.1540
5			2.000	.00100	.00251	2.0580	-.8904	-1.3754	-.1538
6			5.000	.00136	.00343	2.0870	-.9068	-1.3959	-.1539
7			10.000	.00166	.00419	2.1163	-.9227	-1.4165	-.1544
8			20.000	.00195	.00492	2.1530	-.9418	-1.4420	-.1554

Table 7. The parachors of elements[29]

The parachors of elements commonly encountered in chemical transport reactions are tabulated below in alphabetical order. Values in brackets are estimates which may be in error by ± 10 units. Those marked by an asterisk are based on limited data and may be in error by ± 3 units. Otherwise the error is ± 1 unit.

Element	Symbol	[P]	Element	Symbol	[P]
Aluminum	Al	38.6*	Lead	Pb	76.2*
Antimony	Sb	66.0	Lithium	Li	(50)
Argon	A	54.0	Mercury	Hg	69.0
Arsenic	As	50.1	Molybdenum	Mo	(80)
Barium	Ba	(106)	Neon	Ne	25.0
Beryllium	Be	37.8*	Nickel	Ni	(50)
Bismuth	Bi	80*	Nitrogen	N	12.5
Boron	B	16.4	Osmium	Os	80.4*
Bromine	Br	68.0	Oxygen	O	20.0
Cadmium	Cd	(70)	Phosphorus	P	37.7
Calcium	Ca	(68)	Rubidium	Rb	(130)
Carbon	C	4.8	Selenium	Se	62.5
Cesium	Cs	(150)	Silicon	Si	25.0
Chlorine	Cl	54.3	Silver	Ag	63*
Chromium	Cr	54.0*	Sodium	Na	(80)
Copper	Cu	(46)	Sulphur	S	48.2
Fluorine	F	25.7	Thallium	Tl	64*
Gallium	Ga	50*	Tin	Sn	57.9
Gold	Au	61*	Titanium	Ti	45.3*
Helium	He	20.5	Tungsten	W	(90)
Hydrogen	H	17.1	Zinc	Zn	50.7*
Iodine	I	91.0			
Indium	In	(69)			
Iron	Fe	(52)			
Manganese	Mn	(54)			

Table 8. Critical properties of metal halides

Number	Compound	Σ[P]	Boiling Point (°K)	T_c (°K)	P_c (atm)
1	CdI_2	252	1069	1640	35.2
2	MnI_2	236	1100	1701	37.1
3	ZnI_2	232.7	1000	1549	37.5
4	CrI_2	236	1100	1701	37.1
5	CrI_3	327	--	--	28.8
6	InI_3	342	773	1140	27.8
7	GaI_3	323	622	924	29.1
8	GdI_3	353	1610	2365	27.1
9	AlI_3	311.6	695	1037	29.9
10	FeI_2	234	1100	1703	37.4
11	FeI_3	325	--	--	28.9
12	InI_2	251	1000	1535	35.4

BIBLIOGRAPHY

1. H. Schafer, Chemical Transport Reactions (Academic Press, New York and London, 1964).

2. R. B. Bird, W. E. Stewart and E. N. Lightfoot, Transport Phenomenon (John Wiley & Sons, Inc., New York, London and Sydney, 1966) Ch. 16-18).

3. C. F. Curtiss and J. O. Hirschfelder, J. Chem. Phys. 17, 550-5 (1949).

4. H. Schafer et al., Z. Anorg. Chem. 286, 27 (1956).

5. H. Schafer, et al., Z. Anorg. Chem. 286, 42 (1956).

6. R. Nitsche, H. U. Bolsterli and M. Lichtensteiger, J. Phys. Chem. Solids 21, 199 (1961).

7. G. Mandel, J. Phys. Chem. Solids 23, 587-98 (1962).

8. R. F. Lever and G. Mandel, J. Phys. Chem. Solids 23, 599-600 (1962).

9. R. F. Lever, J. Chem. Physics 37 (5), 1078-81 (1962).

10. R. F. Lever, J. Chem. Physics 37 (6), 1174-6 (1962).

11. G. Mandel, J. Chem. Physics 37 (6), 1177-80 (1962).

12. E. Kaldis, J. Crystal Growth 5 376-90 (1969).

13. F. H. Wehmeier, J. Crystal Growth 6, 341-5 (1970).

14. H. D. Lutz, et al., Mon. Fur Chemie 101, 519-24 (1970).

15. B. J. Curtis, F. P. Emmenegger and R. Nitsche, RCA Rev. 31, 647-61 (1970).

16. P. G. Nelson and A. G. Sharpe, Inorg. Phys. Theor., J. Chem. Soc. (A), 1966, p. 501-11.

17. H. L. Pinch and L. Ekstrom, RCA Rev. 31, 692-701 (1970).

18. Laurence L. Quill, Ed., Contributing authors, Leo Brewer, L. A. Bromley et al., The Chemistry and Metallurgy of Miscellaneous Materials: Thermodynamics (McGraw-Hill, 1950).

19. L. Brewer, Report CC-672, May 15, 1945.

20. K. K. Kelley, U. S. Bur. Mines Bull. 383 (1935).

21. R. Colin and J. Drowart, Trans. Faraday Soc. 64(10), 2611-21 (1968).

22. Kenneth A. Kobe and R. Emerson Lynn, Jr. , Chem. Rev. 52, 117 (1953).

23. Meissner and Redding, Ind. Eng. Chem. 34, 521 (1942).

24. Samuel Sugden, The Parachor and Valency (George Routledge and Sons, London, 1930).

25. Robert Herzog, Ind. Eng. Chem. 36 (11), 997-1001 (1944).

26. R. J. Bouchard et al., Inorg. Chem. 4 (5), 685 (1965).

FIGURE CAPTIONS

Fig. 1. Schematic diagram of a closed tube for chemical transport crystal growth of MS compounds.

Fig. 2. Product flux vs iodine feed concentration for transport of CdS by I_2 for different temperature gradients.

Fig. 3. CdS transport by iodine. Product flux vs temperature gradient for a base temperature T_2 = 1100°K.

Fig. 4. Product flux vs iodine feed concentration for transport of MnS by I_2 for different temperature gradients.

Fig. 5. MnS transport by I_2. Product flux vs temperature gradient for a base temperature T_2 = 1100°K.

Fig. 6. Product flux vs iodine feed concentration for transport of ZnS by I_2 for different temperature gradients.

Fig. 7. ZnS transport by I_2. Product flux vs temperature gradient for a base temperature T_2 = 1100°K.

Fig. 8. Standard free energy of formation vs temperature for $CdS_{(s)}$ and $CdI_{2(g)}$.

Fig. 9. Standard free energy of formation vs temperature for $MnS_{(s)}$ and $MnI_{2(g)}$.

Fig. 10. Standard free energy of formation vs temperature for $In_2S_{3(g)}$ and $InI_{3(g)}$.

Fig. 11. Schematic diagram of a closed tube for chemical transport crystal growth of AB_2X_4 compounds.

Fig. 12. Kaldis[12] curve for dependance of the mass transport rate upon the undercooling ΔT. I_2 concentration is 4 mg/cm^3. $T = 1/2 (T_1-T_2)$ is 830°C for CdS and 850°C for ZnSe. Ampoule geometry is d = 35 mm and length = 90 mm.

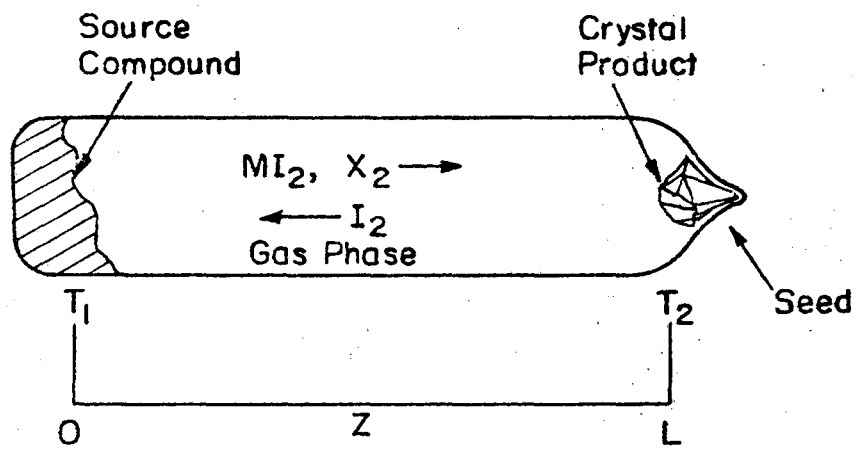

XBL 7212-7341

Fig. 1

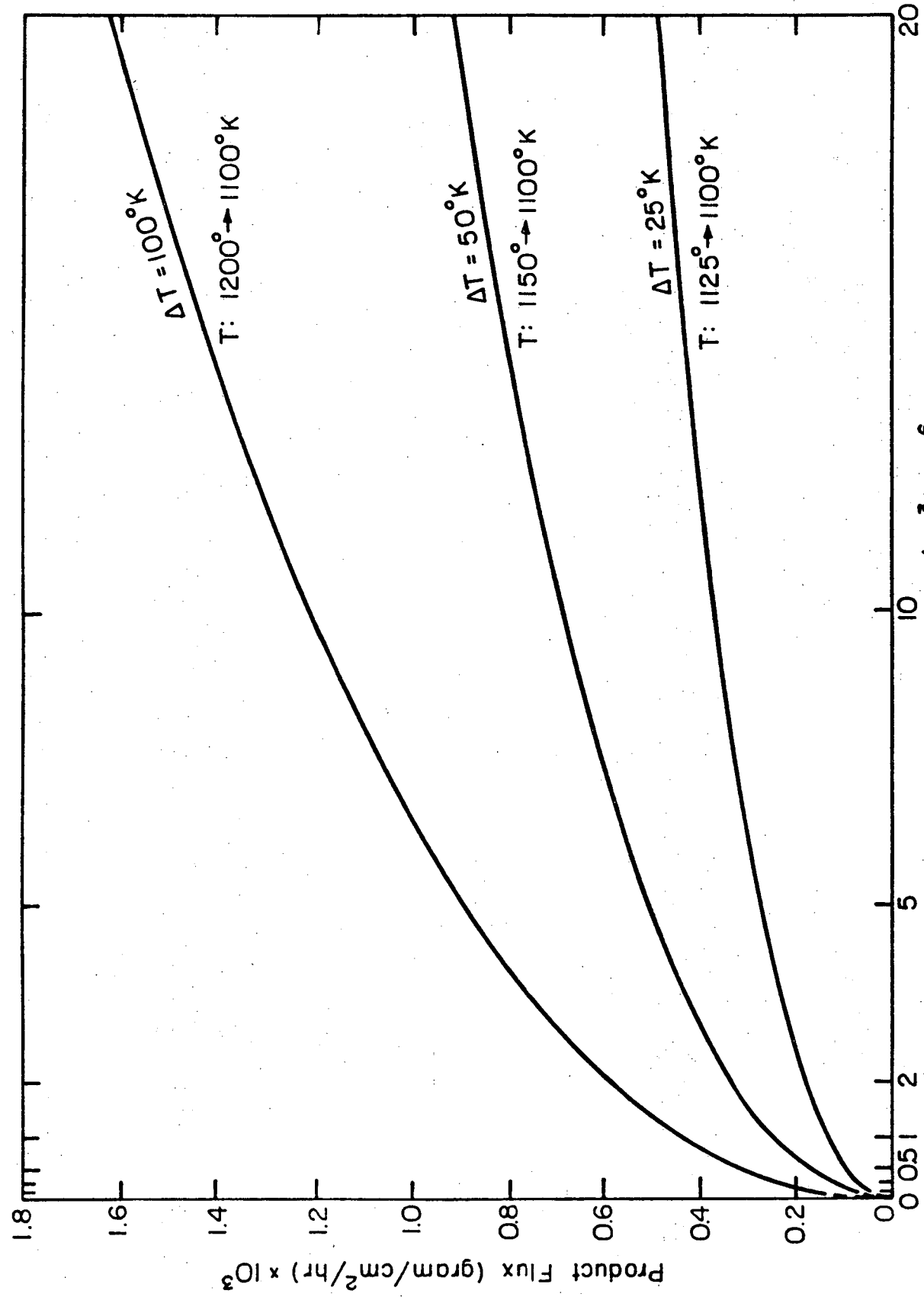

XBL7212-7342

Fig. 2

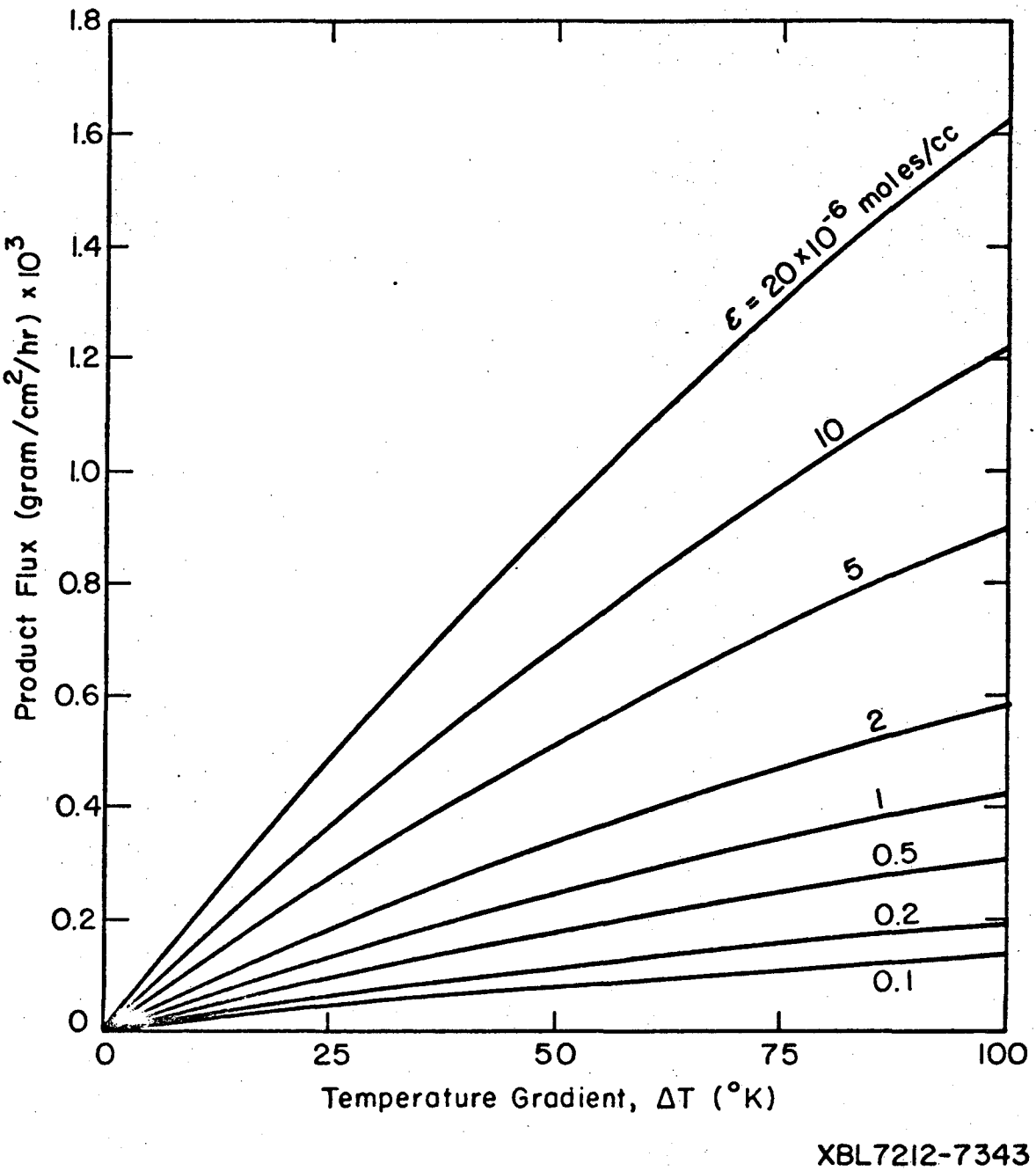
1.8
1.6
1.4
1.2
1.0
0.8
0.6
0.4
0.2
0
Product Flux (gram/cm²/hr) x 10³
ε = 20x10⁻⁶ moles/cc
10
5
2
1
0.5
0.2
0.1
0
25
50
75
100
Temperature Gradient, ΔT (°K)
XBL7212-7343

Fig. 3

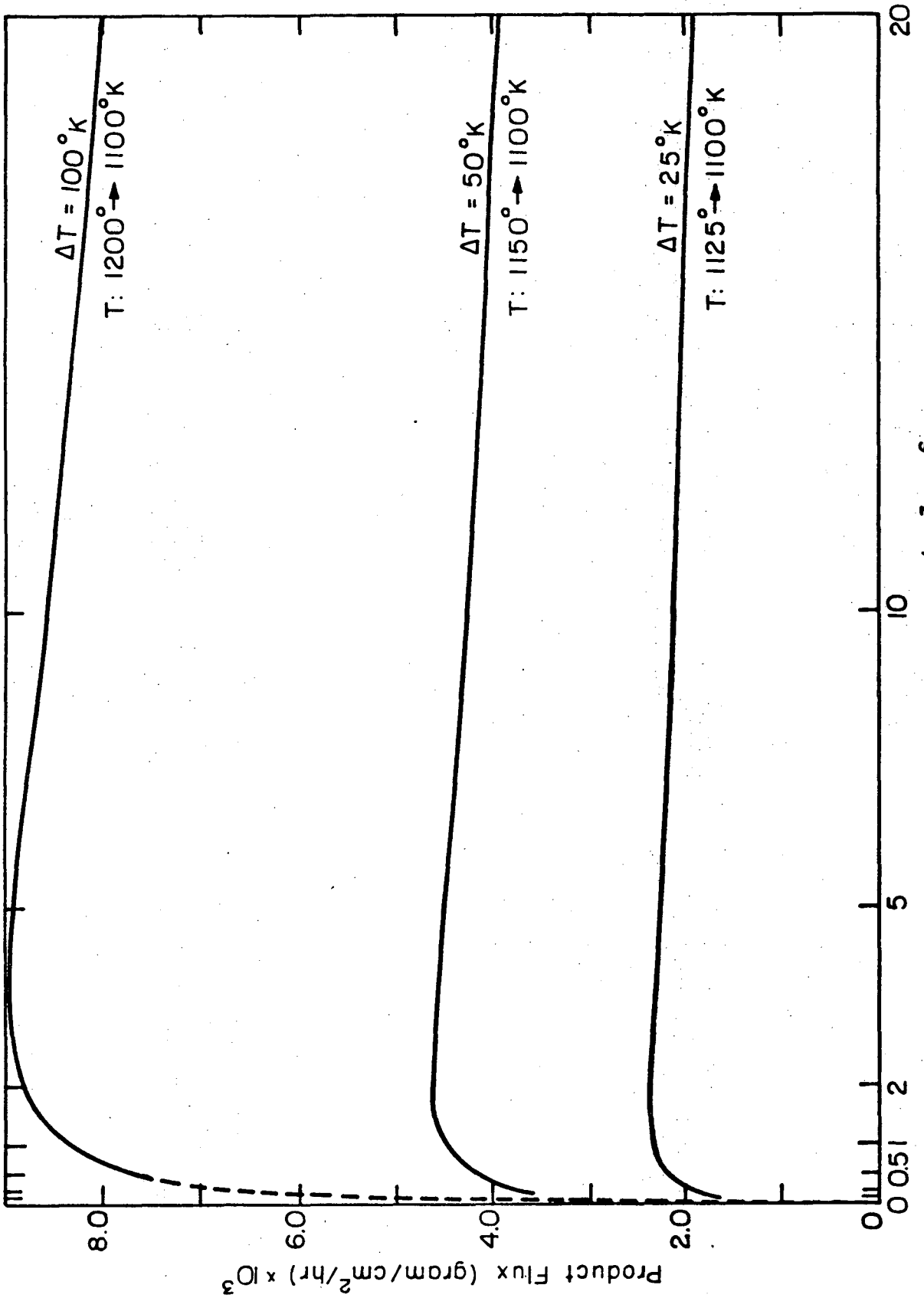

XBL 7212-7344

Fig. 4

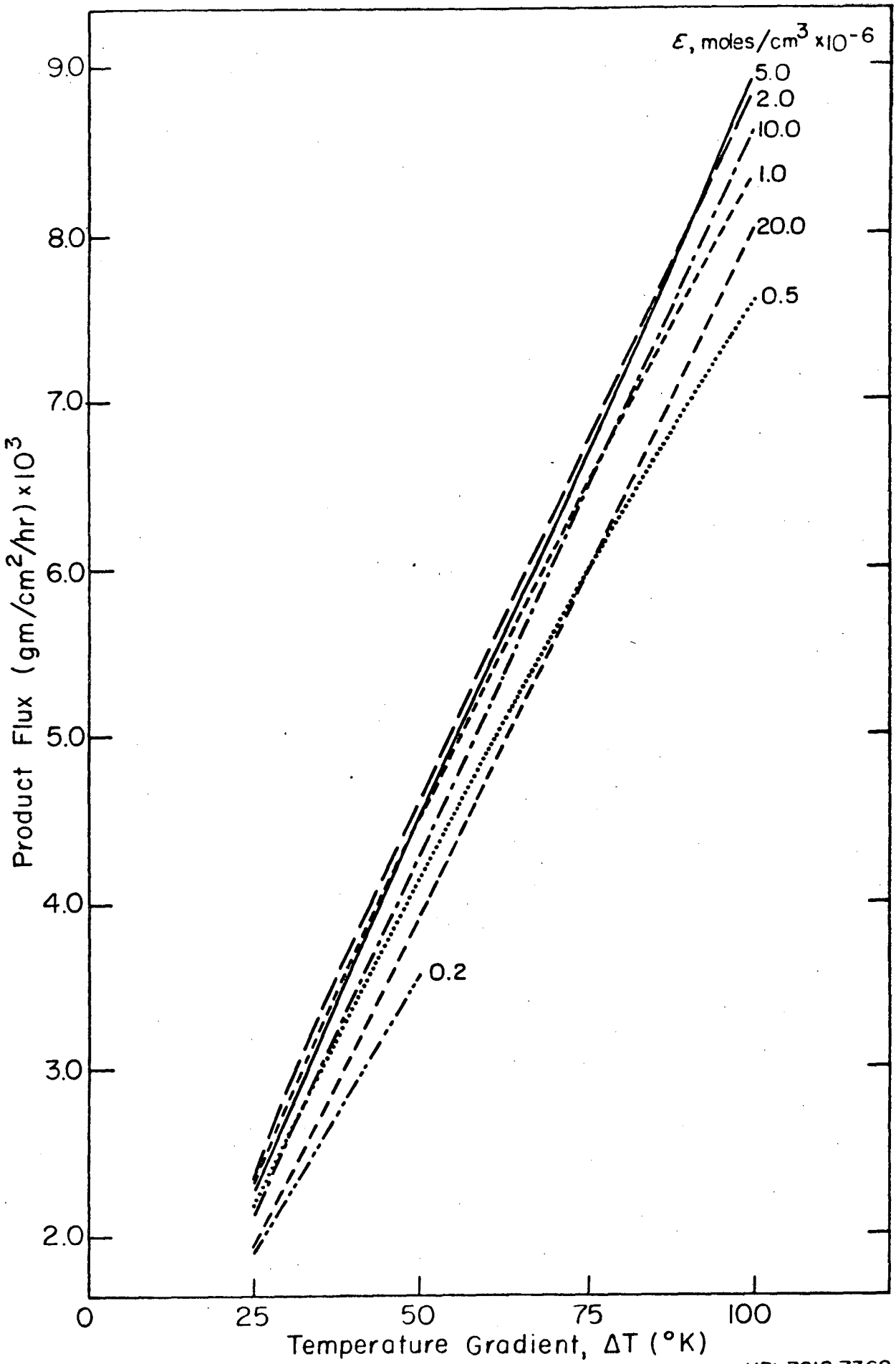
ε, moles/cm³ x10⁻⁶
5.0
2.0
10.0
1.0
20.0
0.5
0.2
9.0
8.0
7.0
6.0
5.0
4.0
3.0
2.0
Product Flux (gm/cm²/hr) x10³
0
25
50
75
100
Temperature Gradient, ΔT (°K)
XBL7212-7362

Fig. 5

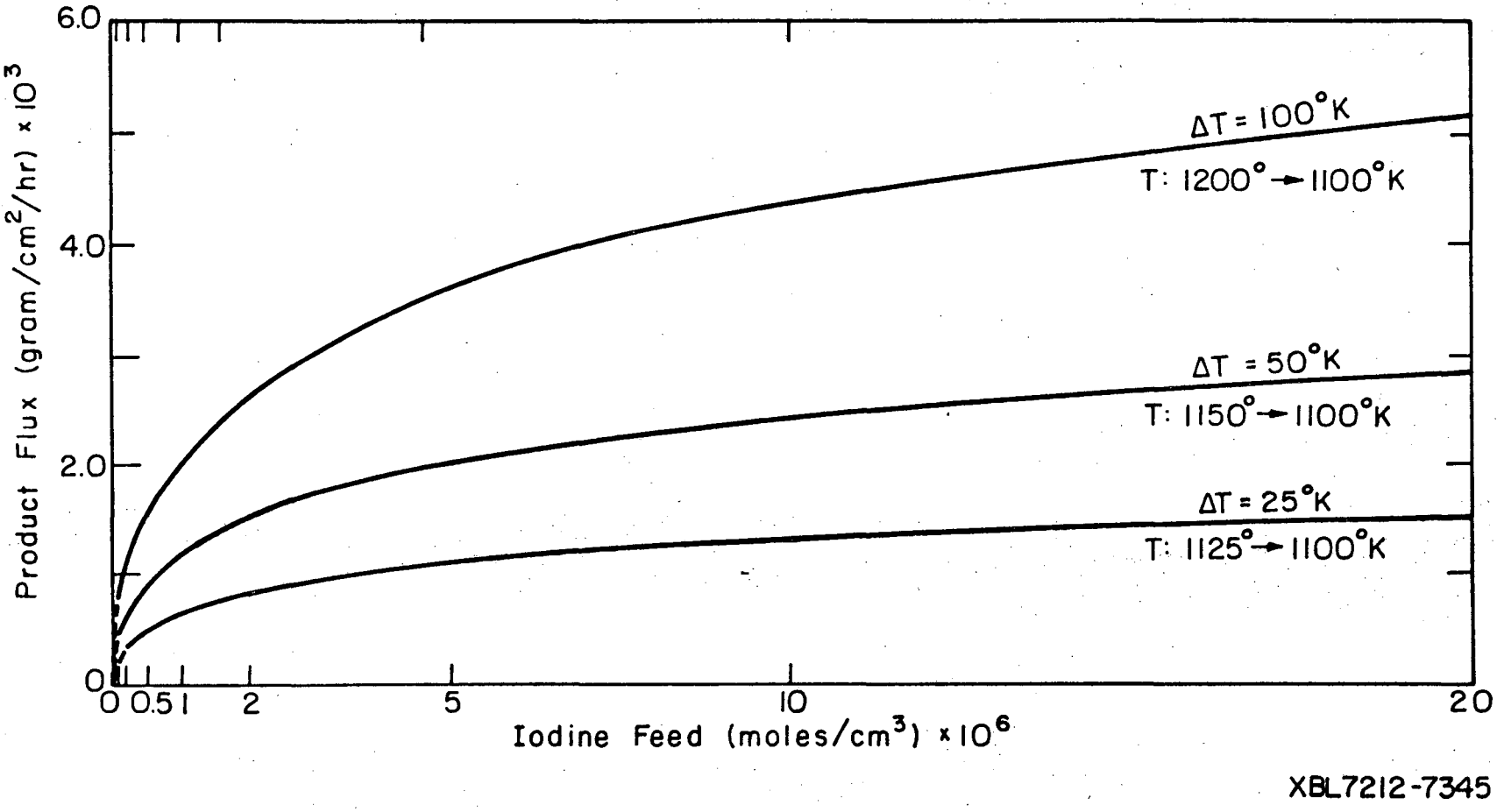
6.0
4.0
2.0
0
Product Flux (gram/cm²/hr) x 10³
ΔT = 100°K
T: 1200° → 1100°K
ΔT = 50°K
T: 1150° → 1100°K
ΔT = 25°K
T: 1125° → 1100°K
0 0.5 1 2 5 10 20
Iodine Feed (moles/cm³) x 10⁶
XBL7212-7345

Fig. 6

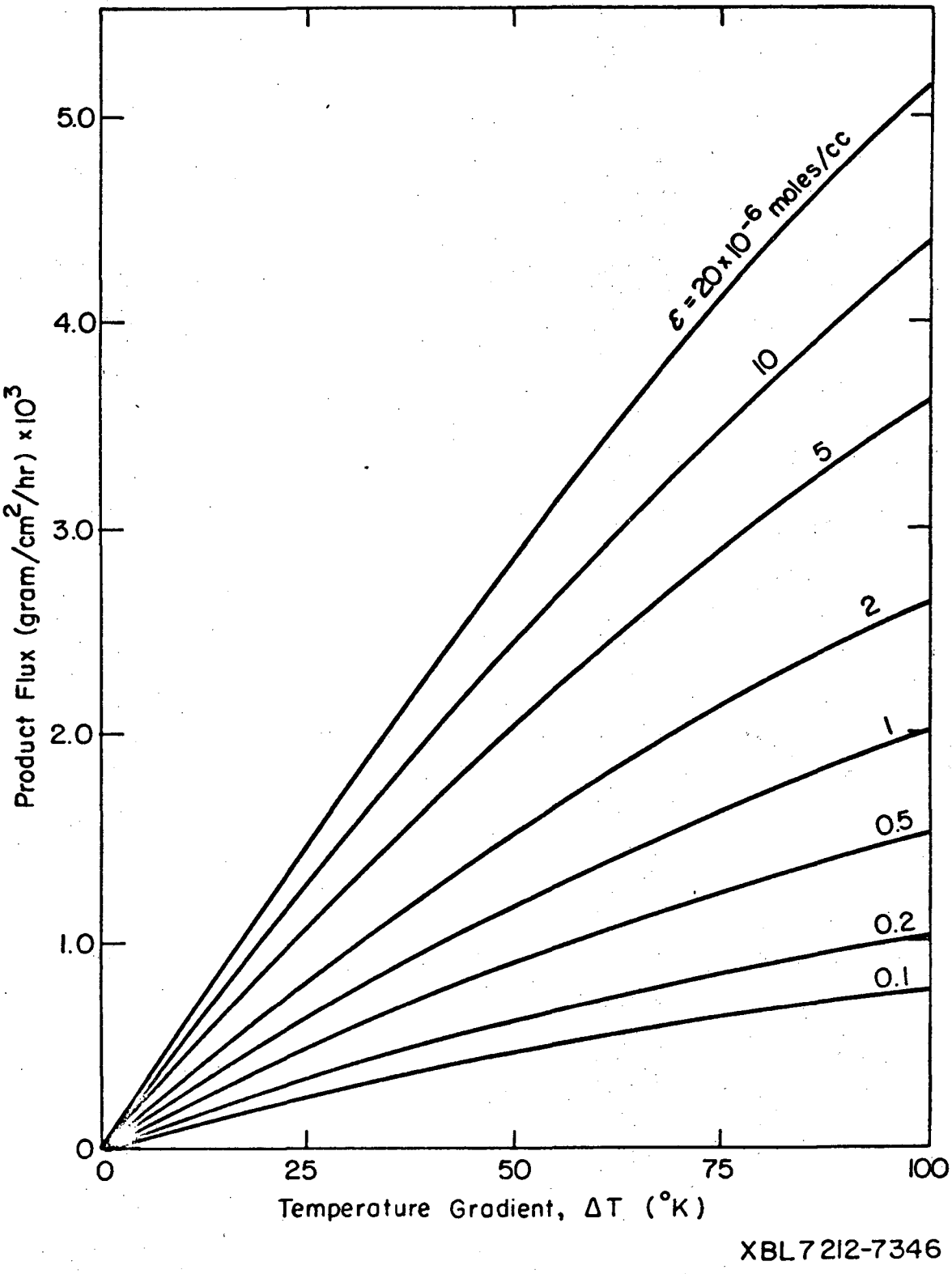
5.0
4.0
3.0
2.0
1.0
0
Product Flux (gram/cm^2/hr) x10^3
ε=20x10-6 moles/cc
10
5
2
1
0.5
0.2
0.1
0
25
50
75
100
Temperature Gradient, ΔT (°K)
XBL7212-7346

Fig. 7

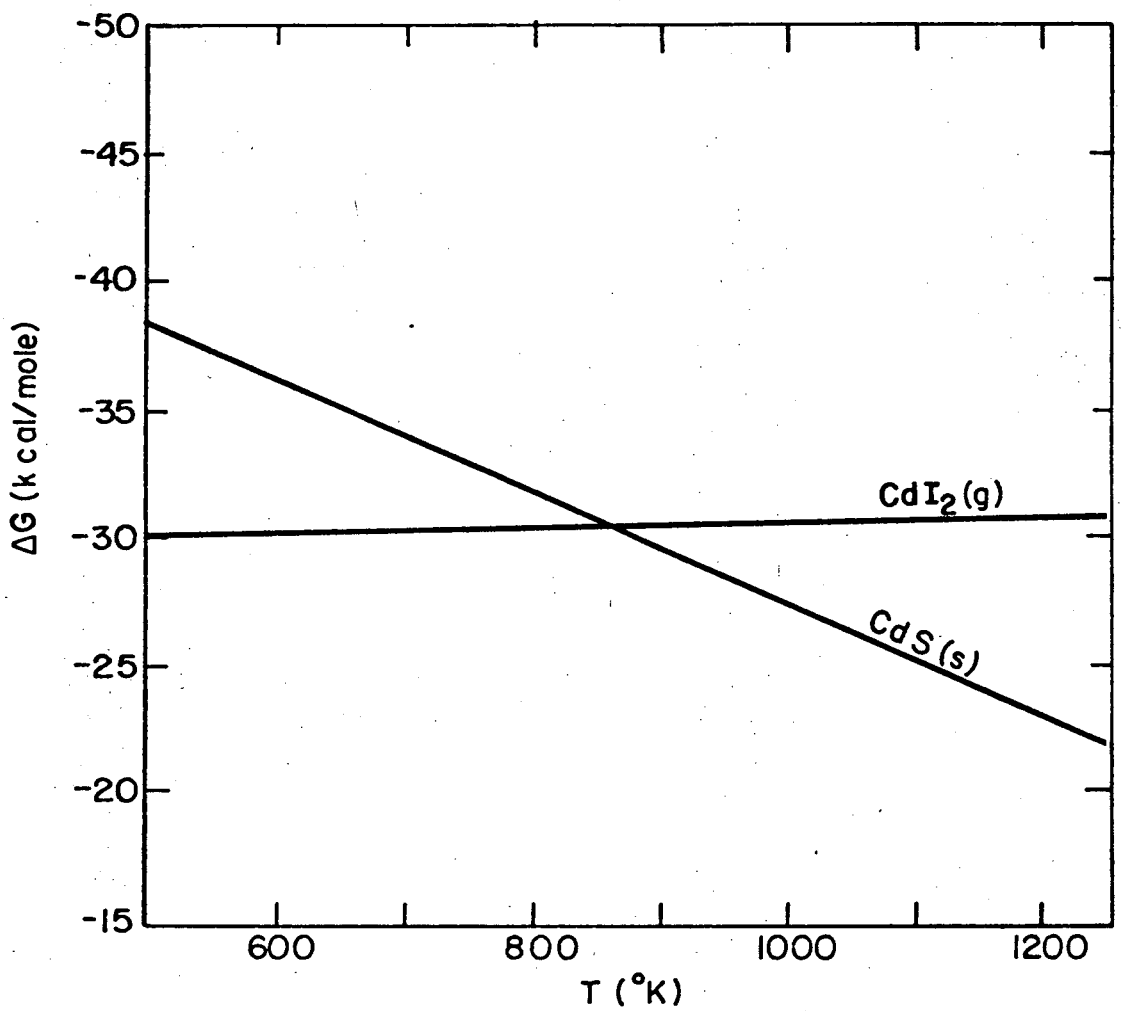
-50
-45
-40
-35
-30
-25
-20
-15
ΔG (k cal/mole)
600
800
1000
1200
T (°K)
CdI2(g)
CdS(s)
XBL7212-7347

Fig. 8

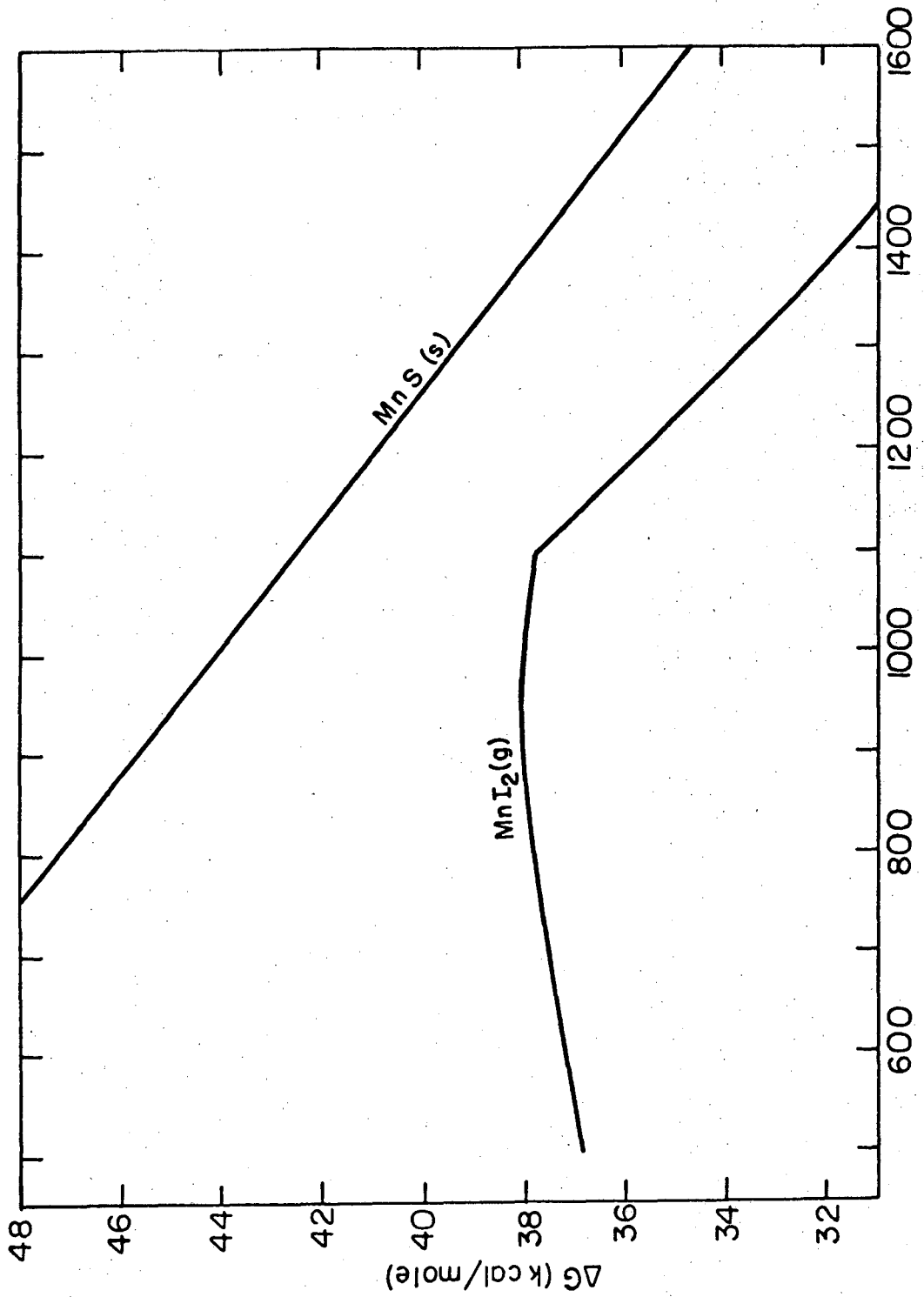

XBL7212-7348

Fig. 9

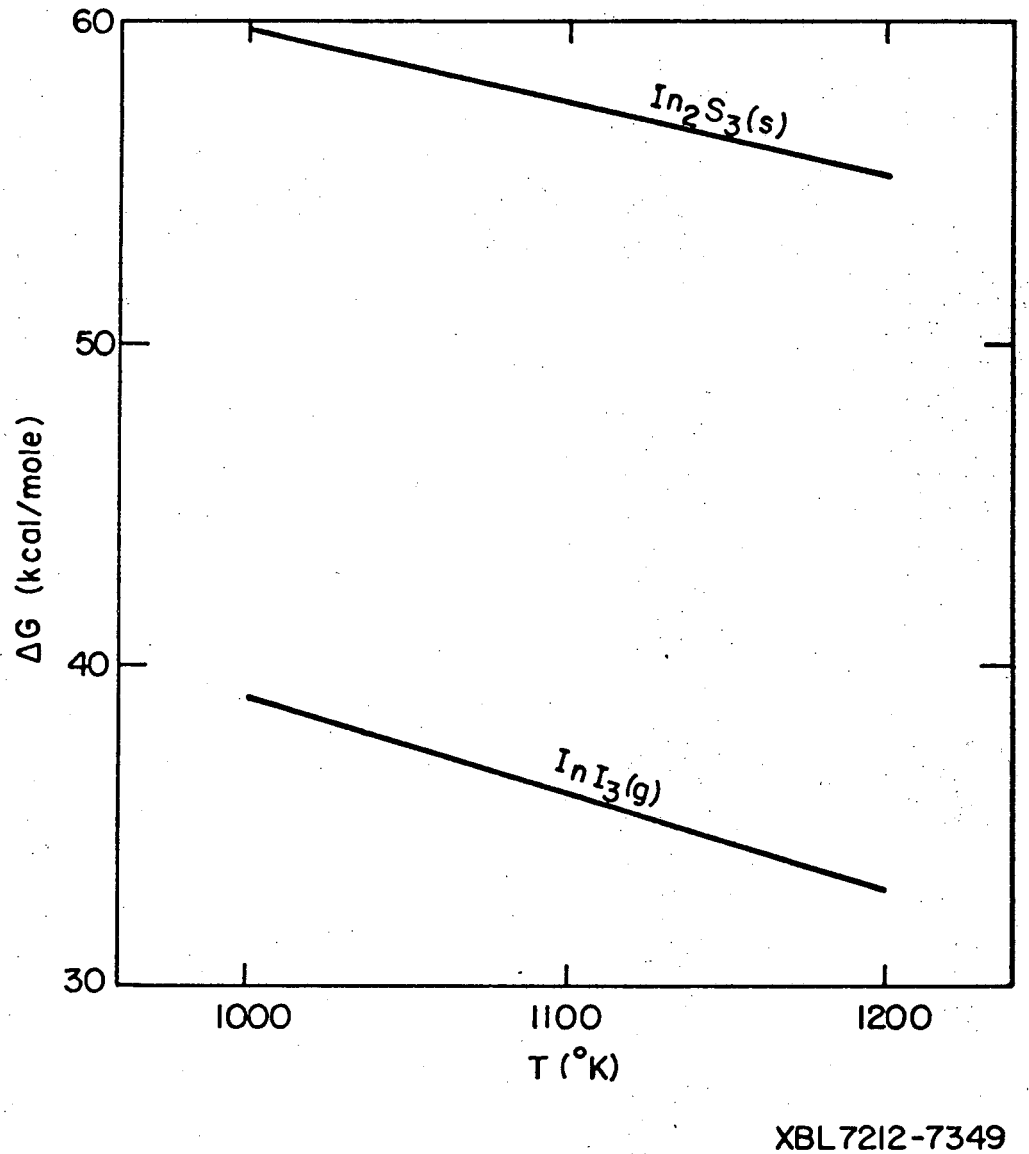
60
50
40
30
ΔG (kcal/mole)
$In_2S_3(s)$
$InI_3(g)$
1000
1100
1200
T (°K)
XBL7212-7349

Fig. 10

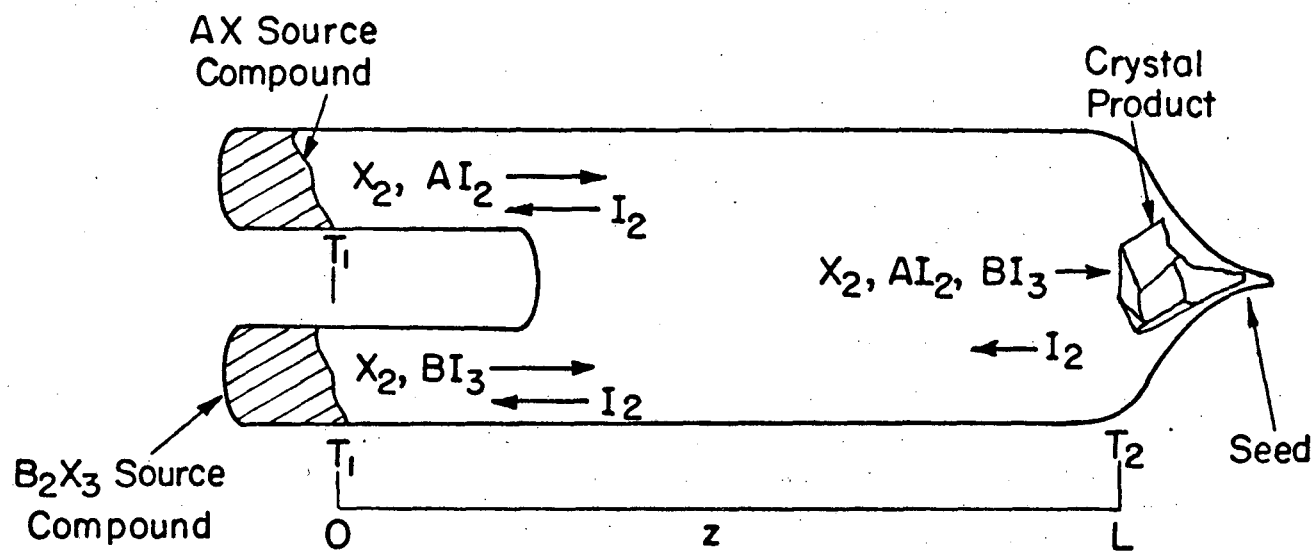
AX Source Compound
Crystal Product
X_2, AI_2
I_2
T_1
X_2, AI_2, BI_3
I_2
X_2, BI_3
I_2
B_2X_3 Source Compound
T_1
T_2
Seed
O
z
L
XBL7212-7351

Fig. 11

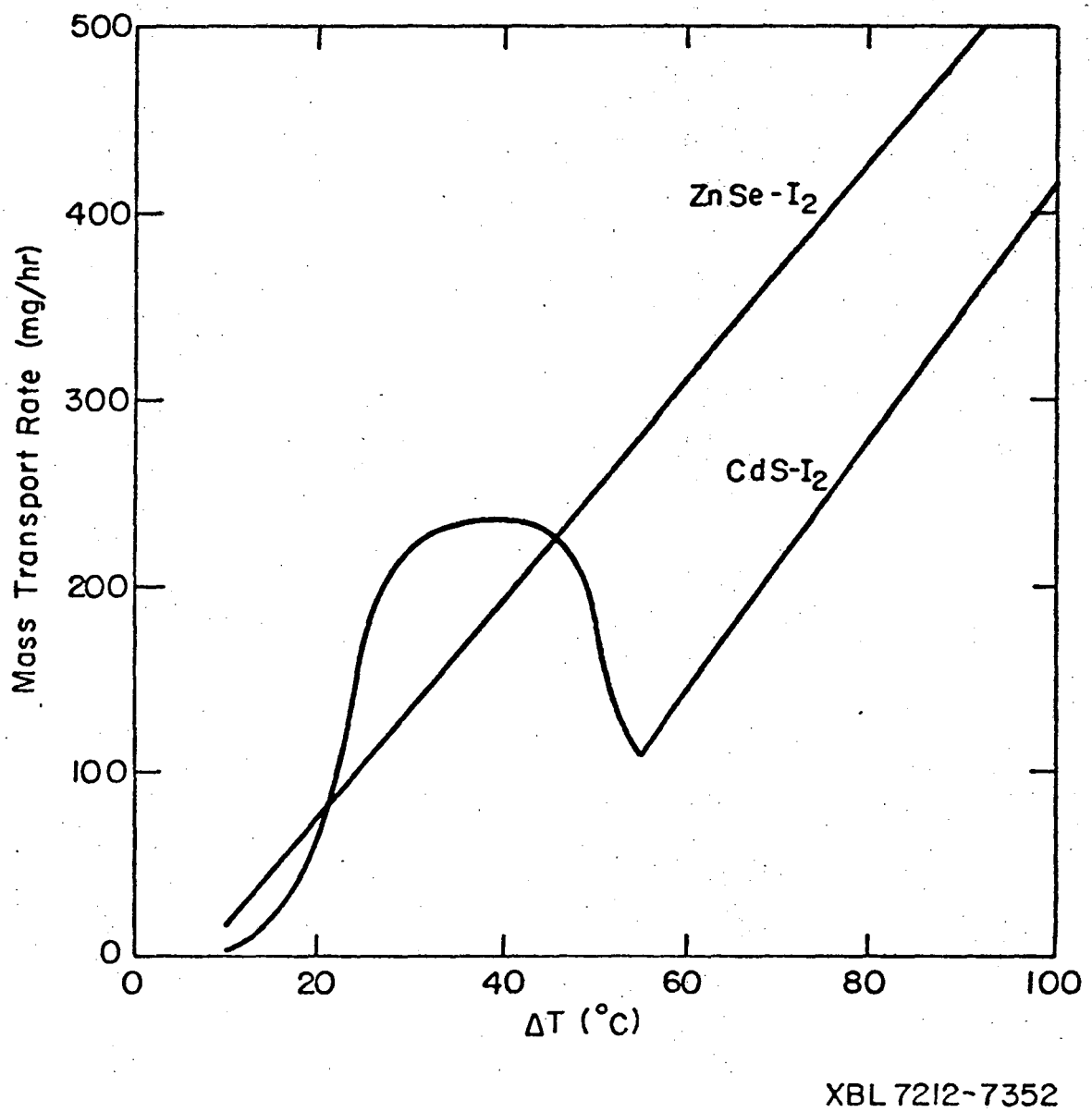
500
400
300
200
100
0
Mass Transport Rate (mg/hr)
ZnSe-I2
CdS-I2
0
20
40
60
80
100
ΔT (°C)
XBL 7212-7352

Fig. 12

III. MAGNETIC SUSCEPTIBILITY

A. Magnetic Behavior of 2-3 Spinels

In this section we will examine the relation between the magnetization of spinels and their structure. Spinels can be ferro-, ferri-, antiferro- or simply paramagnetic.

In transition metal compounds, the orbital angular momentum is quenched.[1] Paramagnetism is then essentially due to the electron spin. At high temperatures these spins are randomly oriented due to thermal agitation. When a magnetic field is applied, the dipoles (caused by the spin) align parallel to the field causing a magnetization M. At lower temperatures, the thermal agitation is lower and M becomes larger until the saturation magnetization is reached. The susceptibility χ at any temperature is the ratio of the magnetization M at that temperature to the field applied.

Ferromagnetism is caused by the exchange interaction of one dipole on a neighboring dipole causing it to align parallel to the first. In this way, all the magnetic dipoles in the system are aligned parallel to each other. At the Curie Temp, T_c however, the thermal agitation overcomes this exchange interaction and the material again becomes paramagnetic above T_c.

In antiferromagnetism, the exchange interaction between neighboring dipoles causes them to align antiparallel to each other. Thus we have every alternate magnetic ion pointing in the same direction. The ions pointing in the same direction may be hypothesized to be part of a sublattice. Hence we have two sublattices interlocked in each other and having magnetic moments in the opposite direction. The net

magnetization of the material is then the difference, and this is equal to zero. At a certain temperature T_N, the Neel Temperature, the thermal agitation again overcomes the exchange interaction and the material becomes paramagnetic.

In ferrimagnetism, the two opposing magnetic sublattices (as mentioned under antiferromagnetism) do not have equal magnetic moments and so the net magnetization is not zero.

Metamagnetism is a phenomenon in which the antiferromagnetic material is converted to a ferromagnetic one on applying a magnetic field.

A ferrimagnetic material consists of two magnetic sublattices A and B. The net magnetic moment of the material is the difference between the magnetic moments of the two sublattices. The temperature dependance of the magnetization of these two sublattices will also be different. Hence the net magnetic moment will change with temperature. Thus from the shape of the χ vs. T curve we will know the kind of magnetism prevalent in the lattice. Knowing this, we can correlate it with the structure of the lattice.

The saturation magnetization of any material is the sum of the saturation magnetization of the individual sublattices. Thus when the composition and consequently the position of ions on different lattice sites in the compound are changed, we would expect a corresponding change in the saturation magnetization. Thus a clue to the compound structure is obtained from the change in saturation magnetization with composition. The following examples illustrate the above.

Example 1

Pinch and Berger[2] substituted trivalent In for divalent Cd on the tetrahedral A-site in the spinel $CdCr_2S_4$. The magnetic moment in μ_B per formula unit measured at 4.2°K in a 10 kOe field is plotted vs. y, the concentration of trivalent In in the compound $In_yCd_{1-y}Cr_2S_4$. In the spinel In_2CrS_4, divalent Cr was found by Flahaut et al.* Hence Pinch posited the following phenomenon: In is substituted for Cd. In^{+3} replaces Cd^{+2} in the A sites. Cr remains on the B sites. But, for charge equilibrium, some Cr^{+3} ions go to Cr^{+2} state. This has 4 unpaired spins compared to 3 for Cr^{+3}. Hence in a compound $Cd_{1-y}In_y[Cr_y^{2+}Cr_{2-y}^{3+}]S_4$ the saturation magnetization will change from $6\mu_B$ to $N\mu_B$

$$N = 3(2-y) \pm 4y.$$

Their experiments showed that the magnetic moment per molecule varied as $N = 3(2-y)-4y$. This meant that Cr^{+2} ions are aligned antiparallel to the Cr^{+3} ions on the same B sublattice. The presence of Cr^{+2} ions is strengthened by the fact that oxidation of the sample leads to decrease in the moment while reduction causes an increase.

Example 2.[3] $FeCr_2S_4$

This compound is a normal spinel and is ferrimagnetic below a T_c of 190°K. The spin arrangement is $Fe^{++}[Cr^{+2}Cr^{+3}]S_4^{=}$. $CuCr_2S_4$ is ferromagnetic below the T_c of 400°K. The spin arrangement is $Cu^{1+}[Cr^{+3}Cr^{+4}]S_4^{=}$. When we substitute Cu in the $FeCr_2S_4$ system, it behaves like a ferromagnetic material at high Cu concentrations, and as a ferrimagnetic material at low Cu concentrations.

*Flahaut et al., c. r. hebd. Seave. Acad. Sc. Paris 253, 1956 (1961).

Example 3.[4] $NiFe_2O_4$

This compound has an inverted structure and is ferrimagnetic. There are 8 Fe^{+3} ions in the A sublattice and 8 Ni^{+2} ions are on the B sublattice. Fe^{+3} has five unpaired spins while Ni^{+2} has two unpaired spins do!p;es/ Forty μ_B on each sublattice (due to Fe^{3+}) compensate each other. The eight Ni^{+2} ions on B give the net magnetic moment = 16 μ_B per unit cell.

$$\underset{\substack{\downarrow \\ 40}}{Fe_{1.0}} \quad [\underset{\substack{\uparrow \\ 16 \text{ net}}}{Ni_{1.0}} \quad \underset{\substack{\uparrow \\ 40}}{Fe_{1.0}}] \quad O_4 \ .$$

Suppose a small amount of nonmagnetic Al^{+3} ion is substituted for Fe^{+3}. For an Al composition of 0.2 Al atoms per formula, the Al^{+3} ions go in the B lattice. Then we have

$$\underset{\substack{\downarrow \\ 32}}{(Fe_{0.8}} \quad \underset{\substack{\downarrow \\ 8}}{Fe_{0.2}}) \ [\underset{\substack{\uparrow \\ 8}}{Ni_{0.5}} \quad \underset{\substack{\uparrow \\ 8 \text{ net}}}{Ni_{0.5}} \quad Al_{0.2} \quad \underset{\substack{\uparrow \\ 32}}{Fe_{0.8}}] \ O_4$$

Thus Ni^{+} ions are used to compensate for the Fe^{+3} ions on the A sublattice.

When Al = 0.4, all the Ni^{+2} ions are used to compensate.

$$\underset{\substack{\downarrow \\ 24}}{(Fe_{0.6}} \quad \underset{\substack{\downarrow \\ 16}}{Fe_{0.4}}) \ [\underset{\substack{\uparrow \\ 16}}{Ni_{1.0}} \quad Al_{0.4} \quad \underset{\substack{\uparrow \\ 24}}{Fe_{0.6}}] \ O_4$$

Hence net magnetization is zero. Further addition of Al^{+3} ions dilutes the B sublattice further and the magnetization is reversed and becomes that of the dominant A sublattice.

Hence we can see that measurement of magnetic susceptibility of a spinel and its variation with composition and temperature gives us a clue to the nature of the charge and the position of an ion in the lattice.

B. Experimental Setup for Measuring Magnetic Susceptibility

Measurements of magnetic susceptibility at different temperatures provides important information on the charge and position of the different ions in a spinel lattice. It allows quantitative comparison of the magnetism exhibited by different spinels (pure and mixed) and give us clues to the different lattice exchange integrals in the crystal.

Methods for measuring magnetic susceptibility belong to two categories:[5] 1) force methods wherein one measures the magnetic force exerted on a sample placed in an inhomogeneous magnetic field and 2) induction methods wherein one measures the signal induced by moving the sample with respect to detecting coils.

The first category, exemplified by the Faraday method has high sensitivity and is suitable for measuring para- and dia-magnetic susceptibilities. The second category (ex. the vibrating sample magnetometer) does not have the sensitivity of the Faraday method but can be used for measuring ferromagnetic susceptibilities which cannot be done by the conventional Faraday technique. This is because of the need of a field gradient in the Faraday method. Conventionally this is done by specially shaped pole pieces on the faces of a large electromagnet. If we had a ferromagnetic sample, this would affect the field gradient which is a function of the field. Therefore the sensitivity of the experiment would become a function of the field. Thus we can never accurately study the field dependance of the magnetization.

To get around this problem, Lewis[6] following the lead of Sucksmith et al.[7] and used a set of coils, rather than specially

shaped pole caps, to provide a field gradient in a Faraday system. The force is now directly proportional to the sample magnetization. Moreover the field gradient can rapidly be turned off or reversed.

1. The Faraday Method

The Faraday method for measuring the magnetic susceptibility involves determining the force on a sample when it is placed in a magnetic field. The force relation is

$$F_z = M_x \left(\frac{\partial H_x}{\partial z}\right)_z$$

where F_z = force acting on the sample

M_x = magnetization of the sample

and $\frac{\partial H_x}{\partial z}$ = the magnetic field gradient.

The magnetization is related to the susceptibility χ by

$M_x = \chi H_x$ where H_x is the field strength.

Thus

$$F_z = \chi H_x \left(\frac{\partial H_x}{\partial z}\right)_z .$$

The schematic of the experimental apparatus constructed is shown in Fig. 1. The sample was suspended by a wire from the pan of a microbalance. The sample was positioned in the gap between the pole faces of a magnet placed vertically below the balance. The suspension wire was isolated from air currents by means of a pyrex tube. The set of coils we had designed to generate a linear field gradient was affixed flat onto the individual pole faces of the magnet and connected to cooling water lines and a dc power supply.

2. Coil Design

A deflection coil system was designed to produce a linear field gradient. In order to be symmetric about the centerline of the magnet pole faces, two pairs of D-shaped coils, one below the centerline and another above it were manufactured. For symmetry, similar coil sets were placed on each pole face (Fig. 2). The current flowing through the coils was such that the field created by the upper coil was opposite to that of the lower coils, and the net effect at $z = 0$ is zero. Our coils were constructed to fit a 4 in. diam. magnet pole face. The return path of the coils was outside this 4 in. diam. so as to minimize image charges in the return lines. The current through the coils could be reversed by a switch in the circuit. This would reverse the field gradient and help give us average values of the susceptibility.

3. Coil Construction

Thin insulated copper ribbon was employed as current carriers to maximize current density and still allow the use of easily available power supplies. The copper ribbon was backed by teflon (Fig. 3). The slight additional width of teflon provides electrical insulation between the copper strip and the copper plate. In a test case, no contact could be detected. The strips are arranged on a copper plate such that each plate has a pair of D-shaped coils (consisting of about 200 turns of the copper strips) lying base to base (Fig. 2). The strips are attached to the plate by an epoxy resin. We have used two copper plates on each pole face. We can add more depending on the gradient required or the magnet gap allowed. The copper plate nearest the pole face has a circular

collar that fits over the pole face. The other copper plate is then attached to this one by copper screws. Thus the assembly is fixed on the magnet. The cooling water lines are made of copper and are soldered onto the plate. They border the inner and outer edges of the D-shaped coils. The cooling water inlet and outlet lines and the current leads were at the outer edge of the plates so they do not come within the gap between the pole faces.

Each coil had an impedance of ~ 0.61 Ω. They were connected in a parallel series arrangement (Fig. 4) such that the overall impedance is ~ 0.62 Ω for each set of two copper plates. The two sets attached to the pole faces were then connected in series to give a total impedance of ~ 1.25 Ω. A dc power supply of capacity 36 V, 20 amp drove the coils.

4. Experimental Observations

The current through each coil was 5 amp. when a current of 10 amp. flowed from the dc power supply. The field gradient measured in a magnet field of 5000 g. was 89 gauss/cm (Fig. 5). The magnetic field of the dc magnet was constant in a region of ~ 1 in. diam. at the center of the pole faces (Fig. 6). The field gradient produced by the coils was linear in a region of ~ 1.50 in. around the center of the pole faces. For the remainder of the section, it was roughly linear. Thus we had a region of ~ 1 in. diam. in the center of the pole faces where the field gradient was linear (Fig. 5).

Measurements of susceptibility were carried out with $CuSO_4 \cdot 5H_2O$ in a sample 3 mm diam. holder tube to minimize the non-uniformity of the magnetic field along the y-axis.

A 5000 oe dc field and 89 eo/cm field gradient produced a force of 0.35 mg on a 0.16 g sample of $CuSO_4 \cdot 5H_2O$ whose known gram susceptibility is 5.85×10^{-6} cgs.

5. Conclusions

It was noted that the maximum dc field differed slightly from the center of the pole faces (Figs. 5 and 6). This could be due to the base of the magnet causing a shift of the lines of force. Linearity was best in the region -0.625 in. $\leq z \leq 0.30$ in. For the larger vertical region -0.75 in. $\leq z \leq 0.5$ in. the deviation was 15%.

There was a slight difference between the measured field gradient and the apparent field gradient as calculated from the experiment on $CuSO_4 \cdot 5H_2O$ (73 gauss/cm).

BIBLIOGRAPHY

1. R. M. Bozorth, Ferromagnetism (Van Nostrand Co., New York, 1951).

2. H. L. Pinch and S. B. Berger, J. Phys. Chem. Solids 29, 2091-9 (1968).

3. G. Haacke and L. C. Beegle, J. Phys. Chem. Solids 28, 1699-1704 (1967).

4. Benjamin Lax and Kenneth J. Button, Microwave Ferrites and Ferrimagnetics (McGraw Hill, 1962) p. 122.

5. H. Zijlstra, Experimental Methods in Magnetism. 2. Measurement of Magnetic Qualities (Wiley, New York 1967).

6. R. T. Lewis, Rev. Sci. Inst. 42(1), 31-34 (1971).

7. W. Sucksmith, C. A. Clark, D. J. Oliver and J. E. Thompson, Rev. Mod. Phys. 25, 34 (1953).

FIGURE CAPTIONS

Fig. 1. Schematic diagram of the apparatus for measuring magnetic susceptibility.

Fig. 2. A view of the deflection coils designed to produce a linear field gradient.

Fig. 3. Cross-sectional view of the copper ribbon.

Fig. 4. Current flow through the deflection coils.

Fig. 5. The magnetic field gradient produced by the deflection coils.

Fig. 6. The magnetic field produced by the dc magnet.

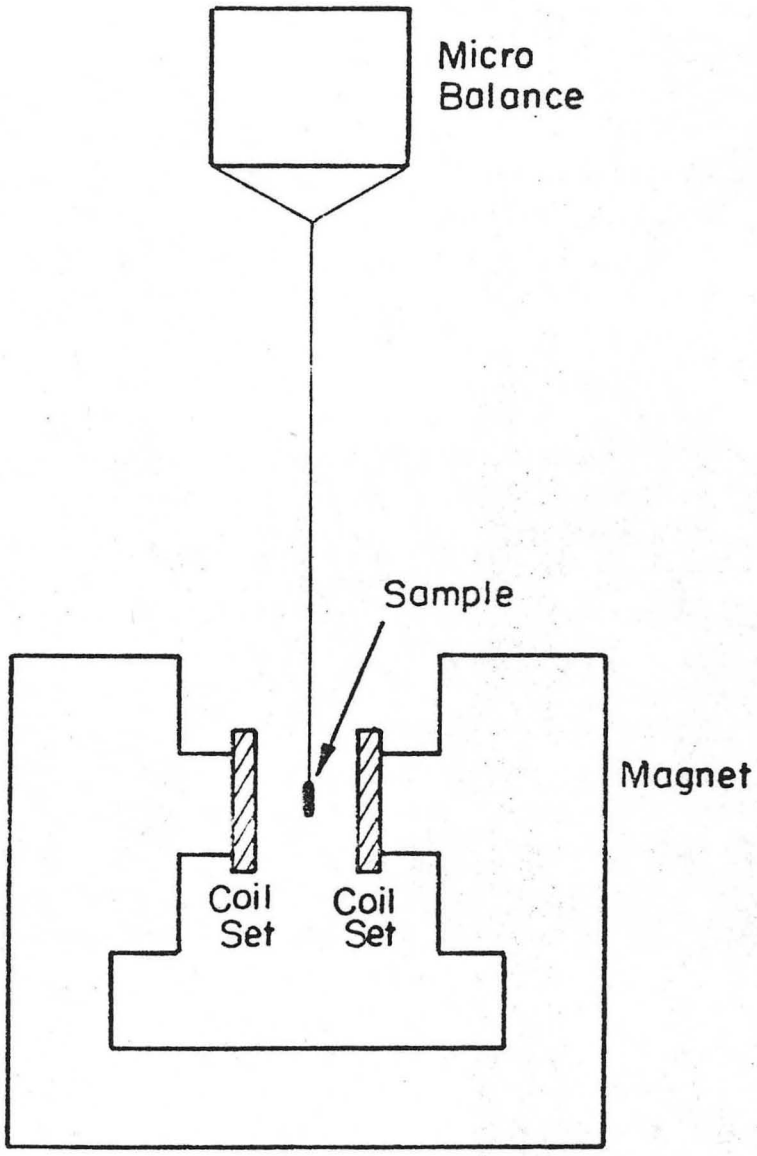

Fig. 1

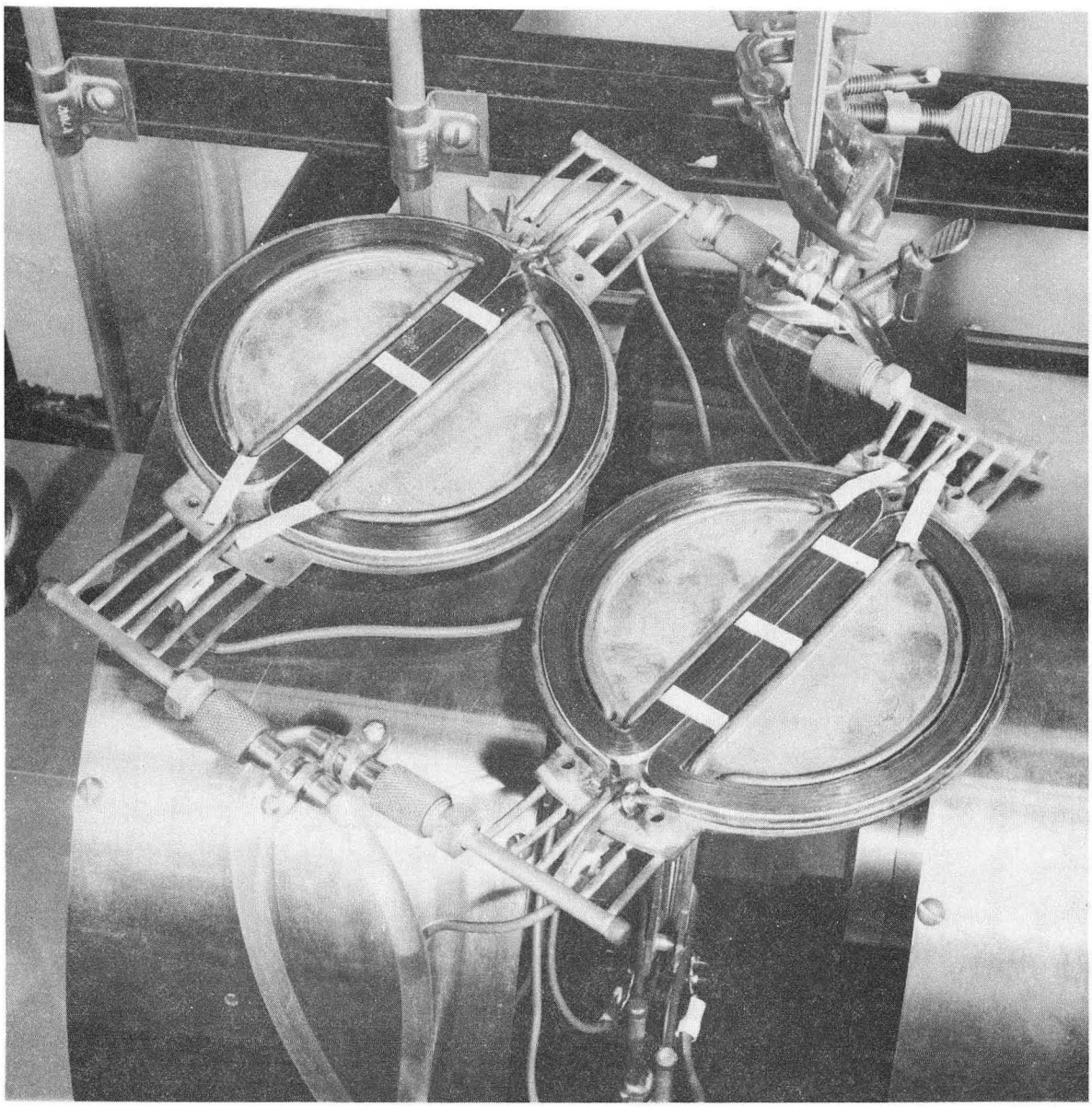

XBB 721-167

Fig. 2

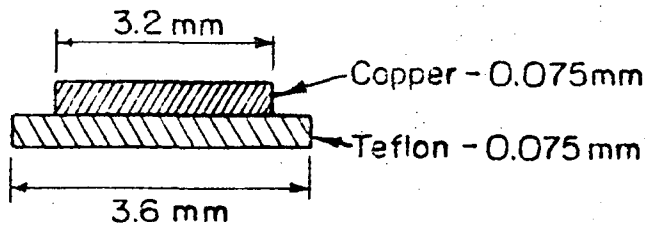
3.2 mm
Copper - 0.075mm
Teflon - 0.075 mm
3.6 mm

Fig. 3

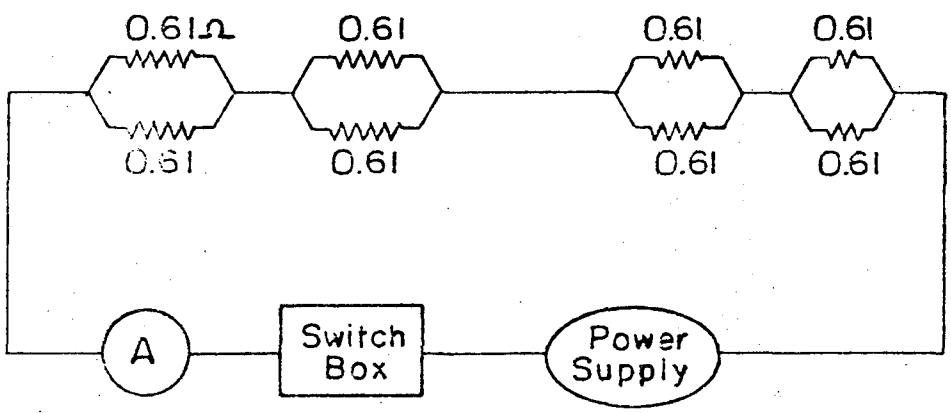
0.61Ω
0.61
0.61
0.61
0.61
0.61
0.61
0.61
A
Switch Box
Power Supply
XBL 7212 - 7355

Fig. 4

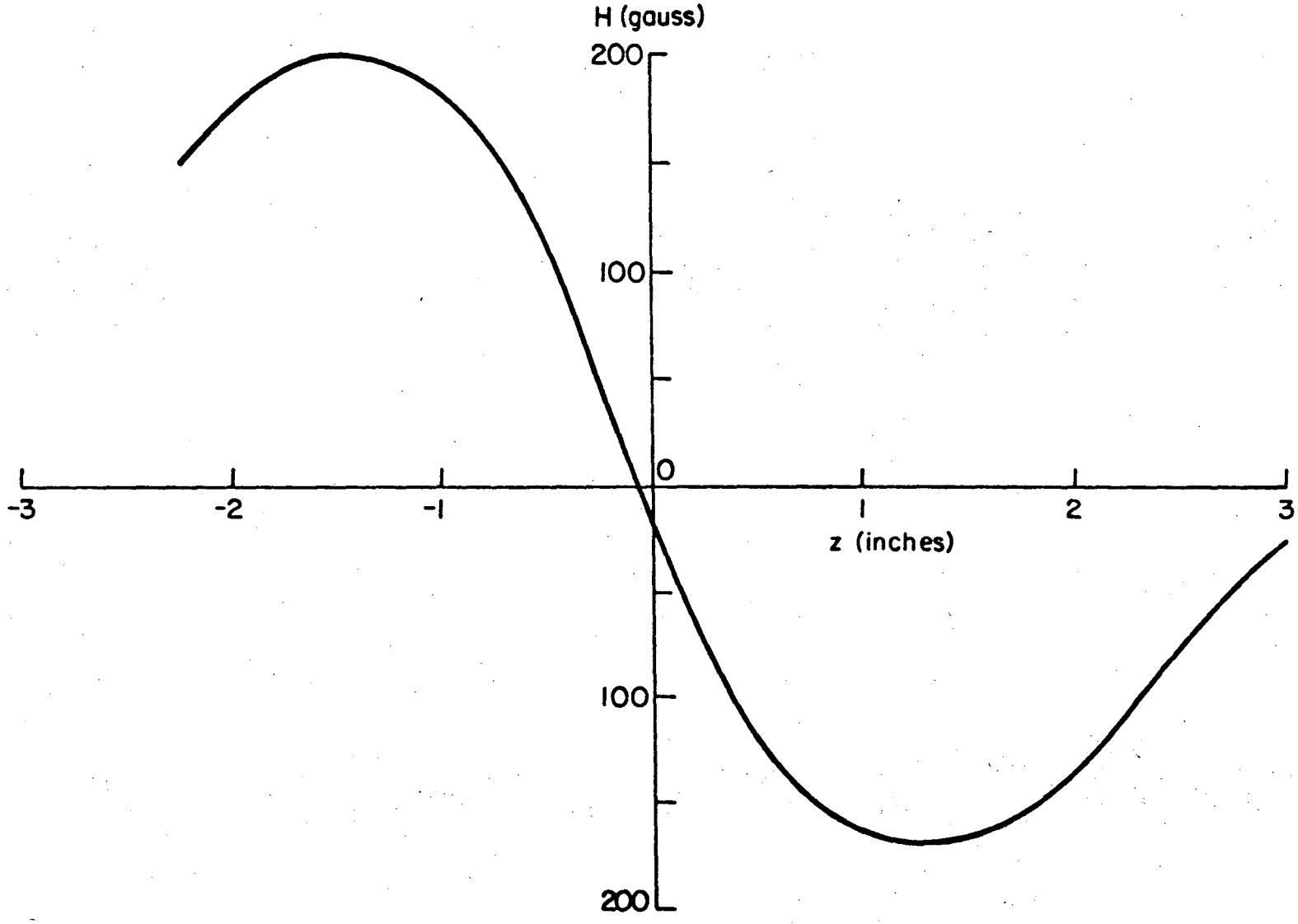

Fig. 5

XBL 7212-7356

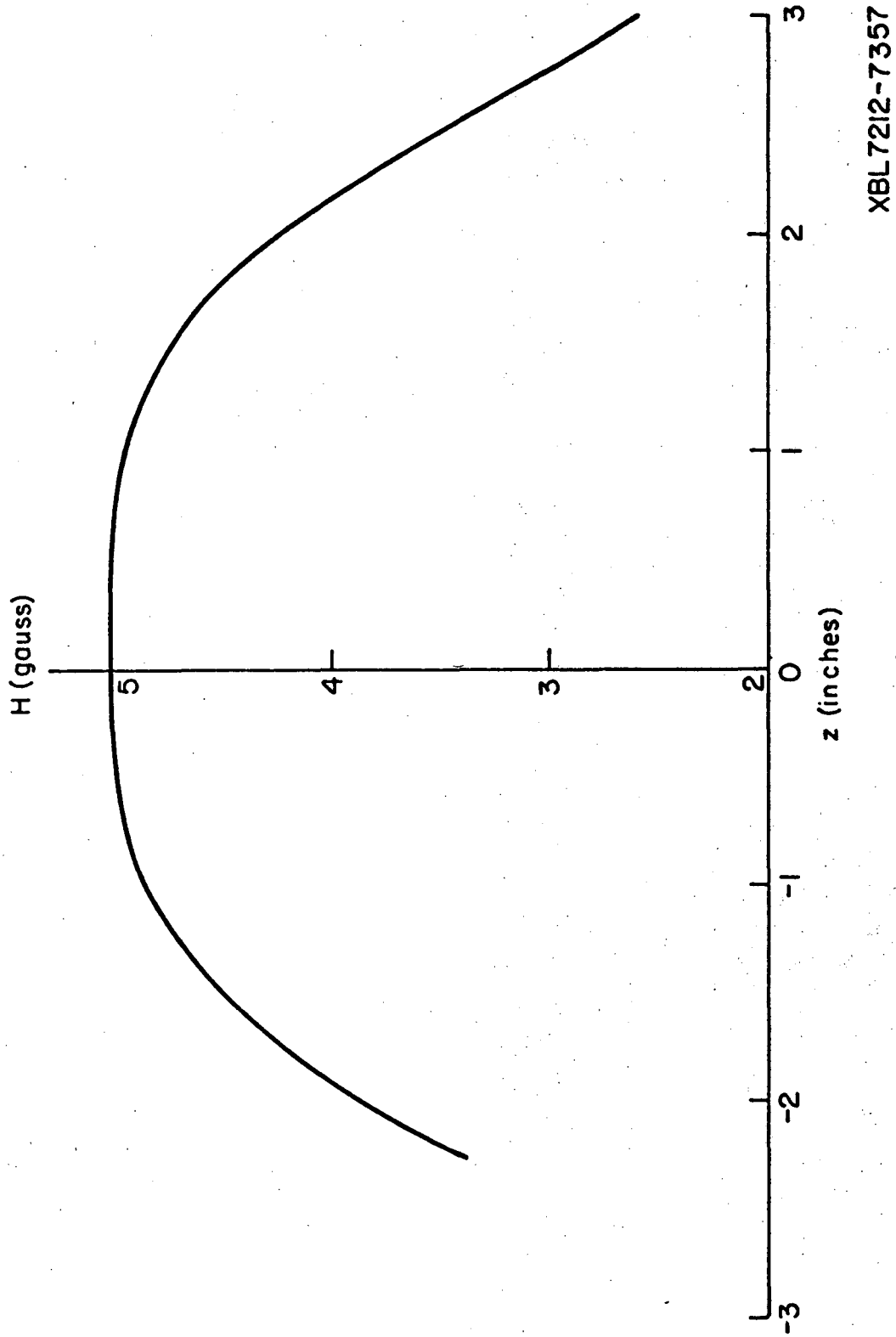

Fig. 6

APPENDIX 1A

Section I.

The multicomponent diffusion Eq. is

$$\nabla x_i = \sum \frac{1}{c\hat{D}_{ij}} \left(N_j x_i - N_i x_j\right) \tag{1}$$

Flux balance at steady state gives us

$$N_{MI_2} = 2N_{S_2} = -N_{I_2} = J \text{ (product flux).} \tag{2}$$

∴ Equations for the three species are

$$\nabla x_1 = \frac{1}{c}\left[\frac{1}{\hat{D}_{12}}\left(x_1 J + x_2 J\right) + \frac{1}{\hat{D}_{13}}\left(\frac{x_1 J}{2} + x_3 J\right)\right] \tag{3}$$

$$\nabla x_2 = \frac{1}{c}\left[\frac{1}{\hat{D}_{21}}\left(-x_2 J - x_1 J\right) + \frac{1}{\hat{D}_{23}}\left(\frac{x_2 J}{2} - x_3 J\right)\right] \tag{4}$$

$$\nabla x_3 = \frac{1}{c}\left[\frac{1}{\hat{D}_{31}}\left(-x_3 J - \frac{x_1 J}{2}\right) + \frac{1}{\hat{D}_{32}}\left(x_3 J - \frac{x_2 J}{2}\right)\right] \tag{5}$$

also

$$x_3 = 1 - x_1 - x_2 \quad \text{for any } z, \text{ and } \hat{D}_{ij} = \hat{D}_{ji} . \tag{6}$$

The variable x_3 can be eliminated from Eqs. 3 and 4 with Eq. 6. Then we have two equations in two unknowns in the form

$$\nabla x_1 = a_1 x_1 + b_1 x_2 + d_1 \tag{7}$$

$$\nabla x_2 = a_2 x_1 + b_2 x_2 + d_2 \tag{8}$$

where

$$a_1 = \frac{J}{c}\left(\frac{1}{\hat{D}_{12}} - \frac{1}{2\hat{D}_{13}}\right) \quad ; \qquad a_2 = \frac{J}{c}\left(\frac{1}{\hat{D}_{23}} - \frac{1}{\hat{D}_{21}}\right)$$

$$b_1 = \frac{J}{c}\left(\frac{1}{\hat{D}_{12}} - \frac{1}{\hat{D}_{13}}\right) \quad . \qquad b_2 = \frac{J}{c}\left(\frac{3}{2\hat{D}_{23}} - \frac{1}{\hat{D}_{21}}\right)$$

$$d_1 = \frac{J}{c\hat{D}_{13}} \quad ; \qquad d_2 = -\frac{J}{c\hat{D}_{23}}$$

Putting Eqs. 7 and 8 into matrix form we have

$$\underline{\nabla x} = \underline{A}\,\underline{x} + \underline{D} \tag{9}$$

where

$$\nabla x = \begin{bmatrix} \nabla x_1 \\ \nabla x_2 \end{bmatrix}, \qquad \underline{A} = \begin{bmatrix} a_1 & b_1 \\ a_2 & b_2 \end{bmatrix}, \qquad \underline{x} = \begin{bmatrix} x_1 \\ x_2 \end{bmatrix}, \qquad \underline{D} = \begin{bmatrix} d_1 \\ d_2 \end{bmatrix}$$

The general solution of Eq. (9) is

$$\underline{x} = \underline{\lambda}\, e^{\underline{A}z} - \underline{A}^{-1}\underline{D} \tag{10}$$

where the arbitrary constant vector $\underline{\lambda}$ is defined by

$$\underline{\lambda} = \begin{bmatrix} \lambda_1 \\ \lambda_2 \end{bmatrix} .$$

The inversion of $\underline{A}$ is then

$$\underline{A}^{-1} = \begin{bmatrix} b_2 & -b_1 \\ -b_2 & a_1 \end{bmatrix} \quad \frac{1}{a_1 b_2 - a_2 b_1}$$

and

$$-\underline{A}^{-1}\underline{D} = \frac{1}{a_2b_1-a_1b_2}\begin{bmatrix} b_2d_1-b_1d_2 \\ a_1d_2-a_2d_1 \end{bmatrix}$$

$\underline{x} = \underline{\lambda}\, e^{\underline{A}z}$ represents the solution to the homogeneous parts of Eqs. 7 and 8, which are Eq. (11) and (12) respectively

$$\nabla x_1 - a_1x_1 - b_1x_2 = 0 \tag{11}$$

$$\nabla x_2 - a_2x_1 - b_2x_2 = 0 \tag{12}$$

Solutions for Eqs. 11 and 12 are

$$x_1 = \lambda_1 e^{m_1 z} + \lambda_2 e^{m_2 z} \tag{13}$$

$$x_2 = \lambda_3 e^{m_1 z} + \lambda_4 e^{m_2 z} \tag{14}$$

where

$$m_{1,2} = \frac{a_1+b_2}{2} + \frac{1}{2}\sqrt{(a_1+b_2)^2 + 4(a_2b_1-a_1b_2)} \quad . \tag{15}$$

We now prove that λ_3 and λ_4 are dependent on λ_1 and λ_2. Replacing values of x_1 and x_2 in Eqs. (11) and (12), we have

$$m_1\lambda_1 e^{m_1 z} + m_2\lambda_2 e^{m_2 z} - a_1\lambda_1 e^{m_1 z} - a_1\lambda_2 e^{m_2 z} - b_1\lambda_3 e^{m_1 z} - b_1\lambda_4 e^{m_2 z} = 0 \tag{16}$$

$$e^{m_1 z}(m_1\lambda_1 - a_1\lambda_1 - b_1\lambda_3) + e^{m_2 z}(m_2\lambda_2 - a_1\lambda_2 - b_1\lambda_4) = 0 \tag{17}$$

Since both exponential terms are positive, each of their coefficients must be 0.

$$\therefore \quad m_1\lambda_1 - a_1\lambda_1 - b_1\lambda_3 = 0 \qquad \text{or} \qquad \lambda_1(m_1 - a_1) - \lambda_3 b_1 = 0 \tag{18}$$

$$m_2\lambda_2 - a_1\lambda_2 - b_1\lambda_4 = 0 \qquad \text{or} \qquad \lambda_2(m_2 - a_1) - \lambda_4 b_1 = 0 \tag{19}$$

Similarly from (12).

$$m_1\lambda_3 - a_2\lambda_1 - b_2\lambda_3 = 0 \qquad \text{or} \qquad \lambda_3(m_1 - b_2) - \lambda_1 a_2 = 0 \tag{20}$$

$$m_2\lambda_4 - a_2\lambda_2 - b_2\lambda_4 = 0 \qquad \text{or} \qquad \lambda_4(m_2 - b_2) - \lambda_2 a_2 = 0 \tag{21}$$

Taking Eqs. (18) and (20)

$$\lambda_1(m_1 - a_1) - \lambda_3 b_1 = 0$$

$$-\lambda_1 a_2 + \lambda_3(m_1 - b_2) = 0$$

if we multiply (18) by $(m_1 - b_2)$ we obtain

$$\lambda_1(m_1 - a_1)(m_1 - b_2) - \lambda_3 b_1(m_1 - b_2) = 0 \tag{22}$$

Since m_1 is a root of

$$(m-a_1)(m-b_2) - a_2b_1 = 0$$

then $$(m_1-a_1)(m_1-b_2) = a_2b_1 \quad .$$

Hence Eq. (22) becomes

$$\lambda_1 a_2 b_1 - \lambda_3 b_1 (m_1-b_2) = 0 \tag{23}$$

or

$$\lambda_3(m_1-b_2) - a_2\lambda_1 = 0 \tag{24}$$

Hence Eqs. (18) and (20) are linearly dependent. Similarly Eqs. (19) and (21) are linearly dependent. Therefore,

$$\lambda_3 = \frac{a_2\lambda_1}{m_1-b_2} = \frac{(m_1-a_1)}{b_1}\ \lambda_1 \tag{25}$$

and

$$\lambda_4 = \frac{a_2\lambda_2}{m_2-b_2} = \frac{(m_2-a_1)}{b_1}\ \lambda_2 \tag{26}$$

Solutions to homogeneous parts of Eqs. (7) and (8) are

$$x_1 = \lambda_1 e^{m_1 z} + \lambda_2 e^{m_2 z} \tag{27}$$

$$x_2 = \frac{a_2\lambda_1 e^{m_1 z}}{m_1-b_2} + \frac{a_2\lambda_2 e^{m_2 z}}{m_2-b_2} \quad . \tag{28}$$

The vector

$$-\underline{A}^{-1}\underline{D} = \frac{1}{a_2b_1-a_1b_2}\begin{bmatrix} b_2d_1-b_1d_2 \\ a_1d_2-a_2d_1 \end{bmatrix}. \tag{29}$$

Hence the general solutions of the nonhomogeneous Eqs.(7) and (8) are

$$x_1 = \frac{b_2d_1-b_1d_2}{a_2b_1-a_1b_2} + \lambda_1 e^{m_1z} + \lambda_2 e^{m_2z} \tag{30}$$

$$x_2 = \frac{a_1d_2-a_2d_1}{a_2b_1-a_1b_2} + \frac{a_2\lambda_1}{m_1-b_2} e^{m_1z} + \frac{a_2\lambda_2}{m_2-b_2} e^{m_2z} \tag{31}$$

$$x_3 = 1 - x_1 - x_2 \ . \tag{32}$$

However, the roots m_1 and m_2 are generally complex and we will now derive solutions in terms of trigonometric functions.

We already have the solution of the homogeneous Eqs. (11) and (12). These were given as Eqs. (27) and (28).

Now assume that m_i are complex with real and imaginary parts defined by

$$m_1 = s + ir$$

$$m_2 = s - ir.$$

Then, on simplifying we find

$$x_1 = e^{sz}\,[(\lambda_1+\lambda_2)\cos rz + i(\lambda_1-\lambda_2)\sin rz]$$

$$x_2 = e^{sz}\left[\left(\frac{a_2\lambda_1}{m_1-b_2} + \frac{a_2\lambda_2}{m_2-b_2}\right)\cos rz + i\left(\frac{a_2\lambda_1}{m_1-b_2} - \frac{a_2\lambda_2}{m_2-b_2}\right)\sin rz\right] \ .$$

where

$$c_1 = \lambda_1 + \lambda_2 \qquad c_2 = i(\lambda_1 - \lambda_2)$$

$$c_3 = a_2\left(\frac{\lambda_1}{m_1-b_2} + \frac{\lambda_2}{m_2-b_2}\right) \qquad c_4 = ia_2\left(\frac{\lambda_1}{m_1-b_2} - \frac{\lambda_2}{m_2-b_2}\right)$$

Only two of these constants are independent since

$$c_3 = a_2\,\frac{c_1(s-b_2)-rc_2}{(s-b_2)^2+r^2} \qquad c_4 = \frac{a_2[c_2(s-b_2)+rc_1]}{(s-b_2)^2+r^2}$$

The final expressions for the concentrations are then

$$x_1 = \alpha_1 + e^{sz}\,(c_1 \cos rz + c_2 \sin rz)$$

$$x_2 = \alpha_2 + e^{sz}\,(c_3 \cos rz + c_4 \sin rz)$$

$$x_3 = 1 - x_1 - x_2$$

where

$$\alpha_1 = \frac{b_2d_1-b_1d_2}{a_2b_1-a_1b_2} \qquad \text{and} \qquad \alpha_2 = \frac{a_1d_2-a_2d_1}{a_2b_1-a_1b_2}\ .$$

$$c_3 = a_2\left(\frac{c_1t-c_2r}{r^2+t^2}\right) \qquad c_4 = a_2\left(\frac{c_1r+c_2t}{r^2+t^2}\right)$$

$$r^2 = 4(a_1b_2-a_2b_1)-(a_1+b_2)^2 \quad \text{and} \quad t = s-b_2\ .$$

Thus, c_1 and c_2 are the arbitrary constants which are determined from the boundary conditions.

APPENDIX 1A

Section II.

The unknowns in the equations derived in App. 1, Sec. I are c_1, c_2 and J (the product flux). Besides these we also need to know c, the total concentration of all gaseous species in the ampoule. Accordingly, we need four equations to obtain the four quantities mentioned above. These equations are:

(i) the equilibrium condition at the source end.

(ii) the equilibrium condition at the product end.

(iii) Iodine conservation in the reactions.

(iv) Conversion criteria at the source. (This gives us 'c', the total concentration)

(i) Equilibrium at the source end:

$$K_1 = \frac{x_2 x_3}{x_1}^{1/2} \Bigg|_{z=0} (cRT_1)^{1/2}$$

This gives us

$$K_1 = \frac{\left[\alpha_2 + \frac{a_2}{r^2+t^2}(tc_1-rc_2)\right]\left[\alpha_3-c_1 - \frac{a_2}{r^2+t^2}(tc_1-rc_2)\right]^{1/2}}{[\alpha_1 + c_1]} (cRT_1)^{1/2}$$

(ii) Equilibrium at the product end:

$$K_2 = \frac{x_2 x_3}{x_1}^{1/2} \Bigg|_{z=L} (cRT_2)^{1/2}$$

$$K_2 = \left[\alpha^2 + \frac{a_2}{r^2+t^2}\, e^{sL}\left\{(c_1t-c_2r)\cos rL + (c_1r+c_2t)\sin rL\right\}\right](cRT_2)^{1/2}$$

$$\times \frac{\left[\alpha_3 - e^{sL}\left\{\left[c_1 + \frac{a_2}{r^2+t^2}(c_1t-c_2r)\right]\cos rL + \left[c_2 + \frac{a_2}{r^2+t^2}(c_1r+c_2t)\right]\sin rL\right\}\right]^{1/2}}{\alpha_1 + e^{sL}(c_1\cos rL + c_2\sin rL)}$$

(iii) Conservation of Iodine

If I_o is the total Iodine fed in,

$$I_o = Ac\int_o^L \{x_1(z) + x_2(z)\}\,dz$$

Putting in the expressions for x_1 and x_2,

$$\frac{I_o}{Ac} = L(\alpha_1+\alpha_2) + \frac{\left[c_1 + \frac{a_2(c_1t-c_2r)}{r^2+t^2}\right]}{r^2+s^2}\left[s(e^{sL}\cos rL - 1) + re^{sL}\sin rL\right]$$

$$+ \frac{\left[c_2 + \frac{a_2(c_1r+c_2t)}{r^2+t^2}\right]}{r^2+s^2}\left[se^{sL}\sin rL - r(e^{sL}\cos rL - 1)\right]$$

(iv) Conversion criterion at the source

At temp T_1,

$$K_1 = \frac{p_2 p_3^{1/2}}{p_1} = \frac{x_2 x_3^{1/2}}{x_1}\Bigg|_{z=0} (cRT_1)^{1/2}$$

Suppose initial iodine feed conc. $= \varepsilon = \frac{I_o}{AL}$. Also, let y be the conversion for the reaction

$$MS + I_2 \rightleftharpoons MI_2 + \frac{1}{2} S_2$$

Then, conc. of I_2, $c_{I_2} = c_1 = (1-y)\varepsilon = c\chi_1$

$$c_{MI_2} = c_2 = \varepsilon y = c\chi_2$$

$$c_{S_2} = c_3 = \frac{\varepsilon y}{2} = c\chi_3$$

$$\therefore \quad K_1 = \varepsilon y \cdot \frac{\varepsilon^{1/2} y^{1/2}}{2^{1/2}} \cdot \frac{1}{(1-y)\varepsilon} \cdot (RT_1)^{1/2}$$

$$\therefore \quad K_1 = \frac{y^{3/2}}{1-y} \left(\frac{\varepsilon RT_1}{2}\right)^{1/2}$$

Since the mole fractions of the gaseous species add up to unity,

$$\frac{\varepsilon y}{2c} + \frac{y\varepsilon}{c} + \frac{(1-y)\varepsilon}{c} = 1$$

$$\frac{c}{\varepsilon} = \frac{3y}{2} + 1-y = 1 + y/2$$

$$y = 2(\frac{c}{\varepsilon} - 1)$$

and

$$K_1 = \frac{(\frac{c}{\varepsilon} - 1)^{3/2}}{(3 - \frac{2c}{\varepsilon})} \quad (4RT_1\varepsilon)^{1/2}$$

These four Eqs. in (i) -(iv) give us the unknowns c_1, c_2, J and c. We can then predict the product flux and also the mole fractions of the gaseous species along a closed ampoule.

APPENDIX 1B

Section I.

If the diffusing species are as represented as

$$I_2 : 1,\ AI_2 : 2,\ BI_3 : 3,\ S_2 : 4,$$

the Stefan Maxwell equations can be represented as

$$\nabla x_1 = \frac{1}{c}\left[\frac{1}{\hat{D}_{12}}(x_1N_2 - x_2N_1) + \frac{1}{\hat{D}_{13}}(x_1N_3 - x_3N_1) + \frac{1}{\hat{D}_{14}}(x_1N_4 - x_4N_1)\right] \quad (1)$$

$$\nabla x_2 = \frac{1}{c}\left[\frac{1}{\hat{D}_{21}}(x_2N_1 - x_1N_2) + \frac{1}{\hat{D}_{23}}(x_2N_3 - x_3N_2) + \frac{1}{\hat{D}_{24}}(x_2N_4 - x_4N_2)\right] \quad (2)$$

$$\nabla x_3 = \frac{1}{c}\left[\frac{1}{\hat{D}_{31}}(x_3N_1 - x_1N_3) + \frac{1}{\hat{D}_{32}}(x_3N_2 - x_2N_3) + \frac{1}{\hat{D}_{34}}(x_3N_4 - x_4N_3)\right] \quad (3)$$

also $x_4 = 1 - x_1 - x_2 - x_3$ at any z. (4)

If N_i is the flux for species 'i', and if diffusion is the controlling phenomenon,

$$N_{AI_2} = \frac{1}{2} N_{BI_3} = \frac{1}{2} N_{S_2} = -\frac{1}{4} N_{I_2} \quad (5)$$

and

$$J = N_2 = \frac{1}{2} N_3 = \frac{1}{2} N_4 = -\frac{1}{4} N_1 . \quad (6)$$

If the product formation rate is F moles/hr then $\frac{F}{A}$ moles/hr-sq cm is the flux of AI_2 because every mole of product ≡ every mole of AI_2 transported. Let J represent $N_{AI_2} = N_2$.

Hence Eq. (1) becomes

$$\nabla x_1 - a_1 x_1 - b_1 x_2 - c_1 x_3 - d_1 = 0 \tag{7}$$

where

$$a_1 = + \frac{J}{c}\left[\frac{1}{\hat{D}_{12}} + \frac{2}{\hat{D}_{13}} - \frac{2}{\hat{D}_{14}}\right]$$

$$b_1 = + \frac{4J}{c}\left[\frac{1}{\hat{D}_{12}} - \frac{1}{\hat{D}_{14}}\right]$$

$$c_1 = + \frac{4J}{c}\left[\frac{1}{\hat{D}_{13}} - \frac{1}{\hat{D}_{14}}\right]$$

$$d_1 = + \frac{4J}{c\hat{D}_{14}}$$

Similarly, Eq. (2) becomes

$$\nabla x_2 - a_2 x_1 - b_2 x_2 - c_2 x_3 - d_2 = 0 \tag{8}$$

where

$$a_2 = - \frac{J}{c}\left(\frac{1}{\hat{D}_{21}} - \frac{1}{\hat{D}_{24}}\right)$$

$$b_2 = - \frac{J}{c}\left(\frac{4}{\hat{D}_{21}} - \frac{2}{\hat{D}_{23}} - \frac{3}{\hat{D}_{24}}\right)$$

$$c_2 = - \frac{J}{c}\left(\frac{1}{\hat{D}_{23}} - \frac{1}{\hat{D}_{24}}\right)$$

$$d_2 = - \frac{J}{c\hat{D}_{24}}$$

Also Eq. (3) has the form

$$\nabla x_3 - a_3 x_1 - b_3 x_2 - c_3 x_3 - d_3 = 0 \tag{9}$$

where

$$a_3 = -\frac{2J}{c}\left(\frac{1}{\hat{D}_{31}} - \frac{1}{\hat{D}_{34}}\right), \qquad b_3 = -\frac{2J}{c}\left(\frac{1}{\hat{D}_{32}} - \frac{1}{\hat{D}_{34}}\right)$$

$$c_3 = -\frac{J}{c}\left(\frac{4}{\hat{D}_{31}} - \frac{1}{\hat{D}_{32}} - \frac{4}{\hat{D}_{34}}\right), \quad d_3 = -\frac{2J}{c\hat{D}_{34}}$$

Putting this set of Eqs. (7), (8) and (9) in matrix form, we obtain

$$\underline{\nabla x} = \underline{A}\underline{X} + \underline{D} \tag{10}$$

where

$$\underline{\nabla x} = \begin{bmatrix} \nabla x_1 \\ \nabla x_2 \\ \nabla x_3 \end{bmatrix}; \qquad \underline{x} = \begin{bmatrix} x_1 \\ x_2 \\ x_3 \end{bmatrix}, \qquad \underline{D} = \begin{bmatrix} d_1 \\ d_2 \\ d_3 \end{bmatrix}$$

$$\underline{A} = \begin{bmatrix} a_1 & b_1 & c_1 \\ a_2 & b_2 & c_2 \\ a_3 & b_3 & c_3 \end{bmatrix}$$

The homogeneous solution for Eq. (10) is $\underline{x} = \underline{\lambda}\, e^{\underline{A}z}$. The non-homogeneous solution is found as follows:

Suppose the solution is $\underline{x} = \underline{\lambda}\, e^{\underline{A}z} + \underline{\beta}$

Then

$$\nabla \underline{x} = \underline{A}\,\underline{\lambda}\, e^{\underline{A}z}$$

Putting these values in Eq. (10), we find

$$\underline{A}\underline{\lambda} - \underline{A}\underline{\lambda} - \underline{A}\underline{B} = \underline{D}$$

hence

$$\underline{\beta} = -\underline{A}^{-1}\underline{D}$$

The general solution of system (10) is then

$$\underline{x} = \underline{\lambda}\, e^{\underline{A}z} - \underline{A}^{-1}\underline{D} \tag{11}$$

We expand the exponential in a Taylor series.

$$e^{\underline{A}z} = \underline{I} + \frac{\underline{A}z}{1!} + \frac{\underline{A}^2 z^2}{2!} + \frac{\underline{A}^3 z^3}{3!} + \cdots\cdots$$

Let us first take a solution to include z^2 terms only. Then

$$A' = A^2 = A \cdot A = \begin{pmatrix} a_1 & b_1 & c_1 \\ a_2 & b_2 & c_2 \\ a_3 & b_3 & c_3 \end{pmatrix}\begin{pmatrix} a_1 & b_1 & c_1 \\ a_2 & b_2 & c_2 \\ a_3 & b_3 & c_3 \end{pmatrix} = \begin{pmatrix} a_1' & b_1' & c_1' \\ a_2' & b_2' & c_2' \\ a_3' & b_3' & c_3' \end{pmatrix}$$

Also we define the inverse matrix $\underline{A}^{-1}$

$$\underline{A}^{-1} = \begin{bmatrix} a_1^\circ & b_1^\circ & c_1^\circ \\ a_2^\circ & b_2^\circ & c_2^\circ \\ a_3^\circ & b_3^\circ & c_3^\circ \end{bmatrix}$$

Thus,

$$e^{\underline{A}z} = \begin{bmatrix} 1 & 0 & 0 \\ 0 & 1 & 0 \\ 0 & 0 & 1 \end{bmatrix} + z \begin{bmatrix} a_1 & b_1 & c_1 \\ a_2 & b_2 & c_2 \\ a_3 & b_3 & c_3 \end{bmatrix} + \frac{z^2}{2} \begin{bmatrix} a_1' & b_1' & c_1' \\ a_2' & b_2' & c_2' \\ a_3' & b_3' & c_3' \end{bmatrix}$$

$$\underline{x} = \underline{I\lambda} + \underline{A\lambda z} + \frac{z^2}{2} \cdot \underline{A'} \cdot \underline{\lambda} - \underline{A}^{-1}\underline{D}$$

In scalar quantities

$$x_1 = \lambda_1 + z(a_1\lambda_1 + b_1\lambda_2 + c_1\lambda_3) + \frac{z^2}{2}(a_1'\lambda_1 + b_1'\lambda_2 + c_1'\lambda_3)$$

$$- (a_1^\circ d_1 + b_1^\circ d_2 + c_1^\circ d_3) \qquad (15)$$

Similarly,

$$x_2 = \lambda_2 + z(a_2\lambda_1 + b_2\lambda_2 + c_2\lambda_3) + \frac{z^2}{2}(a_2'\lambda_1 + b_2'\lambda_2 + c_2'\lambda_3)$$

$$- (a_2^\circ d_1 + b_2^\circ d_2 + c_2^\circ d_3) \qquad (16)$$

$$x_3 = \lambda_3 + z(a_3\lambda_1 + b_3\lambda_2 + c_3\lambda_3) + \frac{z^2}{2}(a_3'\lambda_1 + b_3'\lambda_2 + c_3'\lambda_2)$$

$$- (a_3^\circ d_1 + b_3^\circ d_2 + c_3^\circ d_3) \qquad (17)$$

The boundary conditions given in App. 1B, Sec. II will be used to solve the values of the constants and coefficients in the above relations.

APPENDIX 1B

Section II.

The unknowns in the equations derived in App. 1A Sec I are $\lambda_1, \lambda_2, \lambda_3$, J (the product flux) and c, the total concentration in the tube of the various gaseous species present. Hence, we need 5 equations to solve for the unknowns. Once we know these, we can predict a particular solution for the mole fraction of each species along the ampoule and also, the product formation rate.

The equations we need are supplied by the following boundary conditions

(i) The equilibrium condition for reaction 1A at the source end.

(ii) The equilibrium condition for reaction 1B at the source end.

(iii) The equilibrium condition for reaction 2 at the product end.

(iv) Iodine conservation in the ampoule.

(v) Conversion criteria at the source. (This gives us c , the total molar concentration.)

(i) Equilibrium for rxn - (13) at the source end:

$$K_{1A} = \frac{\left(P_{AI_2}\right)\left(P_{x_2}\right)^{1/2}}{P_{I_2}} = \frac{P_2 \, P_4^{1/2}}{P_1}$$

$$K_{1A} = \frac{x_2 x_4^{1/2}}{x_1} \left(cRT_1\right)^{1/2} \Bigg|_{z=0}$$

(ii) Equilibrium for rxn (14) at the source end.

$$K_{1B} = \frac{\left(P_{BI_3}\right)^2 \left(P_{x_2}\right)^{3/2}}{\left(P_{I_2}\right)^3} = \frac{P_3^{\,2} P_4^{\,3/2}}{P_1^{\,3}}$$

$$= \frac{x_3^{\,2} x_4^{\,3/2}}{x_1^{\,3}} \left(cRT_1\right)^{1/2} \Bigg|_{z=0}$$

(iii) Equilibrium for reaction (15) at the product end.

$$K_2 = \frac{K_s}{K_{1A} K_{1B}} \Bigg|_{T=T_2,\ z=L}$$

where K_s is the equilibrium constant for the reaction

$$AX + B_2X_3 \rightleftharpoons AB_2X_4$$

$$K_s = \frac{a_{AB_2X_4}}{a_{AX} a_{B_2X_3}} = \exp\left(\frac{\Delta G_f\ AB_2X_4 - \Delta G_f\ AX - \Delta G_f\ B_2X_3}{-RT}\right)$$

Generally, data for the standard free energies of formation of AB_2X_4 compounds is not available. We can approximate $K_s = 4$ if AB_2X_4 is an ideal solid solution but generally, $K_s > 4$.

(iv) Iodine conservation in the ampoule.

This condition is based on the fact that all the iodine present in the ampoule whether as free iodine or iodides, is equal to the original amount fed in.

$$I_o = A \int_o^L [c_1(z) + c_2(z) + \frac{3}{2} c_3(z)]dz$$

in terms of a mole balance.

$$\frac{I_o}{Ac} = \int_o^L (x_1 + x_2 + 1{\cdot}5x_3)dz \quad .$$

This gives us

$$\frac{I_o}{Ac} = \frac{I_o}{ALc} \cdot L = \frac{\varepsilon L}{c}$$

where

$$\frac{\varepsilon}{c} = [\lambda_1+\lambda_2+1.5\lambda_3-d_1(a_1^\circ+a_2^\circ+1.5a_3^\circ)-d_2(b_1^\circ+b_2^\circ+1.5b_3^\circ)-d_3(c_1^\circ+c_2^\circ+1.5c_3^\circ)]$$

$$+ \frac{L}{2}[\lambda_1(a_1+a_2+1.5a_3)+\lambda_2(b_1+b_2+1.5b_3)+\lambda_3(c_1+c_2+1.5c_3)]$$

$$+ \frac{L^2}{6}[\lambda_1(a_1'+a_2'+1.5a_3')+\lambda_2(b_1'+b_2'+1.5b_3')+\lambda_3(c_1'+c_2'+1.4c_3')]$$

(v) Conversion criterion at the source end.

Conc. of iodine initially fed in = ε moles/cm^3.

Let

y = conversion in reaction 1A

ω = conversion in reaction 1B.

then for a basis of 1 mole of iodine, y moles of MI_2 are formed and ω moles of MI_3 are formed. The iodine expended = $y + 1.5\,\omega$, the concentration $I_2 = 1 - (y+1.5\,\omega)$, and $x_2 = 0.5\,y + 0.75\,\omega$. Hence if ε moles/cm^3 is the original feed concentration of I_2, then

$$c_1 = cx_1 = \varepsilon[1-y-1.5\,\omega]$$

$$c_2 = cx_2 = \varepsilon y$$

$$c_3 = cx_3 = \varepsilon\omega$$

$$c_4 = cx_4 = \varepsilon(0.5y + 0.75\omega)$$

we know that

$$K_{1A} = \frac{c_2 c_4^{1/2}}{c_1} (RT_1)^{1/2}$$

This simplifies to

$$K_{1A} = \frac{y(y+1.5\omega)^{1/2}}{1-(y+1.5\omega)} \left(\frac{\varepsilon RT_1}{2}\right)^{1/2} \qquad \text{(i)}$$

Also, for the equilibrium constant K_{1B},

$$K_{1B} = \frac{c_3^2 c_4^{3/2}}{c_1^3} (RT_1)^{1/2} = \frac{\omega^2(y+1.5\omega)^{3/2}}{[1-(y+1.5\omega)]^3} \left(\frac{\varepsilon RT_1}{8}\right)^{1/2} . \qquad \text{(ii)}$$

We know that $c = c_1 + c_2 + c_3 + c_4$

and so

$$c = \varepsilon(1-y-1.5\omega) + \varepsilon y + \varepsilon\omega + \frac{\varepsilon}{2}(y+1.5\omega)$$

or

$$\frac{c}{\varepsilon} = 1 + 0.5y + 0.25\omega. \qquad \text{(iii)}$$

Solution of (i), (ii) and (iii) in terms of c, y and ω gives

$$\omega = \sqrt{\frac{K_{1B} y^3 \varepsilon RT_1}{K_{1A}^3}}$$

$$\frac{c}{\varepsilon} = 1 + \frac{y}{2} + \frac{1}{4} \sqrt{\frac{K_{1B} y^3 \varepsilon RT_1}{K_{1A}^3}}$$

and

$$1.5Ay^{5/2} + y^2 + 1.5ABy^{3/2} + By - B = 0 \qquad \text{(iv)}$$

where

$$A = \sqrt{\frac{K_{1B} \varepsilon RT_1}{K_{1A}^3}}$$

and

$$B = \sqrt{\frac{2K_{1A}^2}{\varepsilon RT_1}}$$

Having obtained y from the above Eq. (iv), we can proceed to obtain ω and then c, the total concentration.

APPENDIX 2

Thermodynamic Calculations

Section I

II-VI Compounds transport.

The general reaction is

$$MX_{(s)} + I_{2(g)} \rightleftharpoons MI_{2(g)} + \frac{1}{2} X_{2(g)}$$

$$\therefore \quad \Delta G^\circ_{T,rxn} = \Delta G^\circ_{f,MI_{2(g)}} + \frac{1}{2} \Delta G^\circ_{f,X_{2(g)}} - \Delta G^\circ_{f,I_{2(g)}} - \Delta G^\circ_{f,MX_{(s)}}$$

Most of our thermodynamic data has been taken from Ref. 18 in which the reference state for halogens is the gas (even at 298°K) while the reference state for sulfur is S_2(gas) at 298°K.

Since we have mostly found the ΔG°_f for sulfides, we can represent the free energy balance as

$$\Delta G^\circ_{T,rxn} = \Delta G^\circ_{f,MI_{2(g)}} - \Delta G^\circ_{f,MX_{(s)}}$$

since

$$\Delta G^\circ_{f,I_{2(g)}} = \Delta G^\circ_{f,S_{2(g)}} = 0 .$$

Here, I_2 stands for any helogen.

We are interested in finding the free energy of reaction at high temperatures. Thus, for example, by the use of heat capacities, heats of fusion and heats of vaporization, the values given for 298°K can be

made to apply at greatly increased temperatures. Since, however, for most of these compounds the heat capacities are not known especially at higher temperatures, it has been found useful to approximate the free energy as

$$\Delta G^{\circ}_{rxn,T} = \Delta H_{298} - T\Delta S_{298} \quad ,$$

where the heat and entropy of formation at 298°K are assumed to be constant over the temperature range. Although this is not true, the change in ΔH_{298} and ΔS_{298} is such that the errors tend to balance out. A more detailed discussion of the errors involved is presented by Brewer.[19]

For a given chalcogenide, the calculations are straight forward because the species are assumed to remain in the solid state at such high temperatures as are needed for transport.

For the halides, we have to find the heats and entropies of formation for the gaseous state. Hence after finding the free energy of formation for the solid or liquid state, we will add the free energy of fusion or vaporization as the case may be. Thus,

$$\Delta G^{\circ}_{f(g)} = \Delta G^{\circ}_{f(s)} + \Delta G^{\circ}_{(melting)} + \Delta G^{\circ}_{vap.}$$

or

$$\Delta G^{\circ}_{f(g)} = \Delta G^{\circ}_{f(liq)} + \Delta G^{\circ}_{vap.}$$

For the halides, the ΔG at any temperature can be obtained by finding the value of $(\Delta G-\Delta H_{298})/T$ at the desired temperature through interpolating between the values given in Table 6.3, Ref. 24. The values of ΔH_{298} are also given and so we can obtain $\Delta G_{f(solid)}$ or $\Delta G_{f(liq)}$ as the case may be.

To obtain the free energy of vaporization, we utilize Kelley's method.[20]

$$\Delta G = \Delta H_o - \Delta C_p T \ln T + IT$$

and

$$\Delta H = \Delta H_o + \Delta C_p T$$

where ΔH_o is

$$\Delta H_o = T_1 (\Delta S_v - \Delta C_p)$$

and

$$I = \Delta C_p \ln T_1 + (\Delta C_p - \Delta S_v)$$

where

T_1 = Boiling Point

and

ΔS_v = Entropy of vaporization at the boiling point.

This equation given above is valid for the entire liquid range. For the solids it must be modified. The simplest assumption when data are not available is that ΔC_p is the same for both solid and liquid ranges. Then the free energy of vaporization equation will be the same for the solid as for the liquid except for the addition of the heat

of fusion to ΔH_o and subtracting the entropy of fusion from I.

To use the above equations, a value of ΔC_p is needed. Kelley[20] gives ΔC_p values for many compounds. For those not listed, the rough guidelines are as follows: For vaporization of a liquid to a gaseous MX molecule, ΔC_p = -7 cal/°K/mole; for a gaseous MX_2, ΔC_p = -10; for gaseous MX_3, ΔC_p = -14 and for gaseous MX_4, ΔC_p = -16.

Using the guidelines above, we can proceed to find the thermodynamic values for some chalcogenide transport reactions.

Ex. 1. Cadmium Sulfide Transport by Iodine.

$$CdS_{(s)} + I_{2(g)} \rightleftharpoons CdI_{2(g)} + \frac{1}{2} S_{2(g)}$$

$$\therefore \quad \Delta G^\circ_{T,rxn} = \Delta G^\circ_{T,CdI_{2(g)}} - \Delta G^\circ_{T,CdS_{(s)}} .$$

Calculations for $CdS_{(s)}$:

$$\Delta H_{298} = - 49.9 \text{ kcal/mole}$$

$$\Delta S_{298} = - 22.5 \text{ cal/mole-deg} .$$

$$\Delta G^\circ_{T,CdS_{(s)}} - 49.9 + .0225T \text{ kcal/mole}$$

These functions are plotted in Fig. 8, Ch. II.

Calculations for $CdI_{2(g)}$: At 1000°K, $\Delta G^\circ_{T\,(liq)} = .031T + 63.3$ kcal/mole.

Also, $\Delta C_p = -10$, $T_{BP} = 1069°K$, $\Delta S_{vap} = 23.8$ cal/°mole

Thus $\Delta G^\circ_{vap} = 36.1 + 0.01\ T\ \ell n\ T - 0.1035\ T$

and

$$\Delta G_{T,CdI_{2(g)}} = \Delta G_{T,CdI_{2(liq)}} + \Delta G_{vap}$$

We show this value as a function of T in Fig. 8, Ch. II.

Finally we obtain

$$\Delta G^\circ_{T,rxn} = 0.01\ T\ \ell n\ T - 0.095\ T + 22.7 \text{ kcal/mole.}$$

Ex. 2 <u>Zinc Sulfide Transport by Iodine</u>

$$ZnS_{(s)} + I_{2(g)} \rightleftharpoons ZnI_{2(g)} + \frac{1}{2}S_{2(g)}$$

$$\Delta G^\circ_{T,rxn} = \Delta G^\circ_{T,ZnI_{2(g)}} - \Delta G^\circ_{T,ZnS_{(s)}}$$

For $ZnS_{(s)}$:

$$\Delta H^\circ_{298} = -60.7 \text{ kcal/mole}$$

$$\Delta S^\circ_{298} = -23.4 \text{ cal/mole °K}$$

and

$$\Delta G^\circ_{T,ZnS_{(s)}} - 60.7 + 0.0234\ T$$

For ZnI_2 at 1000°K

$$\Delta G - \Delta H_{298} = 28.1\ T, \text{ at } 1000°K$$

$$\Delta H_{298} = -64.7 \text{ kcal/mole.}$$

$$\Delta G_{ZnI_2(\ell)} = 0.0281\ T - 64.7$$

For the vaporization of $ZnI_{2(\ell)}$

$$T_B \cong 1000°K$$

$$\Delta S_v = 23, \qquad \Delta C_p \cong -10$$

$$\Delta H_o = 1000\ (23+10) = 33000$$

$$I = \Delta C_p\ \ell n\ T - 0.1021\ T = -\ 102.076$$

$$\Delta G_{vap} = 33 + .010\ T\ \ell n\ T - .1021\ T$$

Then,

$$\Delta G_{ZnI_2(g)} = \Delta G_{ZnT_2(\ell)} + \Delta G_{vap}$$

Finally,

$$\Delta G_{T,rxn} = \Delta G_{ZnI_2(g)} - \Delta G_{ZnS(s)}$$

$$\Delta G_{rxn} = -0.0974\ T + 0.01\ T\ \ell n\ T + 29.0 \quad \text{kcal/mole}$$

Ex. 3 <u>Manganese Sulfide Transport by Iodine</u>

$$\Delta G_{T,rxn} = \Delta G^\circ_{T,MnI_2(g)} - \Delta G^\circ_{T,MnS(s)}$$

Calculations for MnS:

$$\Delta H^\circ_{298} = -59.9 \text{ kcal/mole}$$

$$\Delta S_{298} = -15.8 \text{ cal/°K mole}$$

Thus, $\Delta G^\circ_{T,MnS(s)} = -59.9 + 0.0158\ T$

We show this function versus temperature in Fig. 9, Ch. II.

Calculations for MnI_2:

$$T_m = 111°K, \quad \Delta H_{298} = -72 \text{ kcal/mole}$$

$$T_B = 1100°K, \quad \Delta S_{vap} = 21 \text{ cal/mole°K},$$

$$\Delta H_{fusion} = 6.5 \text{ kcal/mole}, \quad \Delta S_{fusion} = 7 \text{ cal/mole°K}.$$

$$\Delta G - \Delta H_{298} = 35\ T \qquad \text{at } T = 500$$

$$\Delta G - \Delta H_{298} = 32\ T \qquad \text{at } T = 1000$$

$$\Delta G - \Delta H_{298} = 28\ T \qquad \text{at } T = 1500$$

From the data given above

$$\Delta G_{vap} = 34.1 + 0.01\ T\ \ell n\ T - 0.101\ T$$

and

$$\Delta G_{sub} = \Delta G_{vap} + \Delta G_{fusion}$$

$$= 40.6 + 0.010\ T\ \ell n\ T - 0.108\ T$$

We show $\Delta G_{MnI_2(g)}$ as a function of T in Fig. 9, Ch. II. Note that for

i) $T < 900°K$, we add ΔG_{sub}, to the ΔG tabulated above.

ii) $T < T < 1100°K$, we add ΔG_{vap} to the ΔG tabulated above.

iii) $T > 1100°K$, we take ΔG values directly from the table, because $\Delta G_{vap} \cong 0$ above the boiling point.

For an analytic equation we can represent the data for a range $T > 1000°K$, the general region for chemical transport by interpolating between $T = 1000°$ and $T = 1500°K$.

For $MnI_{2(liq)}$

$$\frac{\Delta G - \Delta H_{298}}{T} = 32 - 0.008\ (T-1000)\ \text{cal/mole.}$$

Then

$$\Delta G_{MnI_2(\ell)} = 0.032\ T - 0.000008\ T^2 + 0.008\ T - 72\ \text{kcal/mole}$$

$$\Delta G_{(vap)} = 0.01\ T\ \ell n\ T + .724 - .108\ T + 40.6$$

$$\Delta G_{MnI_2(g)} = 0.01\ T\ \ell n\ T - 0.068\ T - 0.000008\ T^2 - 31.4$$

and

$$\Delta G_{MnS(s)} = 0.0158\ T - 59.9$$

Thus $\Delta G^{\circ}_{T,rxn} = 0.01\ T\ \ell n\ T - 0.0838\ T - 0.000008\ T^2 + 28.5$ kcal/mole.

Section 2

The thermodynamics of spinels transport follows similar lines as in Section 1.

We estimate $\Delta G_{T,rxn}$ for the trivalent chalcogenides and obtain the equilibrium constant for conversion into the halides.

The equilibrium constants for these two parallel reactions are then linked in the general equations derived elsewhere.

In this section we calculate $\Delta G_{T,rxn}$ for $M_2X_3 + 3I_2 \rightleftharpoons 2MI_3 + \frac{3}{2} S_2$ defined by

$$\Delta G_{T,rxn} = 2\ \Delta G^{\circ}_{T,MI_3(g)} - \Delta G^{\circ}_{T,M_2X_3(s)}$$

Although the thermodynamic quantities for many trivalent elements were calculated, only those for In are given here.

Ex. 1 Indium Sulfide Transport with Iodine

For $In_2S_{3(s)}$:

$\Delta H_{298,f}$ = -82.3 ± 4.5 kcal/mole (Ref. 21)

$\Delta S_{298,f}$ = -23.0 cal/deg mole (approx. from Th_2S_3)

ΔG°_T = -82.8 + 0.023 T

For $In_2I_{3(g)}$

T_B = 773°K

ΔC_p = -15; $\Delta H_o = T_B(\Delta S_v - \Delta C_p) = 773(24.5+15) = 30533$

ΔG_{vap} = 30.53 + 0.015 T ℓn T - 0.1393 T

$$\Delta G_{InI_3(\ell)} = 0.048\ T - 82$$

$$\Delta G_{InI_3(g)} = \Delta G_{InI_{3(liq)}} + \Delta G_{vap}$$

$$= -0.091\ T + 0.015\ \ell n\ T - 51.47$$

Thus,

$$\Delta G_{T,rxn} = 2\Delta G_{InI_3(g)} - \Delta G_{In_2S_3}$$

$$= -\ .2056\ T + 0.03\ T\ \ell n\ T - 20.2\ kcal$$

The functions $\Delta G_{T,In_2S_3(s)}$ and $\Delta G_{T,InI_3(g)}$ are presented in Fig. 10 Ch. II.

APPENDIX 3

Determination of Gas-Phase Diffusivity

For ordinary diffusion in gases at low density, the Chapman-Enskog theory is used[2]:

$$c\hat{D}_{AB} = 2.2646\times10^{-5}\frac{\sqrt{T\left(\frac{1}{M_A}+\frac{1}{M_B}\right)}}{\sigma_{AB}^{2}\Omega_{\hat{D},AB}} .$$

Since $c = p/RT$,

$$\hat{D}_{AB} = 0.0018583\frac{\sqrt{T^3\left(\frac{1}{M_A}+\frac{1}{M_B}\right)}}{p\sigma_{AB}^{2}\Omega_{\hat{D},AB}}$$

in which $\hat{D}_{AB}$ [$cm^2 sec^{-1}$], c [g-moles cm^{-3}], T[°K], p[atm], σ_{AB} [Å] and Ω_{AB} [dimensionless] are the typical units

For gaseous species whose Lennard Jones parameters σ_A and ε/k are not known, we can use the relation developed by Slattery and Bird,[2]

$$\frac{p\hat{D}_{AB}}{(p_{cA}p_{cB})^{1/3}(T_{cA}T_{cB})^{5/12}\left(\frac{1}{M_A}+\frac{1}{M_B}\right)^{1/2}} = a\left(\frac{T}{\sqrt{T_{cA}T_{cB}}}\right)^{b}$$

in which we use

$\hat{D}_{AB}$ [$cm^2 sec^{-1}$], p[atm], T[°K],

and set $a = 2.745\times10^{-4}$, $b = 1.823$ } for nonpolar gas pairs

or $a = 3.640\times10^{-4}$, $b = 2.334$ } for H_2O with a nonpolar gas.

The accuracy of this relation is ~8% and is less than that of the Chapman-Enskog theory. We have used this relation in our estimation of the binary diffusivities.

For the relation of Slattery and Bird, we can obtain $\hat{D}_{AB}$ from the critical temperatures and pressures. For those compounds whose critical constants are not available, they can be estimated by different relations given in a review by Kobe and Lynn.[22]

Meissner and Redding[23] proposed for the critical temperature for substances boiling below 235°K,

$$T_c = 1.70\ T_B - 2,$$

and for substances containing halogen or sulfur and boiling above 235°K,

$$T_c = 1.41\ T_B + 66 - 11\ F$$

where

T_c = critical temp, °K

T_B = boiling point, °K

F = number of halogen atoms in the molecule.

The reliability of these equations is ~5%.

The concept of a parachor developed by Sugden[24] is really useful for estimating critical constants.

The parachor $[P] = \frac{M\gamma^{1/4}}{D-d} = MC^{1/4}$

where C = Macleod's constant and M = molecules wt.

γ = surface tension at any temperature

D = density of liquid at any temperature

d = density of vapor.

If we use Meissner's relation,[23]

$$T_c = 20.2\ T_B^{0.6} - 143 - 1.2[P] + 10.4[R_D]$$

where

T_B = normal boiling point

and

$$[R_D] = \text{the molar refraction} = \frac{n^2-1}{n^2+2} \cdot \frac{M}{d_L}$$

where n = refractive index of a liquid of density d_L, both determined at the same temperature. Then we can obtain a very good estimate of T_c.

However since we do not have adequate data for $[R_D]$ of inorganic halides, we find it much more convenient to use Herzog's relations[25] for T_c and P_c.

For T_c, we have

$$T_c/T_B = a - b \log[P]$$

and for P_c,

$$\log P_c = a' - b' \log[P].$$

For inorganic halides,

$$a = 2.602,\ b = 0.4449$$

$$a' = 3.4271\quad b' = 0.7829$$

The parachor can be treated as an additive property. For a compound, the parachor is the addition of the various parachors of different atoms in it.

e.g.

$$[P]_{CaCl_2} = [P]_{Ca} + 2[P]_{Cl}$$

Sugden[24] has proposed a table of parachors corresponding to the different elements in the Periodic Table (Table 7). Thus we can easily estimate the critical temperature and pressure of any inorganic halide. Table 8 summarizes calculated critical values for some compounds.

APPENDIX 4

A Computer Program for Chemical Transport of Group II-VI Compounds

The computational program written to solve the equation set derived in App. 1A consists of a main program TRANS which reads in initial data, calls on subroutines needed in the problem and prints output.

The subroutines called by TRANS are:

1. TOCON. This subroutine calculates the total concentration of all gaseous species in the ampoule.
2. DIFUS. This calculates the binary diffusivities $\hat{D}_{ij}$ for the various species in the system.
3. CALFUN. This is actually called by subroutine UTTAM and furnishes the values of the three equations for a given value of the variable set.
4. UTTAM. This estimates the best initial values for the unknown variables.
5. YCOMP. This provides values of the functions f_1, f_2, and f_3 for different values of the variable set. It is called by DHARTI.
6. DHARTI. This subroutine finds the solution to a set of n nonlinear algebraic equations in n real variables. Our problem is 3-dimensional.

DHARTI is a modified version of the program C4 CAL SIMEX obtained through the Computer Center, U.C., Berkeley. The method it utilizes is as follows:

Suppose our variables and equations were represented as $\underline{x}$ for $(x_1,\cdots x_n)$ and $\underline{f}(\underline{x})$ for $[f_1(x),\cdots f_n(x)]$ respectively. The initial problem is represented as

$$f_1(x_1,\cdots x_n) = 0$$

$$f_n(x_1,\cdots x_n) = 0.$$

We use $\max_i |f_i(\underline{x})|$ for the norm $\|\underline{f}(\underline{x})\|$ of $\underline{f}(\underline{x})$. The linear set of equations in matrix form is then

$$A\underline{y} = B \tag{1}$$

where
$A = (\partial_i f_j(x)/\partial x_j)$ and $B \triangleq (-f_i(\underline{x}))$, is solved for the correction vector $\underline{y}$. Then the norm $\|\underline{f}(\underline{x}+\underline{y})\|$ is tested against the norm $\|\underline{f}(\underline{x})\|$. If

$$\|\underline{f}(\underline{x}+\underline{y})\| < \|\underline{f}(\underline{x})\| \tag{2}$$

then the correction is accepted and the cycle is repeated. If Eq. (2) is not satisfied, the correction vector is chopped. $\underline{y}$ is replaced by $0.2\ \underline{y}$ and (2) is tested again. Chopping continues until either (2) is satisfied or the correction is negligible.

The iterative process is repeated until either $\underline{y}$ from Eq. (1) becomes negligible or until the number of iterations exceeds a limit imposed by the programmer. The program arbitrarily takes a correction $\underline{y}$ such that

$$\|\underline{y}\| / \|\underline{x}\| < 10^{-7} \tag{3}$$

as negligible (if $\|x\| \neq 0$, otherwise the denominator in Eq. (3) is taken as unity). The user should scale the variables x_i accordingly.

Of the three unknowns in the problem, λ_1, λ_2 and J, the first two are of the order of unity while J is very small. So J has to be normalized accordingly. One also has to assure that J is a positive quantity. It has been the author's experience that the choice of the initial values has much to do with the successful convergence of the iterative technique.

```
      PROGRAM TRANS (INPUT,OUTPUT)
C     THIS PROGRAM SIMULATES THE CHEMICAL VAPOR TRANSPORT OF 2-6 COMPOUNDS
C     USING HALOGENS AS THE TRANSPORT AGENT. FROM THIS PROGRAM WE CAN FIND
C     THE PRODUCT RATE OF FORMATION OF SINGLE CRYSTALS OF 2-6 COMPOUNDS.
C     WE CAN ALSO FIND THE CONCN. OF THE VARIOUS GASEOUS SPECIES AS A
C     FUNCTION OF THE DISTANCE ALONG THE AMPOULE.
      COMMON/TRAIN/PC(4),TC(4),WM(4),R,EPS,CLONG,A,B
      COMMON/SAFAR/ROTA,CRAS,RIOD,CON,RRR,SSS,TEE,QTEMP1,QTEMP2,EQK1,EQK
     12,RL,SL
      COMMON/PARAM/TEMP1,TEMP2,ORID
      DIMENSION T(10),DLG(10),EQK(10),ORIOD(10),DIFF(4,4)
      DIMENSION V(3),CONE(4),CTWO(4),XJAY(4),FN(3)
      DIMENSION COMP(7)
      DIMENSION AMAT(3,3),DMAT(3,3)
      INTEGER DIM,CNTROL(7)
      READ 200,(COMP(I),I=1,7)
  200 FORMAT(7A6)
      READ 201,N,EPS,R,CLONG,PRESO,NT,NO
  201 FORMAT(I4,7X,F11.8,3F11.4,2I4)
      DO 202 I=1,N
  203 FORMAT(I4,7X,4F11.4)
  202 READ 203,(J,PC(I),TC(I),WM(I))
      READ 205,(ORIOD(I),I=1,NO)
  205 FORMAT(8E10.3)
      READ 207,(T(I),I=1,NT)
  207 FORMAT(8F10.4)
      READ 209,DLAA,DLBB,DLCC,DLDD
  209 FORMAT(4F10.4)
      READ 211,A,B
  211 FORMAT(E11.4,F11.4)
      READ 55,(CONE(I),I=1,3)
   55 FORMAT(3F10.3)
      READ 56,(CTWO(I),I=1,3)
   56 FORMAT(3F10.3)
      PRINT  7
    7 FORMAT(1X,61HTHE MOLE FRACTIONS(X) OF THE SPECIES VARY WITH DISTAN
     1CE(Z) AS//5X,41HX(I2)=-2.+EXP(SZ)*(C1*COS(RZ)+C2*SIN(RZ))//5X,41HX
     1(MI2)=2.+EXP(SZ)*(C3*COS(RZ)+C4*SIN(RZ))//5X,21HX(S2)=1.-X(I2)-X(M
     1I2)/)
      PRINT  8
    8 FORMAT(1X,*THE PARAMETERS R,S,C1,C2,C3 AND C4 WILL BE PRINTED IN E
     1ACH OF THE DIFFERENT CASES BELOW*////)
      PRINT 5,(COMP(I),I=1,7)
    5 FORMAT(1X,*THIS SET OF DATA IS FOR *7A6///)
C     CALCULATE FREE ENERGY AND EQUIL.CONSTANT FOR A GIVEN TEMPERATURE.
      DO 6 I=1,NT
      DLG(I)=DLAA*T(I)+DLBB*T(I)**2+DLCC*T(I)*ALOG(T(I))+DLDD
    6 EQK(I)=EXP(-DLG(I)*1000./(1.98*T(I)))
C     CHOOSE ONE SET OF TEMPERATURE CONDITIONS.
      ND=NT-1
      DO 500 I=1,ND,2
      TEMP1=T(I)
      TEMP2=T(I+1)
      EQK1=EQK(I)
      EQK2=EQK(I+1)
C     SELECT A VALUE FOR INITIAL TRANSPORT AGENT FEED.
      DO 400 KI=1,NO
```

```
      ORID=ORIOD(KI)
      PRINT 100,TEMP1,TEMP2
  100 FORMAT(1X,*DIFFUSION IS FROM TEMP1=*E12.4,*(DEG K) TO TEMP2=*E12.4
     1,*(DEG K)*/)
  101 PRINT 102,EQK1,EQK2
  102 FORMAT(1X,*AT TEMP1, EQUIL. CONST. K1=*E12.4,*AND AT TEMP2,EQUIL.
     1CONST. K2=*E12.4/)
C     FIND TOTAL CONCENTRATION IN AMPOULE
      CALL TOCON(TEMP1,EQK1,ORID,CON)
      IF(CON.LT.0.) GO TO 58
C   CALCULATE PRESSURE IN AMPOULE AT MEAN TEMPERATURE.
      TMEAN=SQRT(TEMP1*TEMP2)
   19 PRESS=CON*R*TMEAN+PRESO/760.
      PRINT 777,PRESS
  777 FORMAT(1X,*PRESSURE IN AMPOULE =*E12.4,*(ATM)*/)
C     FIND BINARY DIFFUSIVITIES AT MEAN TEMPERATURE
      CALL DIFUS(DIFF,N,PRESS,TMEAN)
C     FIND CONSTANT COEFFICIENTS FOR SIMULTANEOUS EQUATIONS
      XXX=1./DIFF(1,2)
      YYY=1./DIFF(1,3)
      ZZZ=1./DIFF(2,3)
      AONE=XXX-0.5*YYY
      ATWO=ZZZ-XXX
      BONE=XXX-YYY
      BTWO=1.5*ZZZ-XXX
      DONE=YYY
      DTWO=-ZZZ
      DDD=ATWO*BONE-AONE*BTWO
      ALPH1=(BTWO*DONE-BONE*DTWO)/DDD
      ALPH2=(AONE*DTWO-ATWO*DONE)/DDD
      ALPH3=1.-ALPH1-ALPH2
      CCC=AONE+BTWO
      CONIN=1./CON
      QTEMP1=SQRT(CON*R*TEMP1)
      QTEMP2=SQRT(CON*R*TEMP2)
      BRKT=CCC**2.+4.*DDD
      IF(BRKT.GT.0.) GO TO 600
C     DISCRIMINANT IS MODULATED
       BRKT=ABS(BRKT)
      DSCRM=SQRT(BRKT)
      SSS=CCC/2.
      RRR=DSCRM/2.
      SL=SSS*CLONG
      RL=RRR*CLONG
      CRAS=RRR**2+SSS**2
      TEE=SSS-BTWO
      ROTA=ATWO/(RRR**2+TEE**2)
      RIOD=ORID*CLONG/CON
      XJAY(1)=.01*CON
      XJAY(2)=.05*CON
      XJAY(3)=.005*CON
      CALL UTTAM(CONE,CTWO,XJAY,V,N)
C   FIND SOLUTION FOR SET OF NONLINEAR EQUATIONS.
      CNTROL(1)=3
      CNTROL(2)=50
      CNTROL(3)=1.
      CNTROL(4)=0
```

```
      CNTROL(5)=3
      CNTROL(6)=0
      DIM=3
      CALL DHARTI(V,AMAT,DMAT,DIM,CNTROL)
C     AFTER FINDING SOLUTIONS FOR SET OF NON-LINEAR ALGEBRAIC EQUATIONS
C     FIND THE PRODUCT RATE AND THE CONSTANTS IN THE CONCENTRATION EQNS.
      V(3)=V(3)**2/1000000.
      RMOD=RRR*V(3)/CON
      SMOD=SSS*V(3)/CON
      COSP=TEE*V(1)-RRR*V(2)
      SINP=RRR*V(1)+TEE*V(2)
      C3=ROTA*COSP
      C4=ROTA*SINP
      SMOW=WM(2)-WM(1)+0.5*WM(3)
      PROD=V(3)*3600.*SMOW
      PRINT 3,PROD
    3 FORMAT(1X,*PRODUCT RATE(GRAM/SQ.CM/HR)=*E10.4/)
      PRINT 9,RMOD,SMOD,V(1),V(2),C3,C4
    9 FORMAT(1X,*R=*F11.5,2X,*S=*F11.5,2X,*C1=*F8.5,2X,*C2=*F8.5,2X,*C3=
     1*F8.5,2X,*C4=*F8.5///)
      GO TO 400
   58 PRINT 59
   59 FORMAT(1X,* TOTAL CONCENTRATION IS NEGATIVE*/)
      GO TO 400
  600 PRINT 60
   60 FORMAT (1X,*POSITIVE DISCRIMINANT*/)
  400 CONTINUE
  500 CONTINUE
      STOP
      END
```

```
      SUBROUTINE TOCON (T,EQLB,ORID,CON)
C     THIS SUBROUTINE CALCULATES THE TOTAL CONCENTRATION OF ALL VAPOR
C     SPECIES IN THE AMPOULE.IT ALSO FINDS THE CONVERSION AT THE SOURCE.
      COMMON/TRAIN/PC(4),TC(4),WM(4),R,EPS,CLONG,A,B
      FACT=EQLB*EQLB/(R*T)
      ITER=0
      CON=ORID
      UUU=3.*ORID+FACT
      VVV=3.*ORID*ORID+3.*ORID*FACT
   11 FUNC=CON**3-CON**2*UUU+CON*VVV-ORID**3-2.25*FACT*ORID*ORID
   13 DIFC=3.*CON*CON-2.*CON*UUU+VVV
      CONEW=CON-FUNC/DIFC
      DIFF=(CONEW-CON)/CON
      CON=CONEW
      IF(ABS(DIFF)-EPS) 22,22,23
   22 GO TO 99
   23 ITER=ITER+1
      IF(ITER-25)16,16,17
   16 GO TO 11
   17 PRINT 18
   18 FORMAT(1X,*OVERALL CONCENTRATION NOT CONVERGENT IN 25 ITERATIONS*)
      STOP
   99 PRINT 100,T,ORID,CON
  100 FORMAT(1X,*TOTAL CONC AT*E12.4,*(DEG K) FOR INITIAL IODINE CONC OF
     1*E12.4,*(MOLES/CU CM) IS =*E12.4,*(MOLES/CU CM)*/)
      CONVR=2.*(CON/ORID-1.)
      PRINT 98,CONVR
   98 FORMAT(1X,*CONVERSION=*F10.6/)
      RETURN
      END



      SUBROUTINE DIFUS(D,N,P,T)
C     THIS SUBROUTINE CALCULATES THE BINARY DIFFUSIVITIES FOR THE VARIOUS
C     GASEOUS SPECIES IN THE AMPOULE.
      COMMON/TRAIN/PC(4),TC(4),WM(4),R,EPS,CLONG,A,B
      DIMENSION D(4,4)
      DO 10 L=1,N
      DO 10 M=1,N
   10 D(L,M)=0.
      DO 20 L=1,N
      DO 20 M=1,N
      IF(L-M) 14,20,14
   14 D(L,M)=D(M,L)
      IF(D(L,M).GT. 0.) GO TO 20
      D(L,M)=A/P*T**B*(PC(L)*PC(M))**0.333*(TC(L)*TC(M))**(0.417-B/2.)*S
     1QRT(1./WM(L)+1./WM(M))
   20 CONTINUE
      RETURN
      END
```

```
      SUBROUTINE UTTAM(CONE,CTWO,XJAY,BZ,N)
C     THIS SUBROUTINE IN CONJUNCTION WITH ,CALFUN, FINDS THE BEST INITIAL
C     VALUES FOR THE VARIABLES TO BE FOUND IN  ,DHARTI,.
      DIMENSION Z(3),CONE(4),CTWO(4),XJAY(4),BZ(3),BF(3),FN(4)
      DATA (BF(I),I=1,3)/3*0./
      DO 20 I=1,N
      FN(I)=1000.
   20 BZ(I)=0.
      BEST=1000.
      DO 70 I=1,3
      Z(1)=CONE(I)
      DO 80 J=1,3
      Z(2)=CTWO(J)
      DO 90 K=1,3
      Z(3)=SQRT(XJAY(K))*1000.
      CALL CALFUN(N,FN,Z)
      SUM=SQRT(FN(1)**2+FN(2)**2+FN(3)**2)
      IF(SUM.GE.BEST) GO TO 90
      BEST=SUM
      DO 25 IS=1,N
      BZ(IS)=Z(IS)
   25 BF(IS)=FN(IS)
   90 CONTINUE
   80 CONTINUE
   70 CONTINUE
      RETURN
      END

      SUBROUTINE CALFUN(N,FN,Z)
      COMMON/SAFAR/ROTA,CRAS,RIOD,CON,RRR,SSS,TEE,QTEMP1,QTEMP2,EQK1,EQK
     12,RL,SL
      DIMENSION FN(N),Z(N)
      REAL MOD
      MOD=Z(3)**2/(CON*1000000.)
      RMOD=RRR*MOD
      SMOD=SSS*MOD
      SLMOD=SL*MOD
      IF(SLMOD.GT.50.) GO TO 90
      EXPS=EXP(SLMOD)
      COSR=COS(RL*MOD)
      SINR=SIN(RL*MOD)
      CRAP=CRAS*MOD**2
      COSP=TEE*Z(1)-RRR*Z(2)
      SINP=Z(1)*RRR+TEE*Z(2)
      RSVP=Z(1)+ROTA*COSP
      IF(RSVP.GT.1.) GO TO 90
      ABCD=EXPS*(COSR*RSVP+SINR*(Z(2)+ROTA*SINP))
      IF(ABCD.GT.1.) GO TO 90
      FN(1)=(2.+ROTA*COSP)*QTEMP1*SQRT(1.-RSVP)/(-2.+Z(1))-EQK1
      FN(2)=(2.+ROTA*EXPS*(COSP*COSR+SINP*SINR))*QTEMP2*SQRT(1.-ABCD)/(-
     12.+EXPS*(Z(1)*COSR+Z(2)*SINR))-EQK2
      FN(3)=((Z(1)+ROTA*COSP)*(SMOD*(EXPS*COSR-1.)+RMOD*EXPS*SINR)+(Z(2)
     1+ROTA*SINP)*(SMOD*EXPS*SINR-RMOD*(EXPS*COSR-1.)))/CRAP-RIOD
   90 CONTINUE
      RETURN
      END
```

```
      FUNCTION YCOMP(Z,NFN,NPROB)
C     THIS FUNCTION FURNISHES THE VALUES OF FUNCTIONS AND GRADIENTS AS
C     REQUIRED IN SUBROUTINE ,DHARTI,.
      REAL Z(1),MOD
      COMMON/SAFAR/ROTA,CRAS,RIOD,CON,RRR,SSS,TEE,QTEMP1,QTEMP2,EQK1,EQK
     12,RL,SL
      MOD=Z(3)**2/(CON*1000000.)
      RMOD=RRR*MOD
      SMOD=SSS*MOD
      SLMOD=SL*MOD
      IF(SLMOD.GT.50.) RETURN
      EXPS=EXP(SLMOD)
      COSR=COS(RL*MOD)
      SINR=SIN(RL*MOD)
      COSP=TEE*Z(1)-RRR*Z(2)
      SINP=Z(1)*RRR+TEE*Z(2)
      CRAP=CRAS*MOD**2
  100 GO TO (11,12,13),NFN
   11 RSVP=Z(1)+ROTA*COSP
      IF (RSVP.LE.1.) GO TO 92
      RETURN
   92 YCOMP=(2.+ROTA*COSP)*QTEMP1*SQRT(1.-RSVP)/(-2.+Z(1))-EQK1
      RETURN
   12 ABCD=EXPS*(COSR*RSVP+SINR*(Z(2)+ROTA*SINP))
      IF (ABCD.LE.1.) GO TO 91
      RETURN
   91 YCOMP=(2.+ROTA*EXPS*(COSP*COSR+SINP*SINR))*QTEMP2*SQRT(1.-ABCD)/(-
     12.+EXPS*(Z(1)*COSR+Z(2)*SINR))-EQK2
      RETURN
   13 YCOMP=((Z(1)+ROTA*COSP)*(SMOD*(EXPS*COSR-1.)+RMOD*EXPS*SINR)+(Z(2)
     1+ROTA*SINP)*(SMOD*EXPS*SINR-RMOD*(EXPS*COSR-1.)))/CRAP-RIOD
      RETURN
      END
```

ACKNOWLEDGEMENTS

I am indebted to Dr. Lee F. Donaghey for his continuous guidance, encouragement and constructive suggestions throughout the course of this investigation. I would also like to thank Dr. Alexis T. Bell and Dr. Norman Phillips for their criticism and comments which helped shape the final manuscript.

I also wish to acknowledge the assistance of D. Ray and A. F. Kabir for numerous discussions concerning the mathematical equations and the computer program; Jim Byce for help in constructing the deflection coils; Phillip Eggers for his help in the electronic instrumentation and Jerry Smith for his help in obtaining certain computer subroutines.

Shirley Ashley and Alice Ramirez deserve special praise for coping with the typing of the thesis. I would also like to thank Gloria Pelatowski for the drawings.

Finally, I am grateful to the U. S. Atomic Energy Commission for providing financial support through the Inorganic Materials Research Division of the Lawrence Berkeley Laboratory.

TECHNICAL INFORMATION DIVISION
LAWRENCE BERKELEY LABORATORY
UNIVERSITY OF CALIFORNIA
BERKELEY, CALIFORNIA 94720